

Modeling Sulfur Oxides (SO_x) Emissions Transport from Ships at Sea

Modeling Sulfur Oxides (SO_x) Emissions Transport from Ships at Sea

Assessment and Standards Division
Office of Transportation and Air Quality
U.S. Environmental Protection Agency

Prepared for EPA by
Atmospheric & Environmental Research, Inc.
EPA Contract No. GS-10F-0615P

NOTICE

This technical report does not necessarily represent final EPA decisions or positions. It is intended to present technical analysis of issues using data that are currently available. The purpose in the release of such reports is to facilitate the exchange of technical information and to inform the public of technical developments which may form the basis for a final EPA decision, position, or regulatory action.



TABLE OF CONTENTS

1.	Introduction.....	1-1
2.	Modeling Approach	2-1
2.1	Air Quality Model (CALPUFF).....	2-1
2.2	Meteorological Model (CALMET).....	2-3
2.3	Approach.....	2-3
	2.3.1 Receptors.....	2-4
	2.3.2 Sources.....	2-4
	2.3.3 Modeling domains	2-5
3.	Model Inputs	3-1
3.1	Meteorology	3-1
	3.1.1 Measurements	3-2
	3.1.2 MM5 outputs.....	3-7
	3.1.3 CALMET winds.....	3-7
	3.1.4 CALMET mixing heights	3-17
3.2	Emissions	3-17
	3.2.1 Emission rates	3-26
	3.2.2 Stack parameters	3-27
4.	Results.....	4-1
4.1	Results for the Southern Pacific U.S. Coastline	4-2
4.2	Results for the Northern Pacific U.S. Coastline	4-16
4.3	Results for the Gulf of Mexico Coastline	4-32
4.4	Results for the Atlantic Ocean Coastline	4-43
5.	Summary and Conclusions	5-1
6.	References.....	6-1

Appendices

LIST OF TABLES

Table 3-1	Stack characteristics.....	3-28
Table 5-1	Percentage of SO ₂ concentrations below the design value as a function of the distance from the coastline.....	5-2
Table 5-2	Percentage of sulfate concentrations below the design value as a function of the distance from the coastline.	5-2

LIST OF FIGURES

Figure 2-1	Modeling domain for the Southern Pacific Ocean U.S. coastline.	2-6
Figure 2-2	Modeling domain for the Northern Pacific Ocean U.S. coastline.	2-7
Figure 2-3	Modeling domain for the Gulf of Mexico coastline.	2-9
Figure 2-4	Modeling domain for the Atlantic Ocean coastline.	2-10
Figure 3-1	Land-based surface stations and over-water stations for the Southern Pacific Ocean U.S. coastline.....	3-3
Figure 3-2	Land-based surface stations and over-water stations for the Northern Pacific Ocean U.S. coastline.....	3-4
Figure 3-3	Land-based surface stations and over-water stations for the Gulf of Mexico coastline	3-5
Figure 3-4	Land-based surface stations and over-water stations for the Atlantic Ocean coastline	3-6
Figure 3-5	MM5 modeling domain	3-8
Figure 3-6a	Wind roses based on CALMET outputs for the southern Pacific Ocean during winter and spring 2002	3-9
Figure 3-6b	Wind roses based on CALMET outputs for the southern Pacific Ocean during summer and fall 2002	3-10
Figure 3-7a	Wind roses based on CALMET outputs for the northern Pacific Ocean during winter and spring 2002	3-11
Figure 3-7b	Wind roses based on CALMET outputs for the northern Pacific Ocean during summer and fall 2002	3-12
Figure 3-8a	Wind roses based on CALMET outputs for the Gulf of Mexico during winter and spring 2002.....	3-13
Figure 3-8b	Wind roses based on CALMET outputs for the Gulf of Mexico during summer and fall 2002.....	3-14
Figure 3-9a	Wind roses based on CALMET outputs for the Atlantic Ocean during winter and spring 2002.....	3-15
Figure 3-9b	Wind roses based on CALMET outputs for the Atlantic Ocean during summer and fall 2002.....	3-16
Figure 3-10a	Mixing heights for the southern Pacific Ocean during winter and spring 2002.....	3-18
Figure 3-10b	Mixing heights for the southern Pacific Ocean during summer and fall 2002.....	3-19
Figure 3-11a	Mixing heights for the northern Pacific Ocean during winter and spring 2002.....	3-20

Figure 3-11b	Mixing heights for the northern Pacific Ocean during summer and fall 2002.....	3-21
Figure 3-12a	Mixing heights for the Gulf of Mexico during winter and spring 2002	3-22
Figure 3-12b	Mixing heights for the Gulf of Mexico during summer and fall 2002 ..	3-23
Figure 3-13a	Mixing heights for the Atlantic Ocean during winter and spring 2002 .	3-24
Figure 3-13b	Mixing heights for the Atlantic Ocean during summer and fall 2002 ...	3-25
Figure 4-1	Ratios of annual-average SO ₂ concentrations due to sea-going ships burning high-sulfur fuel at 125 km from the Southern Pacific U.S. coastline to the concentrations (target values) due to dockside ships at the coastline burning low-sulfur fuel	4-3
Figure 4-2	Cumulative frequency distribution of design ratios of SO ₂ concentrations from ships at 125 km from the Southern Pacific U.S. coastline	4-4
Figure 4-3	Ratios of annual-average sulfate concentrations due to sea-going ships burning high-sulfur fuel at 125 km from the Southern Pacific U.S. coastline to the concentrations (target values) due to dockside ships at the coastline burning low-sulfur fuel	4-5
Figure 4-4	Cumulative frequency distribution of design ratios of sulfate concentrations from ships at 125 km from the Southern Pacific U.S. coastline	4-6
Figure 4-5	Ratios of annual-average SO ₂ concentrations due to sea-going ships burning high-sulfur fuel at 250 km from the Southern Pacific U.S. coastline to the concentrations (target values) due to dockside ships at the coastline burning low-sulfur fuel	4-8
Figure 4-6	Cumulative frequency distribution of design ratios of SO ₂ concentrations from ships at 250 km from the Southern Pacific U.S. coastline	4-9
Figure 4-7	Ratios of annual-average sulfate concentrations due to sea-going ships burning high-sulfur fuel at 250 km from the Southern Pacific U.S. coastline to the concentrations (target values) due to dockside ships at the coastline burning low-sulfur fuel	4-10
Figure 4-8	Cumulative frequency distribution of design ratios of sulfate concentrations from ships at 250 km from the Southern Pacific U.S. coastline	4-11
Figure 4-9	Ratios of annual-average SO ₂ concentrations due to sea-going ships burning high-sulfur fuel at 375 km from the Southern Pacific U.S. coastline to the concentrations (target values) due to dockside ships at the coastline burning low-sulfur fuel	4-12
Figure 4-10	Cumulative frequency distribution of design ratios of SO ₂ concentrations from ships at 375 km from the Southern Pacific U.S. coastline	4-13
Figure 4-11	Ratios of annual-average sulfate concentrations due to sea-going ships burning high-sulfur fuel at 375 km from the Southern Pacific U.S.	

	coastline to the concentrations (target values) due to dockside ships at the coastline burning low-sulfur fuel	4-14
Figure 4-12	Cumulative frequency distribution of design ratios of sulfate concentrations from ships at 375 km from the Southern Pacific U.S. coastline	4-15
Figure 4-13	Ratios of annual-average sulfate concentrations due to sea-going ships burning high-sulfur fuel at 500 km from the Southern Pacific U.S. coastline to the concentrations (target values) due to dockside ships at the coastline burning low-sulfur fuel	4-17
Figure 4-14	Cumulative frequency distribution of design ratios of sulfate concentrations from ships at 500 km from the Southern Pacific U.S. coastline	4-18
Figure 4-15	Ratios of annual-average SO ₂ concentrations due to sea-going ships burning high-sulfur fuel at 125 km from the Northern Pacific U.S. coastline to the concentrations (target values) due to dockside ships at the coastline burning low-sulfur fuel	4-19
Figure 4-16	Cumulative frequency distribution of design ratios of SO ₂ concentrations from ships at 125 km from the Northern Pacific U.S. coastline	4-20
Figure 4-17	Ratios of annual-average sulfate concentrations due to sea-going ships burning high-sulfur fuel at 125 km from the Northern Pacific U.S. coastline to the concentrations (target values) due to dockside ships at the coastline burning low-sulfur fuel	4-22
Figure 4-18	Cumulative frequency distribution of design ratios of sulfate concentrations from ships at 125 km from the Northern Pacific U.S. coastline	4-23
Figure 4-19	Ratios of annual-average SO ₂ concentrations due to sea-going ships burning high-sulfur fuel at 250 km from the Northern Pacific U.S. coastline to the concentrations (target values) due to dockside ships at the coastline burning low-sulfur fuel	4-24
Figure 4-20	Cumulative frequency distribution of design ratios of SO ₂ concentrations from ships at 250 km from the Northern Pacific U.S. coastline	4-25
Figure 4-21	Ratios of annual-average sulfate concentrations due to sea-going ships burning high-sulfur fuel at 250 km from the Northern Pacific U.S. coastline to the concentrations (target values) due to dockside ships at the coastline burning low-sulfur fuel	4-26
Figure 4-22	Cumulative frequency distribution of design ratios of sulfate concentrations from ships at 250 km from the Northern Pacific U.S. coastline	4-27
Figure 4-23	Ratios of annual-average sulfate concentrations due to sea-going ships burning high-sulfur fuel at 375 km from the Northern Pacific U.S.	

	coastline to the concentrations (target values) due to dockside ships at the coastline burning low-sulfur fuel	4-28
Figure 4-24	Cumulative frequency distribution of design ratios of sulfate concentrations from ships at 375 km from the Northern Pacific U.S. coastline	4-29
Figure 4-25	Ratios of annual-average sulfate concentrations due to sea-going ships burning high-sulfur fuel at 500 km from the Northern Pacific U.S. coastline to the concentrations (target values) due to dockside ships at the coastline burning low-sulfur fuel	4-30
Figure 4-26	Cumulative frequency distribution of design ratios of sulfate concentrations from ships at 500 km from the Northern Pacific U.S. coastline	4-31
Figure 4-27	Ratios of annual-average SO ₂ concentrations due to sea-going ships burning high-sulfur fuel at 125 km from the Gulf of Mexico coastline to the concentrations (target values) due to dockside ships at the coastline burning low-sulfur fuel	4-33
Figure 4-28	Cumulative frequency distribution of design ratios of SO ₂ concentrations from ships at 125 km from the Gulf of Mexico coastline	4-34
Figure 4-29	Ratios of annual-average sulfate concentrations due to sea-going ships burning high-sulfur fuel at 125 km from the Gulf of Mexico coastline to the concentrations (target values) due to dockside ships at the coastline burning low-sulfur fuel	4-35
Figure 4-30	Cumulative frequency distribution of design ratios of sulfate concentrations from ships at 125 km from the Gulf of Mexico coastline	4-36
Figure 4-31	Ratios of annual-average SO ₂ concentrations due to sea-going ships burning high-sulfur fuel at 250 km from the Gulf of Mexico coastline to the concentrations (target values) due to dockside ships at the coastline burning low-sulfur fuel	4-37
Figure 4-32	Cumulative frequency distribution of design ratios of SO ₂ concentrations from ships at 250 km from the Gulf of Mexico coastline	4-38
Figure 4-33	Ratios of annual-average sulfate concentrations due to sea-going ships burning high-sulfur fuel at 250 km from the Gulf of Mexico coastline to the concentrations (target values) due to dockside ships at the coastline burning low-sulfur fuel	4-39
Figure 4-34	Cumulative frequency distribution of design ratios of sulfate concentrations from ships at 250 km from the Gulf of Mexico coastline	4-40
Figure 4-35	Ratios of annual-average sulfate concentrations due to sea-going ships burning high-sulfur fuel at 375 km from the Gulf of Mexico coastline to the concentrations (target values) due to dockside ships at the coastline burning low-sulfur fuel	4-41

Figure 4-36	Cumulative frequency distribution of design ratios of sulfate concentrations from ships at 375 km from the Gulf of Mexico coastline	4-42
Figure 4-37	Ratios of annual-average sulfate concentrations due to sea-going ships burning high-sulfur fuel at 500 km from the Gulf of Mexico coastline to the concentrations (target values) due to dockside ships at the coastline burning low-sulfur fuel	4-44
Figure 4-38	Cumulative frequency distribution of design ratios of sulfate concentrations from ships at 500 km from the Gulf of Mexico coastline	4-45
Figure 4-39	Ratios of annual-average SO ₂ concentrations due to sea-going ships burning high-sulfur fuel at 125 km from the Atlantic Ocean coastline to the concentrations (target values) due to dockside ships at the coastline burning low-sulfur fuel	4-46
Figure 4-40	Cumulative frequency distribution of design ratios of SO ₂ concentrations from ships at 125 km from the Atlantic Ocean coastline	4-47
Figure 4-41	Ratios of annual-average sulfate concentrations due to sea-going ships burning high-sulfur fuel at 125 km from the Atlantic Ocean coastline to the concentrations (target values) due to dockside ships at the coastline burning low-sulfur fuel	4-48
Figure 4-42	Cumulative frequency distribution of design ratios of sulfate concentrations from ships at 125 km from the Atlantic Ocean coastline	4-49
Figure 4-43	Ratios of annual-average SO ₂ concentrations due to sea-going ships burning high-sulfur fuel at 250 km from the Atlantic Ocean coastline to the concentrations (target values) due to dockside ships at the coastline burning low-sulfur fuel	4-50
Figure 4-44	Cumulative frequency distribution of design ratios of SO ₂ concentrations from ships at 250 km from the Atlantic Ocean coastline	4-51
Figure 4-45	Ratios of annual-average sulfate concentrations due to sea-going ships burning high-sulfur fuel at 250 km from the Atlantic Ocean coastline to the concentrations (target values) due to dockside ships at the coastline burning low-sulfur fuel	4-52
Figure 4-46	Cumulative frequency distribution of design ratios of sulfate concentrations from ships at 250 km from the Atlantic Ocean coastline	4-53
Figure 4-47	Ratios of annual-average sulfate concentrations due to sea-going ships burning high-sulfur fuel at 375 km from the Atlantic Ocean coastline to the concentrations (target values) due to dockside ships at the coastline burning low-sulfur fuel	4-55
Figure 4-48	Cumulative frequency distribution of design ratios of sulfate concentrations from ships at 375 km from the Atlantic Ocean coastline	4-56
Figure 4-49	Ratios of annual-average sulfate concentrations due to sea-going ships burning high-sulfur fuel at 500 km from the Atlantic Ocean coastline to	

the concentrations (target values) due to dockside ships at the coastline
burning low-sulfur fuel 4-57

Figure 4-50 Cumulative frequency distribution of design ratios of sulfate
concentrations from ships at 375 km from the Atlantic Ocean coastline 4-58

EXECUTIVE SUMMARY

A screening study was conducted to determine the air quality impacts (annual average ground-level concentrations of SO₂ and sulfate) on land due to SO_x emissions from ships burning high-sulfur fuel at sea at various distances from the coastline. The CALPUFF dispersion model was used for this screening study. Meteorological inputs were prepared with the CALMET model using the outputs of a prognostic meteorological model, MM5, in combination with surface measurements over water and on land. The meteorology represents the year 2002 because it was the most recent year for which an MM5 simulation covering the contiguous United States was available. CALPUFF tends to overestimate the conversion of SO₂ to sulfate in the gas phase and the results presented here are likely to provide conservative estimates of the impacts of emissions from ships at sea on inland air quality (because of the simplified treatment of aqueous-phase chemistry in CALPUFF, this overestimation may not hold for cases where the interactions of the ship plumes with fog dominate sulfate formation).

Four domains were studied: the southern Pacific coastline, the northern Pacific coastline, the Gulf of Mexico coastline and the Atlantic coastline. The results were compared with those calculated for ships burning low-sulfur fuel at the coastline to determine upper bounds for Sulfur Emission Control Areas (SECAs), i.e., off-shore distances at which the switch to high-sulfur fuel would not impair air quality. For each offshore distance investigated, the percentage of receptors for which the air quality impacts of ships at sea were lower than the impacts of ships at the coastline was calculated.

Emission rates were estimated to be representative of ocean-going ships along U.S. coastlines. The sulfur content of the fuel was assumed to be 15,000 ppm within the SECA (i.e., here at the coastline) and 27,000 ppm outside the SECA (i.e., at the four off-shore distances considered here, 125, 250, 375 and 500 km). The gas-phase SO₂ and particulate-phase sulfate emissions per ship were estimated to be 100,320 g/h and 3,040 g/h, respectively, within the SECA and 180,640 g/h and 5,600 g/h, respectively, outside the SECA. Based on an analysis of ship traffic off the Pacific coastline, a distance of 25 km between ships was used for all coastlines.

The results are summarized in Tables E-1 and E-2 for concentration ratios of SO₂ and sulfate, i.e., the ratio of the concentration calculated for ships at sea to the concentration calculated for ships at the coastline (the design value).

The results for SO₂ were different from those for sulfate, primarily due to differences in the behavior of these two species downwind of a source. For all the coastlines studied, the majority of the SO₂ concentration ratios were less than one at shorter off-shore distances than for sulfate. Thus, sulfate concentration ratios were the limiting factor for defining the upper bounds of the SECA for each coastline.

The results showed some differences in results among the various coastlines studied. These differences are due to differences in the wind fields bringing the offshore ship emissions and their secondary products to land as well as differences in precipitation, which removes pollutants from the atmosphere.

The results from the two Pacific Ocean coastline simulations were qualitatively similar. For both Pacific Ocean coastlines, over 90% of the receptors showed SO₂ concentration ratios less than one for ships at 250 km from the coastline. For sulfate, only about 49% and 56% of the receptors had concentrations less than one for ships at 500 km from the southern Pacific Ocean and northern Pacific Ocean coastlines, respectively.

For the other two coastlines (Atlantic Ocean and Gulf of Mexico), the SO₂ results were qualitatively similar to those for the Pacific Ocean coastlines, i.e., over 90% of the receptors showed SO₂ concentration ratios less than one for ships at 250 km from the coastline. However, there were some large differences for sulfate. For the Gulf of Mexico coastline, over 70% of the receptors showed sulfate concentration ratios less than one for ships at 250 km from the coastline. For the Atlantic Ocean coastline, nearly 60% of the receptors showed sulfate concentration ratios less than one for ships at 250 km from the coastline.

Table E-1. Percentage of SO₂ concentrations below the design value as a function of the distance from the coastline.

Distance from coastline	125 km	250 km	375 km	500 km
Southern Pacific	40.7%	90.7%	100%	100%
Northern Pacific	46.6%	97.9%	100%	100%
Gulf of Mexico ^a	84.4%	98.1%	100%	100%
Atlantic	86.6%	100%	100%	100%

^aNote that Florida values correspond to a shorter ship-coastline distance and the values presented in the table should be seen as lower limits.

Table E-2. Percentage of sulfate concentrations below the design value as a function of the distance from the coastline.

Distance from coastline	125 km	250 km	375 km	500 km
Southern Pacific	4.4%	24.9%	41.9%	48.7%
Northern Pacific	0.01%	3.6%	20.3%	55.7%
Gulf of Mexico ^a	40.4%	72.0%	80.5%	84.0%
Atlantic	1.2%	57.9%	92.5%	100%

^aNote that Florida values correspond to a shorter ship-coastline distance and the values presented in the table should be seen as a lower limits.

These results suggest that an off-shore distance of 500 km should be sufficient when conducting refined modeling of the potential impacts of ship emissions on air quality inland, if a criterion of about 50% of inland receptors having sulfate concentrations below the design value is acceptable to define the SECA.

1. INTRODUCTION

This document describes a screening study to model on-shore SO₂ and sulfate concentrations due to emissions of SO_x from ships at sea. The objective of this screening study is to obtain quantitative information on the shortest distance at which ships burning high sulfur fuel (fuel content of 27,000 ppm) will have air quality impacts at land receptors that are less than those anticipated from emissions from ships burning low sulfur fuel (fuel content of 15,000 ppm) within coastal waters. This distance can subsequently be used as the basis for defining the modeling domain for a more refined Eulerian modeling study using the U.S. EPA Community Multiscale Air Quality model (CMAQ). The results of the CMAQ modeling will yield the information required to define the outer boundary of a Sulfur Emission Control Area (SECA) for various U.S. coastlines. Because of differences in meteorology and other factors governing the transport and transformation of ship emissions among the various coastlines, each coastline is modeled separately in the screening study described here.

A review of available models and data was conducted prior to defining our modeling approach (Seigneur et al., 2005a; see Appendix A). The modeling approach was then formally documented in an analysis plan that was reviewed by EPA (Seigneur et al., 2005b; see Appendix B).

This report is organized as follows. Section 2 describes the modeling approach, including brief descriptions of the air quality model (CALPUFF) used for the screening study, and the meteorological preprocessor for CALPUFF, referred to as CALMET. CALPUFF is recommended by EPA for regulatory applications to assess the long-range transport of pollutants. While CALPUFF has some limitations, as discussed in Section 2, it is suitable for a screening study since it will tend to overestimate the oxidation of SO₂ to sulfate in the gas phase (Karamchandani et al., 2006) and may thus provide a conservative bound for the distance of interest for defining the SECA (because of the simplistic treatment of aqueous-phase chemistry in CALPUFF, one cannot assess whether sulfate concentrations would be overestimated if fog processes dominate sulfate formation). Section 3 describes the development of meteorological, emissions and geophysical data inputs for the CALPUFF simulations. Section 4 presents the results for

the various U.S. coastlines that were simulated, and Section 5 provides a summary of the study and presents some conclusions.

2. MODELING APPROACH

2.1 Air Quality Model (CALPUFF)

We used the EPA-recommended long-range transport model, CALPUFF, for this screening study. CALPUFF is a multi-layer, multi-species non-steady-state puff dispersion model that can simulate the effects of time- and space-varying meteorological conditions on pollutant transport, transformation, and removal. It can accommodate arbitrarily varying point source, area source, volume source, and line source emissions. It is intended for use on scales from tens of meters to hundreds of kilometers from a source.

Detailed descriptions of the formulation and features of CALPUFF are provided in the CALPUFF documentation (Scire et al., 2000a). Here, we briefly summarize some of the features of CALPUFF that are relevant to our study and discuss the limitations of CALPUFF in its treatment of atmospheric chemistry. CALPUFF includes algorithms for near-source effects such as building downwash, transitional plume rise, partial plume penetration, sub-grid scale terrain interactions as well as longer range effects such as pollutant removal due to wet and dry deposition, simplified chemical transformations, vertical wind shear, over-water transport and coastal interaction effects. Because the latter features were relevant to simulating the transport and chemistry of SO_x emissions from ships, they were activated for our study.

CALPUFF offers several options to simulate the formation of secondary sulfate and nitrate particles from the oxidation of the emitted primary gaseous pollutants, SO₂ and NO_x respectively. Since the oxidation of SO₂ to sulfate was of interest for this study, we selected the more advanced chemistry module available in CALPUFF, which is based on the RIVAD/ARM3 chemical mechanism (Morris et al., 1988). This option treats the NO and NO₂ conversion processes in addition to the NO₂ to inorganic nitrate and SO₂ to sulfate conversions. The scheme assumes low background VOC concentrations and is not suitable for urban regions. The NO-NO₂-O₃ chemical system is first solved to get pseudo-steady-state concentrations of NO, NO₂, and O₃. During the day, this system consists of the NO₂ photolysis reaction to yield NO and O₃ and the NO-O₃ titration reaction to yield NO₂. During the night, only the NO-O₃ titration reaction is considered.

In the implementation of the RIVAD/ARM3 scheme in CALPUFF, the background O₃ concentration is used as the initial O₃ concentration at each puff chemistry time step (i.e., the plume O₃ concentration does not evolve as a function of the downwind distance but instead it is replenished at each time step). This may lead to errors if the sources that are being simulated are large NO_x emitters. For such sources, the high NO concentrations in the plume deplete the O₃ concentrations near the source and, as a result, OH concentrations are very low and the gas-phase rates of NO₂ and SO₂ oxidation to HNO₃ and H₂SO₄, respectively, are negligible (Karamchandani et al., 1998; Karamchandani and Seigneur, 1999). In CALPUFF, the lack of depletion of O₃ in the plume leads to an overestimate of the steady-state daytime concentration of the hydroxyl radical, OH, which is calculated from the final O₃ concentration after the solution of the NO-NO₂-O₃ system and is, therefore, also overestimated in the near field. Because the OH concentrations are overestimated, CALPUFF overestimates the rates of formation of HNO₃ and H₂SO₄ in the near field.

CALPUFF uses dry deposition velocities to calculate the dry deposition of gaseous and particulate pollutants to the surface. These dry deposition velocities can either be user-specified or calculated internally in CALPUFF using a resistance-based model. For this study, we selected the latter option to calculate dry deposition velocities. For gaseous pollutants, the resistances that are considered are the atmospheric resistance, the deposition layer resistance, and the canopy resistance. For particles, a gravitational settling term is included and the canopy resistance is assumed to be negligible. The various resistances and particle settling rates are calculated as functions of atmospheric variables (e.g., stability and wind speed), surface characteristics (e.g., surface roughness, vegetation type, physiological state), and the properties of the depositing material (gas diffusivity, solubility, and reactivity; particle size, shape, and density).

CALPUFF uses the scavenging coefficient approach to parameterize wet deposition of gases and particles. The scavenging coefficient depends on pollutant characteristics (e.g., solubility and reactivity), as well as the precipitation rate and type of precipitation. The model provides default values for the scavenging coefficient for various species and two types of precipitation (liquid and frozen).

2.2 Meteorological Model (CALMET)

The recommended meteorological inputs for applying CALPUFF are the time-dependent outputs of CALMET, a meteorological model that contains a diagnostic wind field module and overwater and overland boundary layer modules (Scire et al., 2000b). The outputs of CALMET are hourly gridded fields of micro-meteorological parameters and three-dimensional wind and temperature fields. The wind field module in CALMET combines an objective analysis procedure using wind observations with parameterized treatments of slope flows, valley flows, terrain kinematic effects, terrain blocking effects, and sea/lake breeze circulations. The boundary layer modules of CALMET produce gridded fields of micrometeorological parameters, such as friction velocity, convective velocity scale, and Monin-Obukhov lengths, as well as mixing heights and PGT stability classes.

Inputs to CALMET include surface and upper air meteorological data. Optionally, CALMET can also use the outputs of prognostic meteorological models, such as MM5 and CSUMM, to supplement observations and create the meteorological fields required by CALPUFF. A processor (CALMM5) is available to convert MM5 data to the format required for CALMET. For this study, we used the U.S. EPA's MM5 simulation outputs for 2002. The MM5 domain contains the entire contiguous United States and portions of Canada and Mexico and extends out to the Pacific Ocean in the west, the Gulf of Mexico to the south and the Atlantic Ocean in the east. Thus, MM5 results for all the coastlines relevant to our study were available from the EPA. Section 3 provides additional details on the preparation of the meteorological data inputs for CALPUFF for this study.

2.3 Approach

For each coastline, a number of annual CALPUFF simulations were conducted. We used 2002 as our reference year because it corresponds to the most recent year for which an MM5 simulation covering all coastlines was available. The first simulation for each coastline was to establish the target values of annual-average SO₂ and sulfate concentrations at an array of inland receptors (the placement of the receptors is described in Section 2.3.1 below). These target values correspond to emissions from ships at

dockside, i.e., those ships that are within the SECA and, therefore, will likely have to burn low sulfur fuel (15,000 ppm fuel content). Then, we conducted annual CALPUFF simulations for ships located at various distances from the coastline. For these simulations, the ship emissions used were those based on ships burning high sulfur fuel (i.e., 27,000 ppm fuel content). The comparisons of annual-average concentrations of SO₂ and sulfate from these simulations with the target values determined previously provide a basis for defining the SECA modeling domain for the CMAQ simulations to be conducted by EPA.

In the following sections, we provide additional details on the placement of receptors and sources for the simulations as well as the modeling domain for each coastline.

2.3.1 Receptors

Ground-level receptors were located on land along the coastline and at various distances from the coastline. The first line of receptors was located along the coastline, with a distance of 10 km between adjacent receptors. This distance provides a finer spatial resolution than that of the ship emissions (see Section 3). Nine additional lines of receptors were then located inland parallel to the coastline receptors. The distances between adjacent lines of receptors were variable, with higher resolutions near the coastline and coarser resolutions further inland. The first line of inland receptors was located at 10 km from the coastline receptors, while the last line of receptors was located at 240 km (about 150 miles) from the coastline. Depending on the coastline being simulated, the total number of receptors varied from about 1100 to 2800.

2.3.2 Sources

Ship emissions were represented by a set of stationary point sources. Each point source represents one ship. The use of stationary sources to represent moving ships is an appropriate approximation for this screening modeling study, because using stationary sources will overestimate the downwind air quality impacts (emissions will be

concentrated in specific locations rather than continuously distributed along the shipping lane, thereby leading to greater ambient air concentrations).

For each simulation, the sources were located at a selected distance from shore (along the coastline for the target value simulations, and at 125 km, 250 km, 375 km, and 500 km from the coastline for the SECA boundary simulations). The spacing between adjacent ships for a given simulation was determined from ship traffic and estimated shipping lane density (see Section 3). We maintained the same number of ships for the at-sea emissions scenarios as the number of ships for the dockside emissions scenario. This number varied from about 40 to 100 depending on the coastline being simulated.

2.3.3 Modeling domains

The following U.S. coastlines were simulated in this screening study:

- Southern Pacific Ocean coastline
- Northern Pacific Ocean coastline
- Gulf of Mexico coastline
- Atlantic Ocean coastline

All modeling domains were selected to allow an off-shore distance of at least 500 km from the coastline to include all ship-at-sea scenarios (see above) and an inland distance of at least 240 km from the coastline to provide sufficient spatial coverage for calculating air quality impacts.

The modeling domain for the Southern Pacific U.S. coastline extends from about 30 degrees North to 38 degrees North and includes Southern California, the Central California coastline, and the southern portion of Northern California. Figure 2-1 shows this domain as well as the locations of coastline ships for the target value simulation and the locations of the receptors at the coastline and inland where SO₂ and sulfate concentrations were calculated.

Figure 2-2 shows the domain for the Northern Pacific U.S. coastline, which extends from about 35 degrees North to about 52 degrees North and includes Northern California,

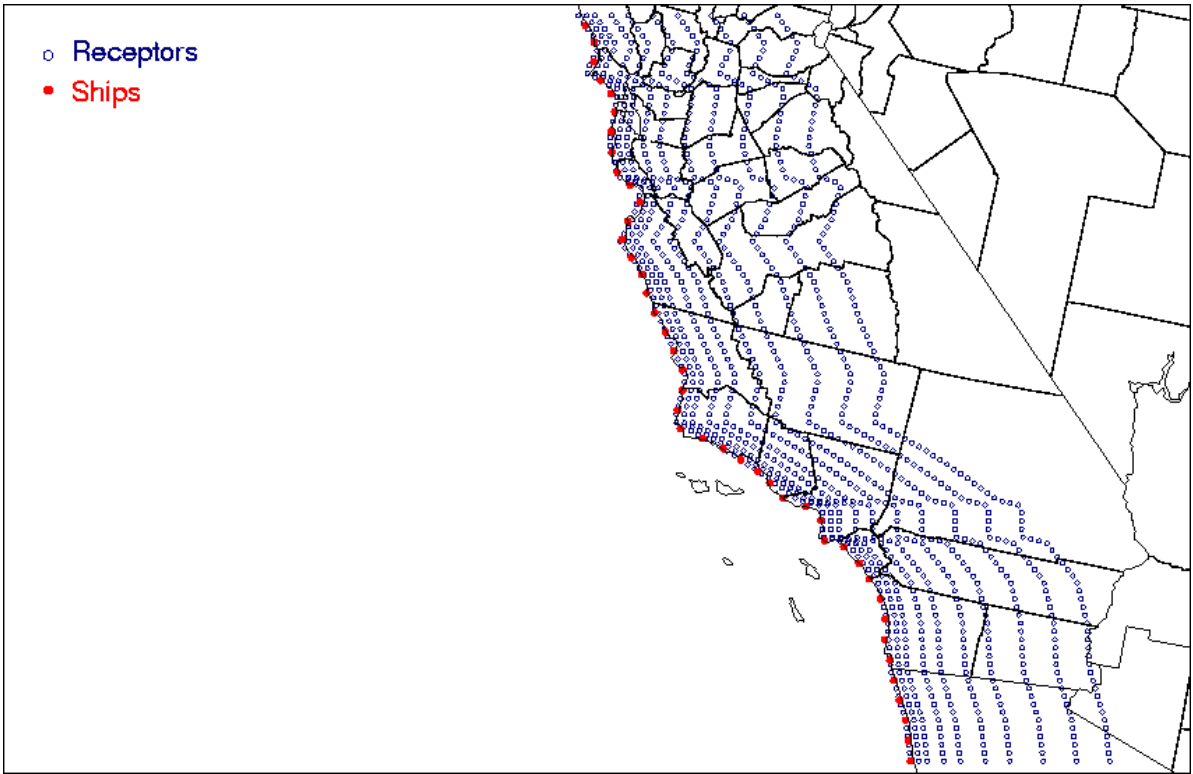


Figure 2-1. Modeling domain for the Southern Pacific Ocean U.S. coastline.

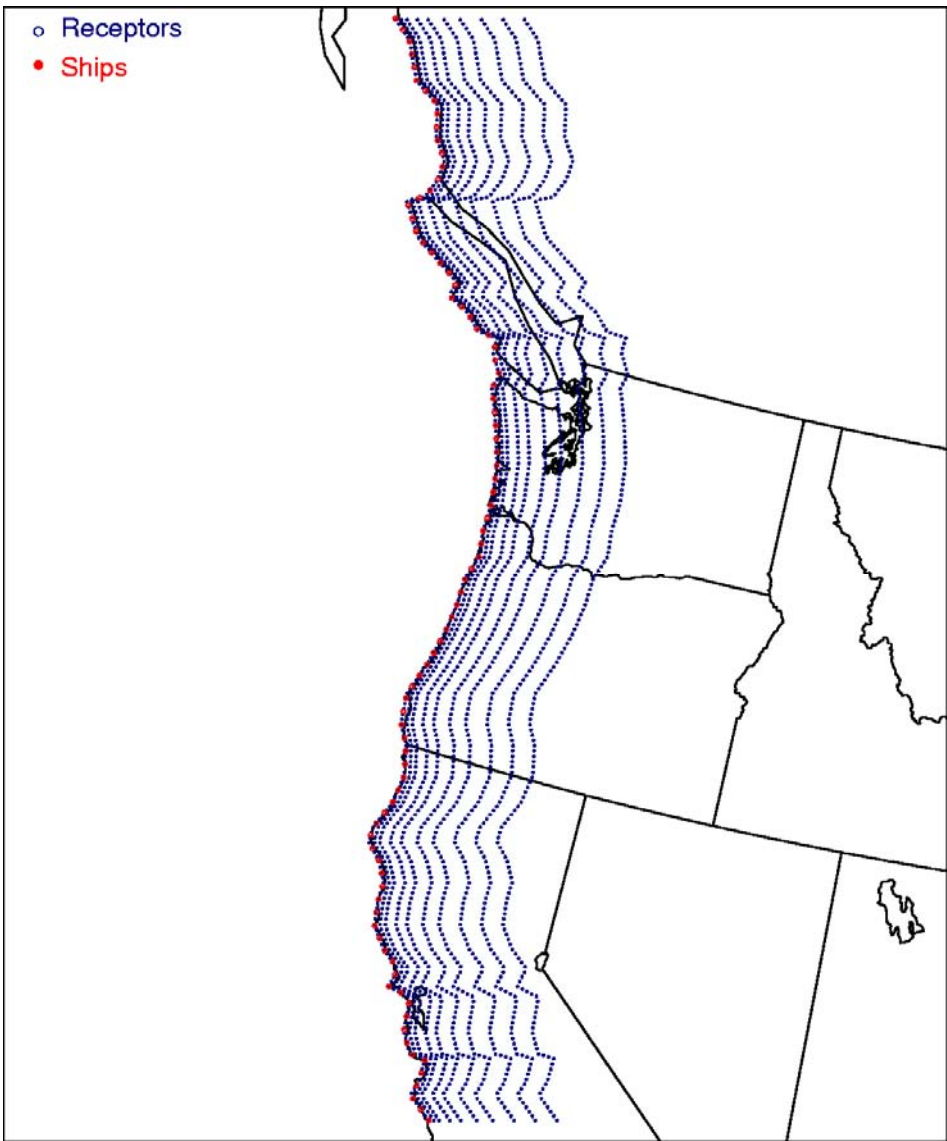


Figure 2-2. Modeling domain for the Northern Pacific Ocean U.S. coastline.

Oregon, and Washington in the U.S., and the southern half of the British Columbia coastline in Canada.

In the east-west direction, the modeling domains for both the Southern Pacific and Northern Pacific coastlines begin at the western boundary of the modeling domain for the MM5 simulations that provided the hourly 3-D meteorological inputs for our study (see Section 3). The eastern boundaries of the modeling domains for the Southern and Northern Pacific coastline extend to about 115 degrees West and 112 degrees West, respectively.

The modeling domain for the Gulf of Mexico coastline is shown in Figure 2-3. The east-west extent of the modeling domain is from Western Texas (about 105 degrees West) in the west to Florida and the Atlantic Ocean (about 75 degrees West). The southern boundary of the modeling domain coincides with the southern boundary of the MM5 domain while the northern boundary is at about 34 degrees North.

The southern boundary of the Atlantic Ocean modeling domain, shown in Figure 2-4, also coincides with the southern boundary of the MM5 domain. The northern boundary is at about 52 degrees North, just a few degrees lower than the northern boundary of the MM5 domain. The western boundary of the Atlantic Ocean domain is at about 85 degrees West, while the eastern boundary coincides with the eastern boundary of the MM5 domain.

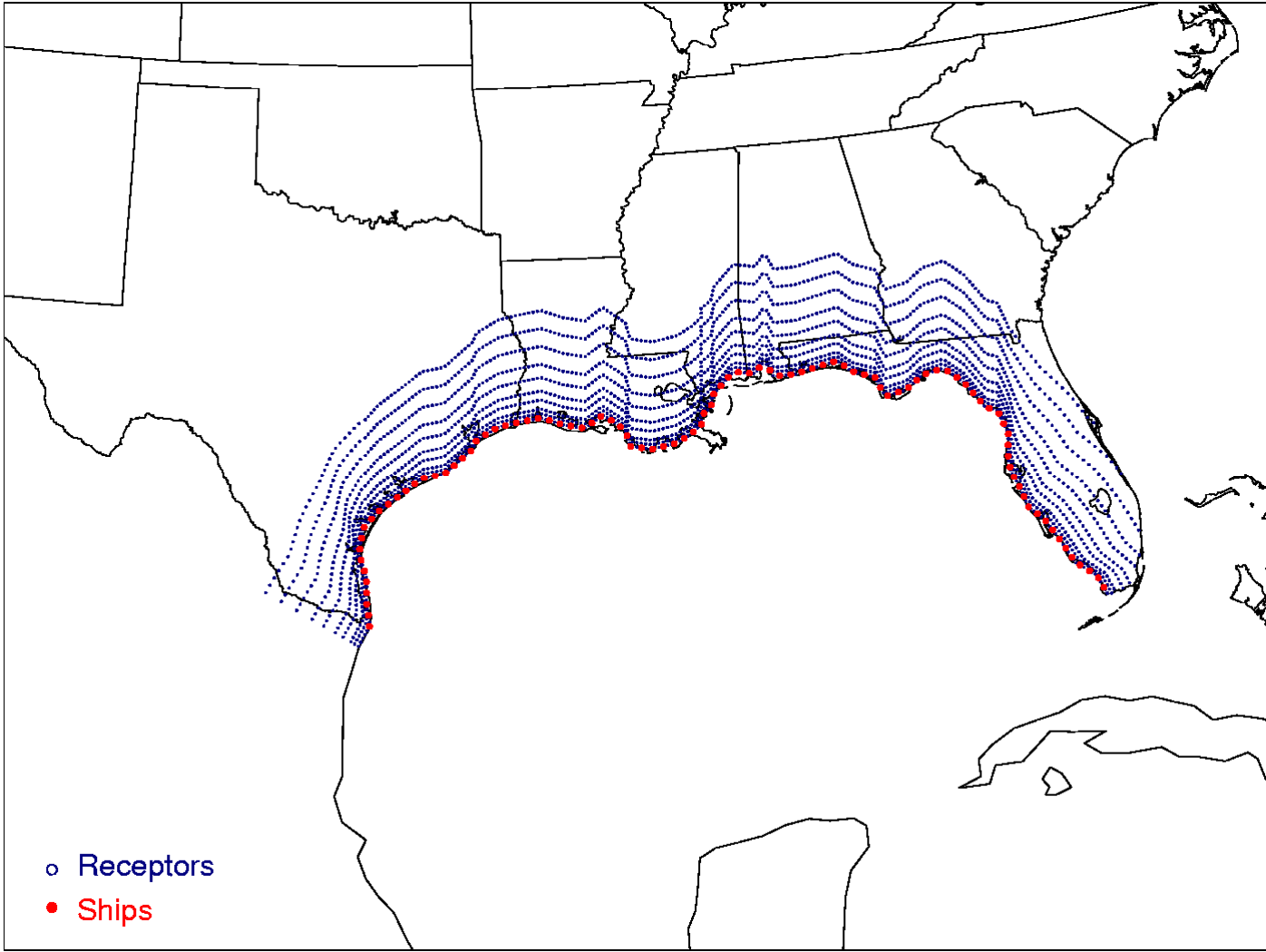


Figure 2-3. Modeling domain for the Gulf of Mexico coastline.

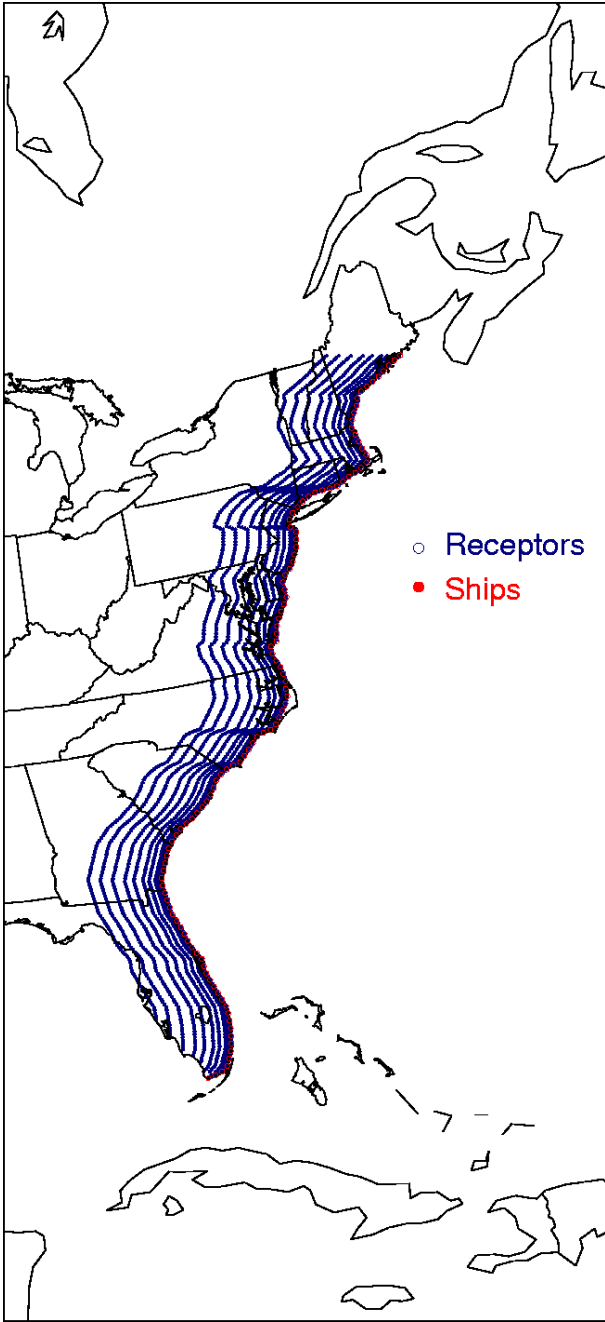


Figure 2-4. Modeling domain for the Atlantic Ocean coastline.

3. MODEL INPUTS

The following inputs were required for the CALPUFF simulations

- Meteorology
- Emissions
- Land use and terrain elevation data
- Coastline data

Terrain elevation data at 1 degree DEM (Digital Elevation Model) resolution were downloaded from the U.S. Geological Survey (USGS). Land use data were also obtained from the USGS at a 1:250,000 scale. These data were processed by the CALPUFF/CALMET preprocessors: TERREL, CTGCOMP, CTGPROC, and MAKEGEO.

Coastline data were obtained using the ZXPLLOT package from the Center for the Analysis and Prediction of Storms at the University of Oklahoma.

The preparation of meteorological and emission inputs for the CALPUFF simulations is described below.

3.1 Meteorology

As described in Section 2.2, CALMET is the companion meteorological model that is used to prepare the meteorological fields used by CALPUFF. CALMET is a diagnostic meteorological model that can use standard surface and upper air meteorological data, and also has an over-water option that allows the use of special over-water measurements for grid cells that are over the ocean. In addition, CALMET can use 3-D gridded meteorological fields from prognostic models, such as MM5, to either supplement observations or to provide an initial guess field for the diagnostic procedure.

For this study, we used a combination of land-based surface measurements, over-water measurements, and MM5 outputs to create the CALPUFF meteorological fields. The MM5 fields provide the vertical structure with sufficient temporal (hourly) and

spatial (36 km) resolution to supplement the surface measurements. This approach provides consistency with the subsequent grid-based modeling that will be conducted by OAQPS to define SECAs using CMAQ, because CMAQ will be driven with the MM5 meteorology. It also addresses a weakness in the official release of CALMET (Scire et al., 2005) in its calculation of mixing heights over-water surfaces. The mixing height algorithm in CALMET underestimates over-water mixing heights, especially during light wind conditions over warm water, since it only calculates mechanically-derived mixing over water surfaces. This weakness has been corrected in a new version of CALMET described by Scire et al. (2005). However, this new version was not available to us at the time we performed the CALMET simulations for this study. Based on our discussions with the CALMET developers (Scire, 2005), we used the MM5 mixing heights directly in CALMET.

3.1.1 Measurements

The National Climatic Data Center (NCDC) Integrated Surface Hourly Observations database provided the land-based hourly surface measurements. These include wind speed, wind direction, temperature, and dew point temperature. Over-water measurements were available for all the coastlines from the National Data Buoy Center (NDBC) (<http://www.ndbc.noaa.gov>). These measurements are taken from buoys. The buoys are at varying distances from the coast. Those near the coast are frequently near harbors or bays. Most of the buoys are owned and operated by NDBC but there are also several other agencies that submit their data to the NDBC database. The over-water measurement coverage is sparse, as shown in Figures 3-1 through 3-4, which show the locations of the land-based surface and over-water measurements for each of the coastlines that were simulated in this study. We used 2002 observations for consistency with the MM5 outputs (see below).

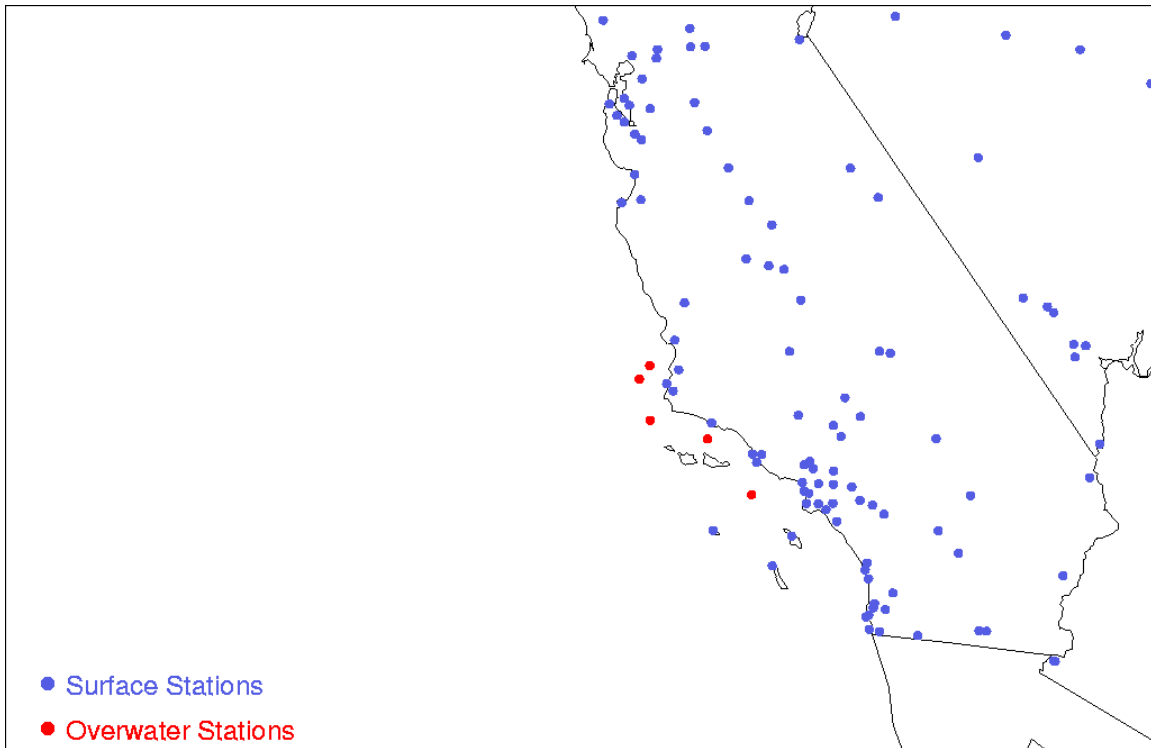


Figure 3-1. Land-based surface stations and over-water stations for the Southern Pacific Ocean U.S. coastline.

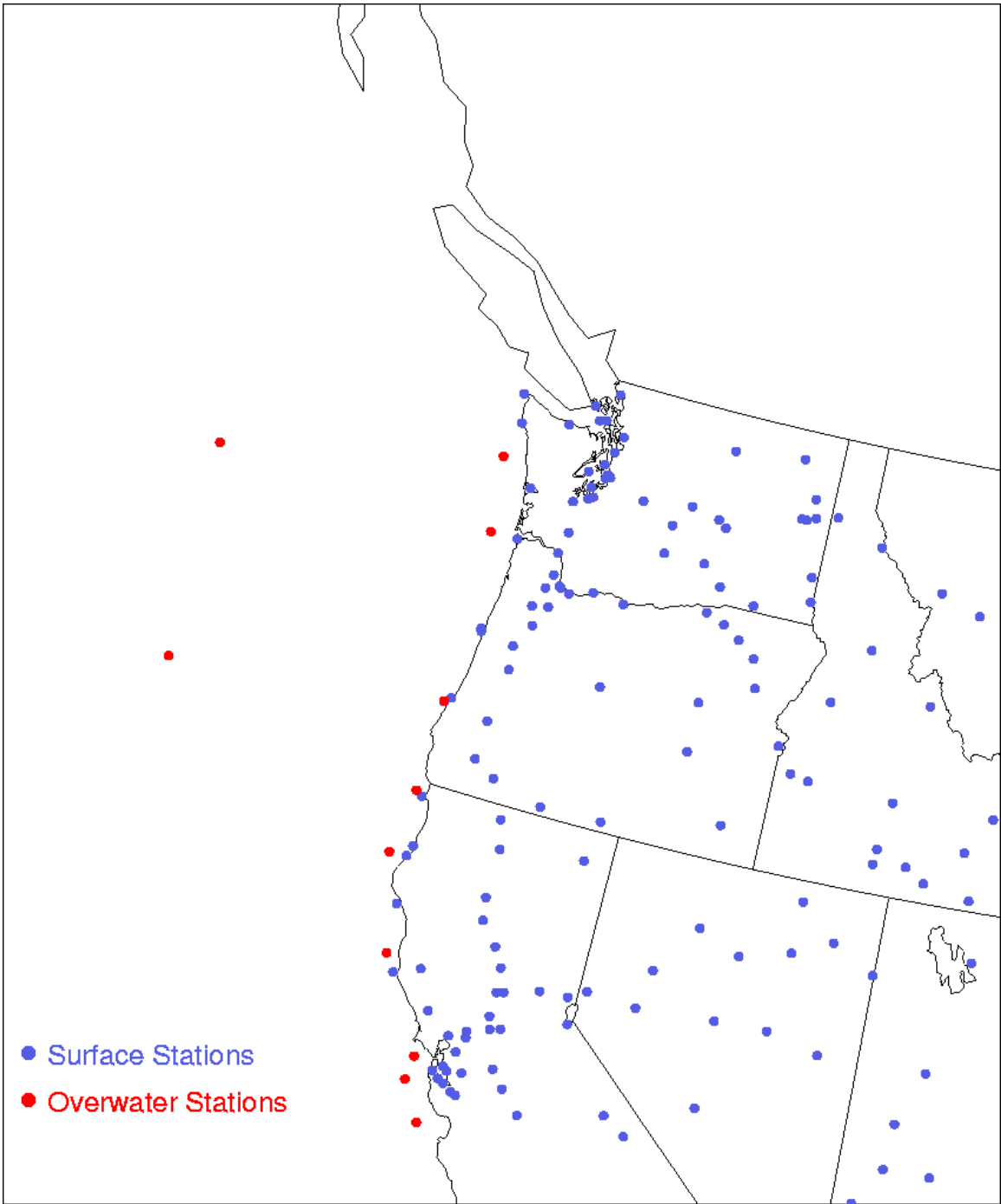


Figure 3-2. Land-based surface stations and over-water stations for the Northern Pacific Ocean U.S. coastline.

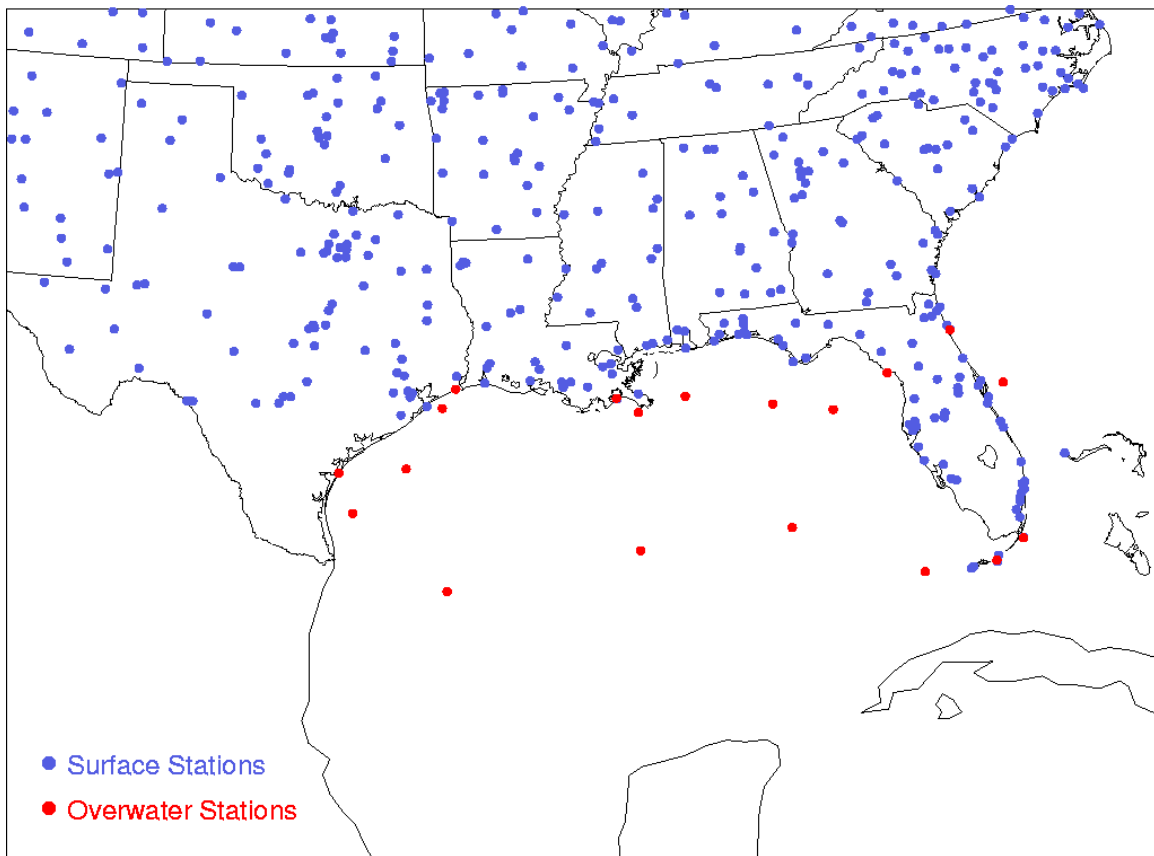


Figure 3-3. Land-based surface stations and over-water stations for the Gulf of Mexico coastline.

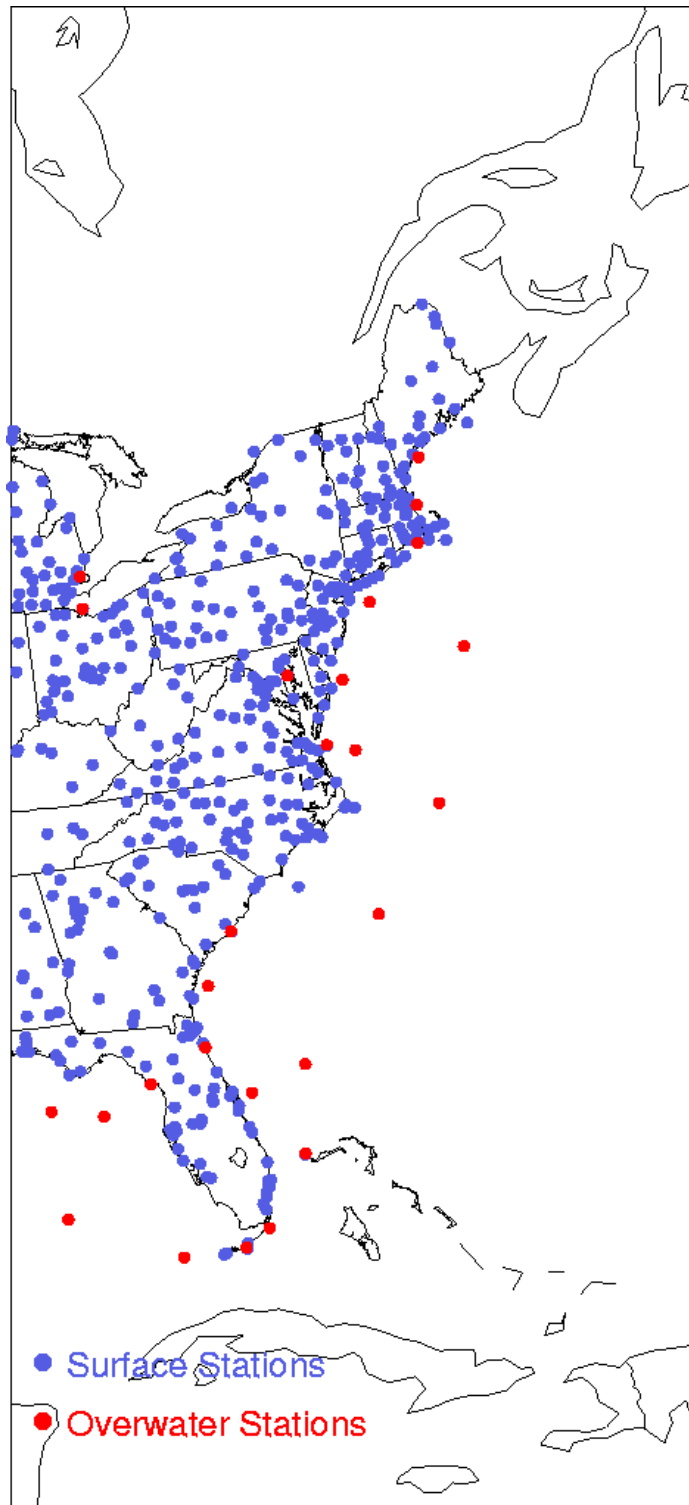


Figure 3-4. Land-based surface stations and over-water stations for the Atlantic Ocean coastline.

3.1.2 MM5 outputs

We used the outputs of the 2002 MM5 simulations sponsored by the U.S. EPA to supplement the meteorological measurements. These outputs were provided to us by ENVIRON Corporation. The MM5 modeling domain, shown in Figure 3-5, covers the entire contiguous United States and extends significantly over the oceans. The horizontal spatial resolution for the MM5 outputs is 36 km.

An interface program (CALMM5) converts the MM5 data into a form compatible with CALMET. A beta version (not yet officially approved by the EPA) of CALMM5 processes MM5 Version 3 output data directly. This processor is available from the CALPUFF-CALMET Download BETA-Test page.

3.1.3 CALMET Winds

As mentioned above, the wind fields were calculated with CALMET using the outputs of MM5 in combination with available data. To illustrate the variability of wind speed and direction with location and season, we present wind roses over the ocean based on the calculated CALMET wind fields for the southern Pacific coastline, northern Pacific coastline, Gulf of Mexico coastline and Atlantic coastline in Figures 3-6, 3-7, 3-8 and 3-9, respectively.

In the southern Pacific Ocean, winds are mostly from the southwest except during winter in the northern part of the domain where the wind direction is more variable. In the northern Pacific, the prevailing winds are from the west in the southern part of the domain (i.e., off the coast of California and Oregon) during spring, summer and fall. Wind direction is variable during winter in the southern part of the domain and for all seasons in the northern part of the domain.

In the Gulf of Mexico, the wind direction varies with season and location. During winter, in the western part of the domain, the prevailing winds are from the southwest and the northeast; they are mostly from the west and north in the central part of the domain and with more variable direction near the Florida coast. During spring and

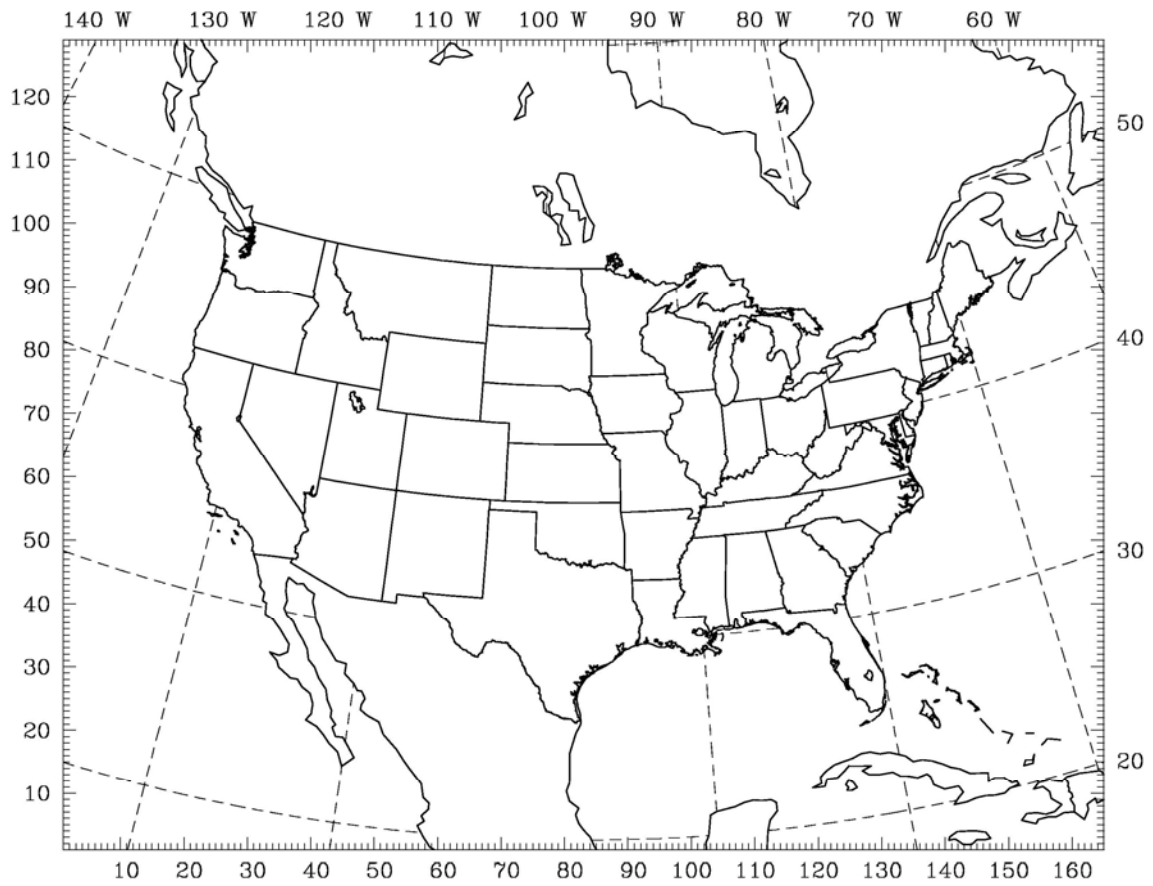


Figure 3-5. MM5 modeling domain.

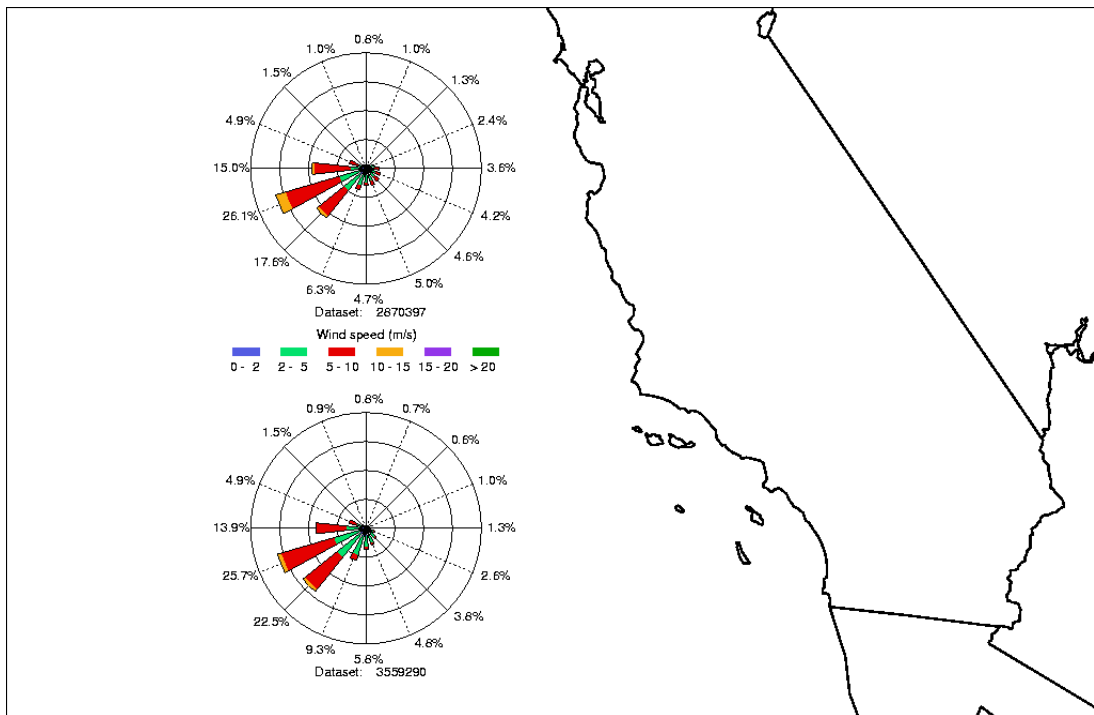
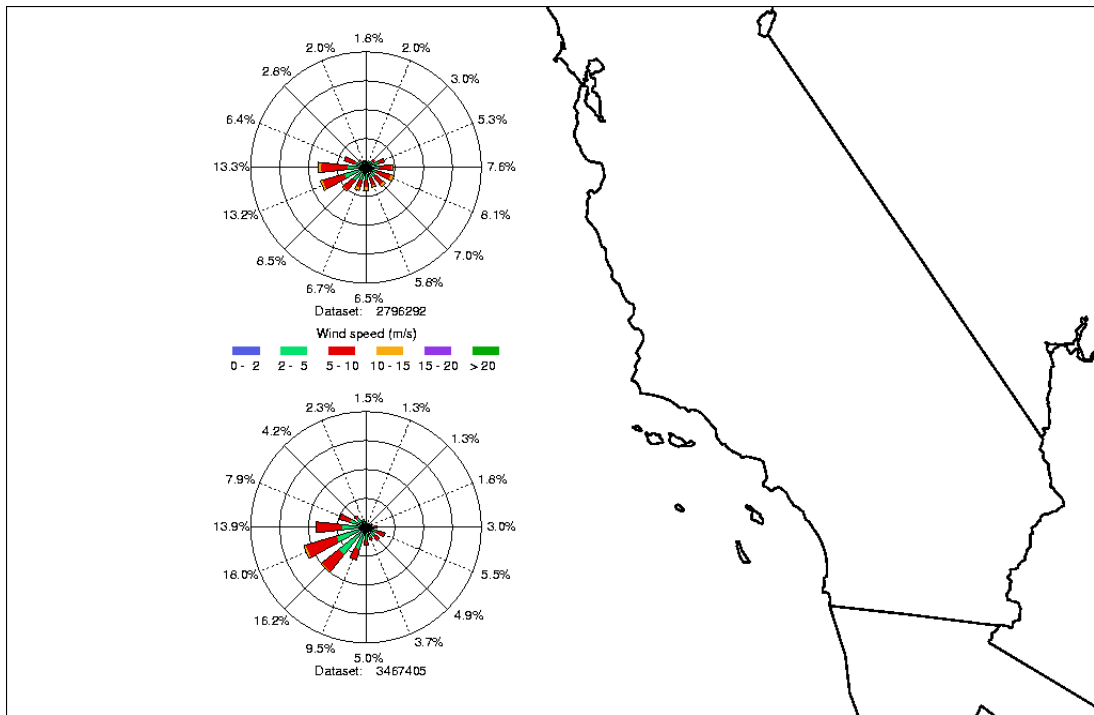


Figure 3-6a. Wind roses based on CALMET outputs for the southern Pacific Ocean during winter 2002 (top) and spring 2002 (bottom).

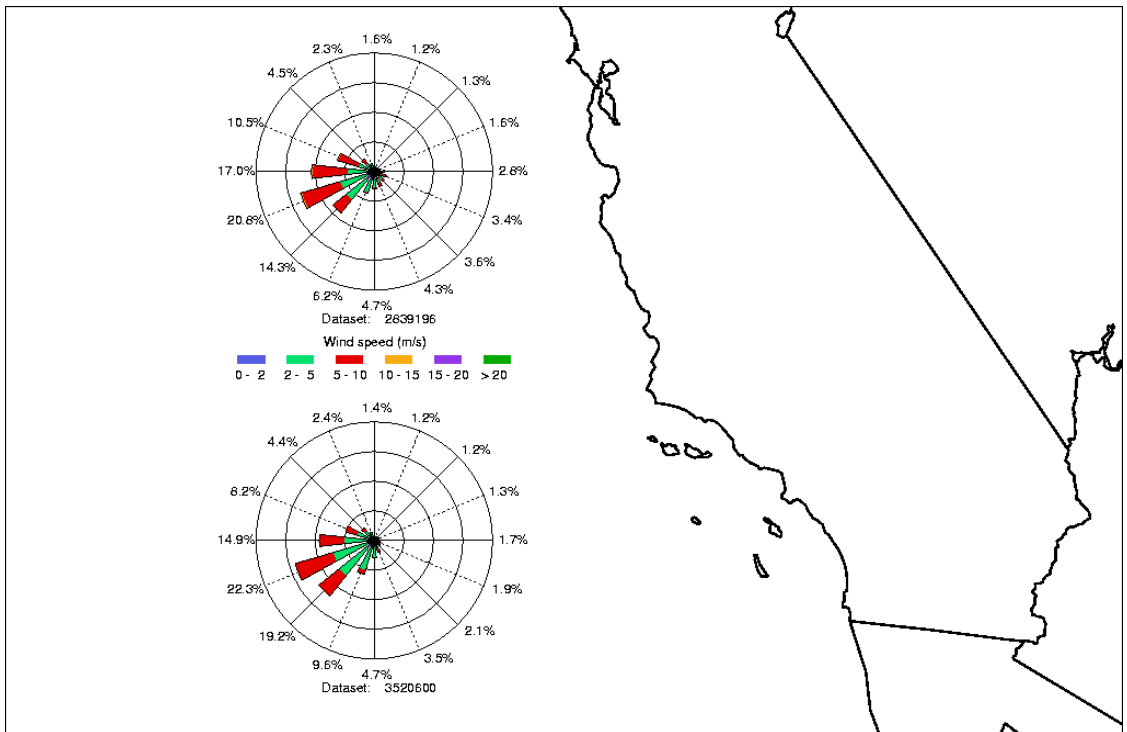
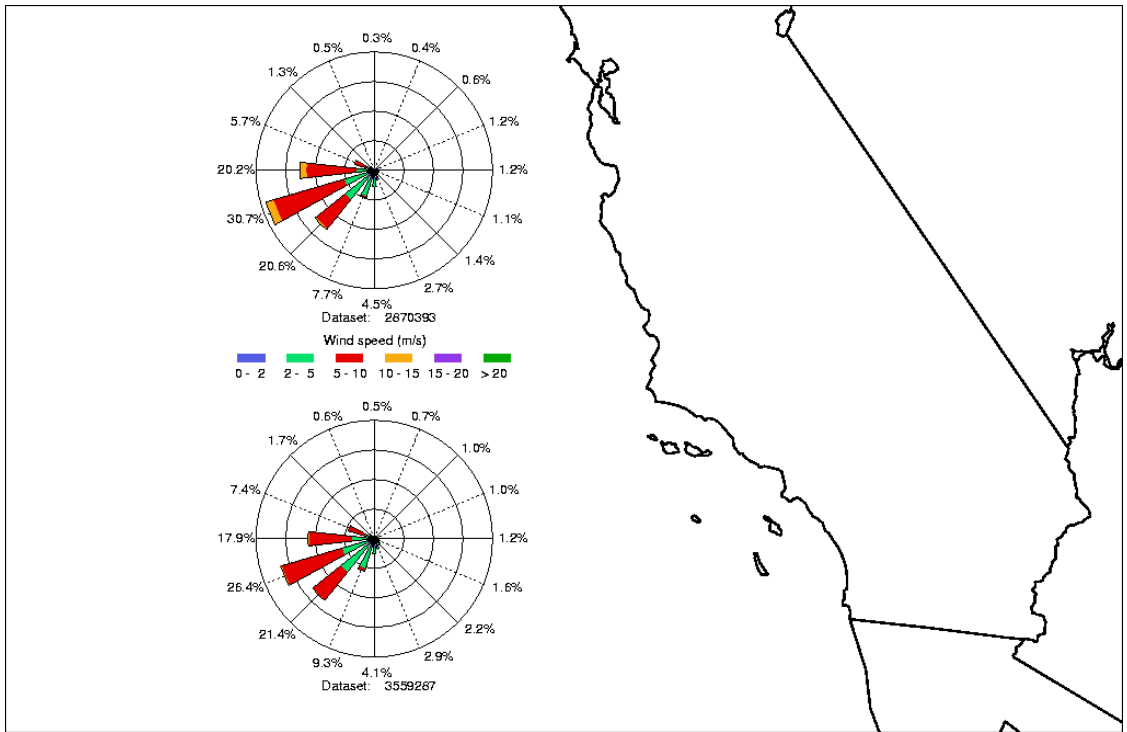


Figure 3-6b. Wind roses based on CALMET outputs for the southern Pacific Ocean during summer 2002 (top) and fall 2002 (bottom).

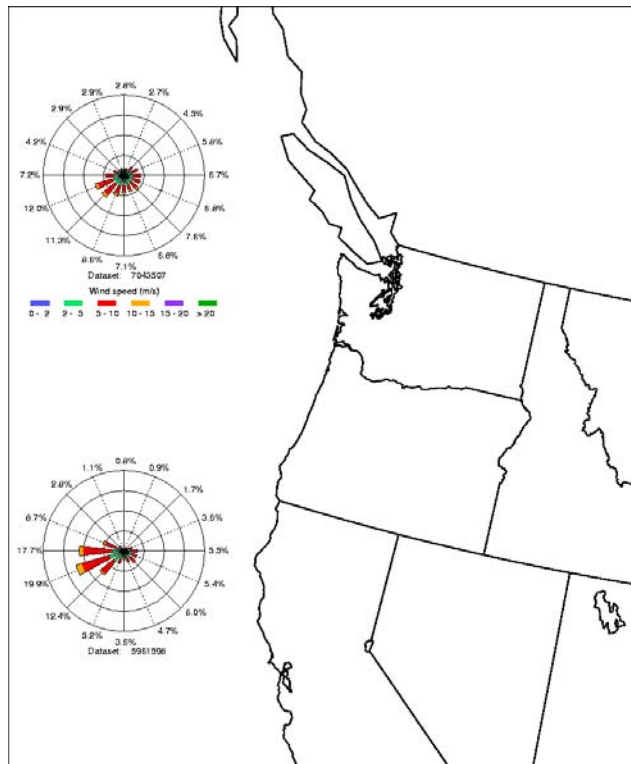
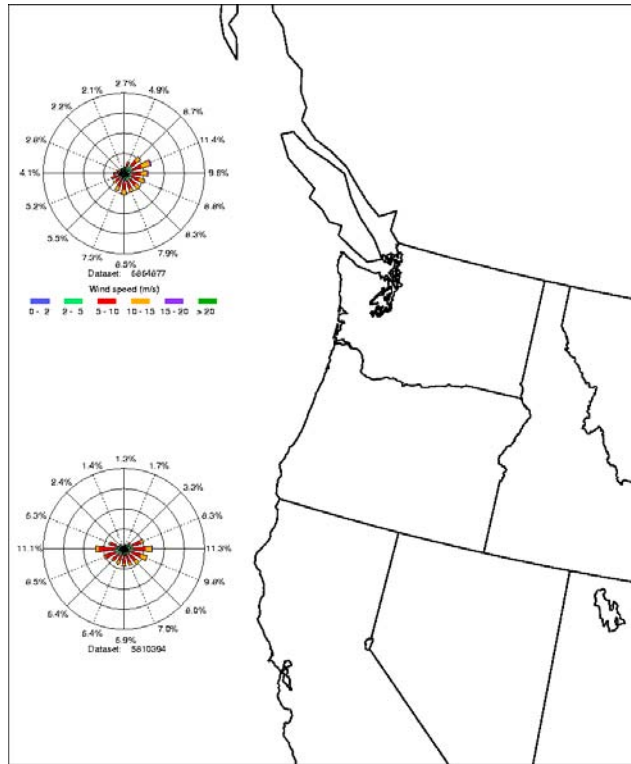


Figure 3-7a. Wind roses based on CALMET outputs for the northern Pacific Ocean during winter 2002 (top) and spring 2002 (bottom).

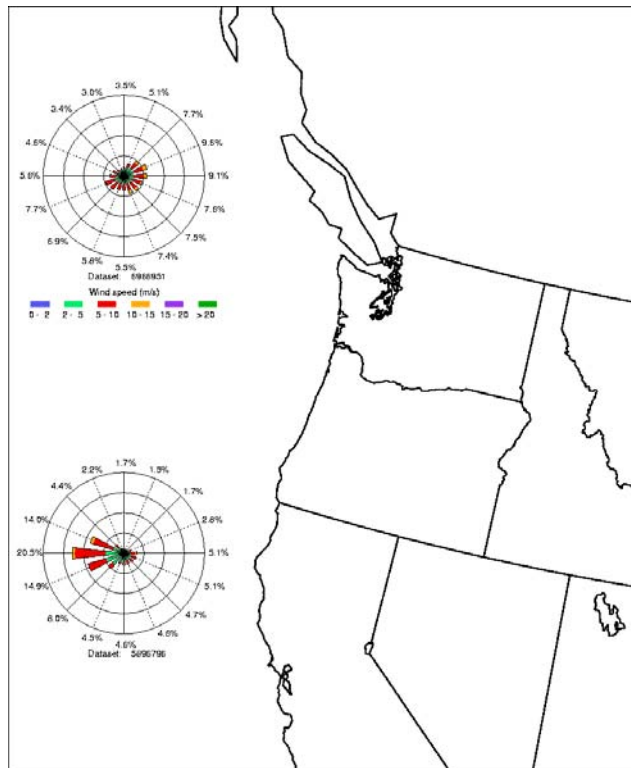
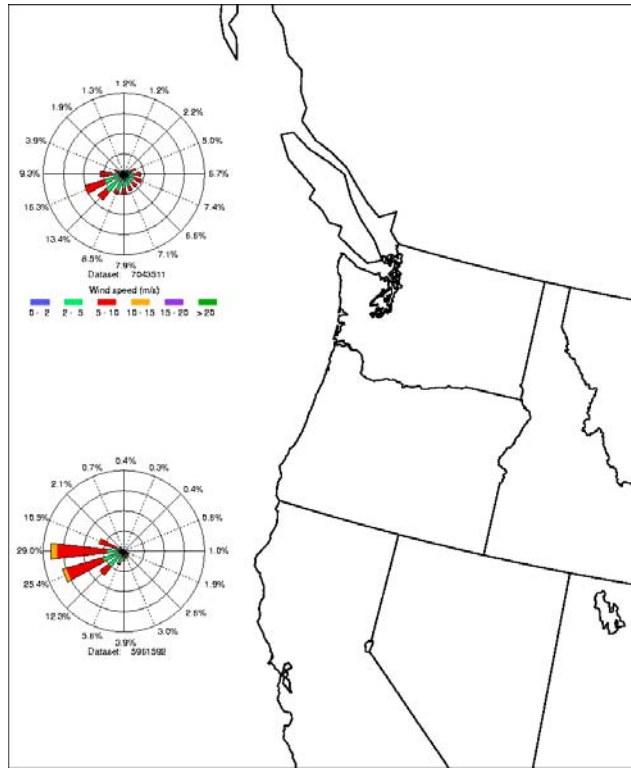


Figure 3-7b. Wind roses based on CALMET outputs for the northern Pacific Ocean during summer 2002 (top) and fall 2002 (bottom).

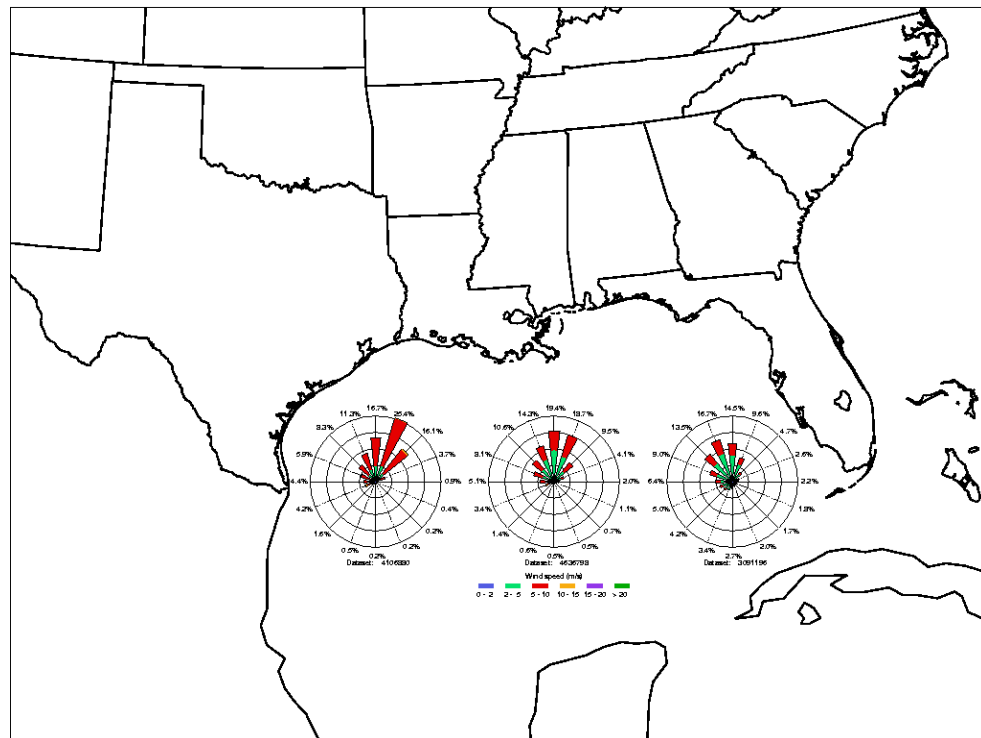
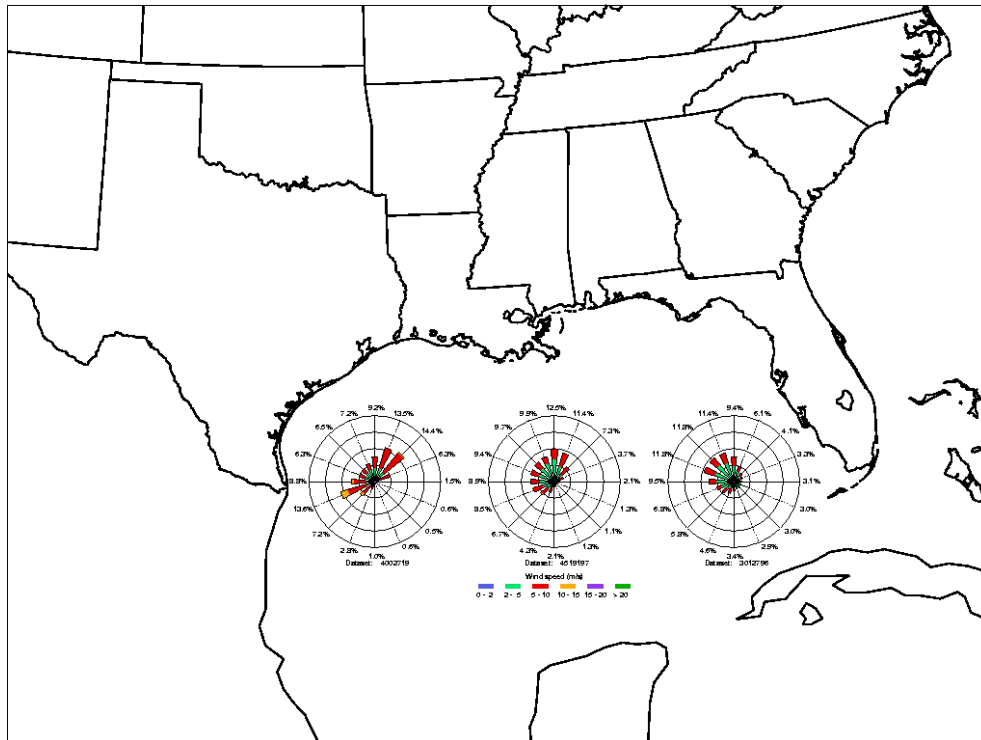


Figure 3-8a. Wind roses based on CALMET outputs for the Gulf of Mexico during winter 2002 (top) and spring 2002 (bottom).

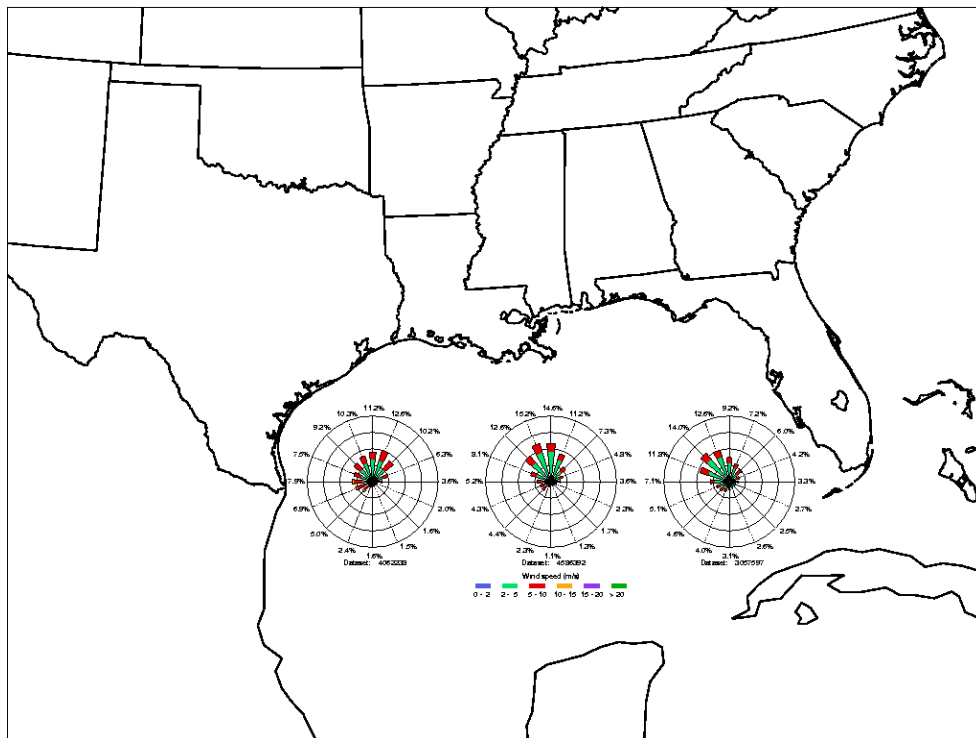
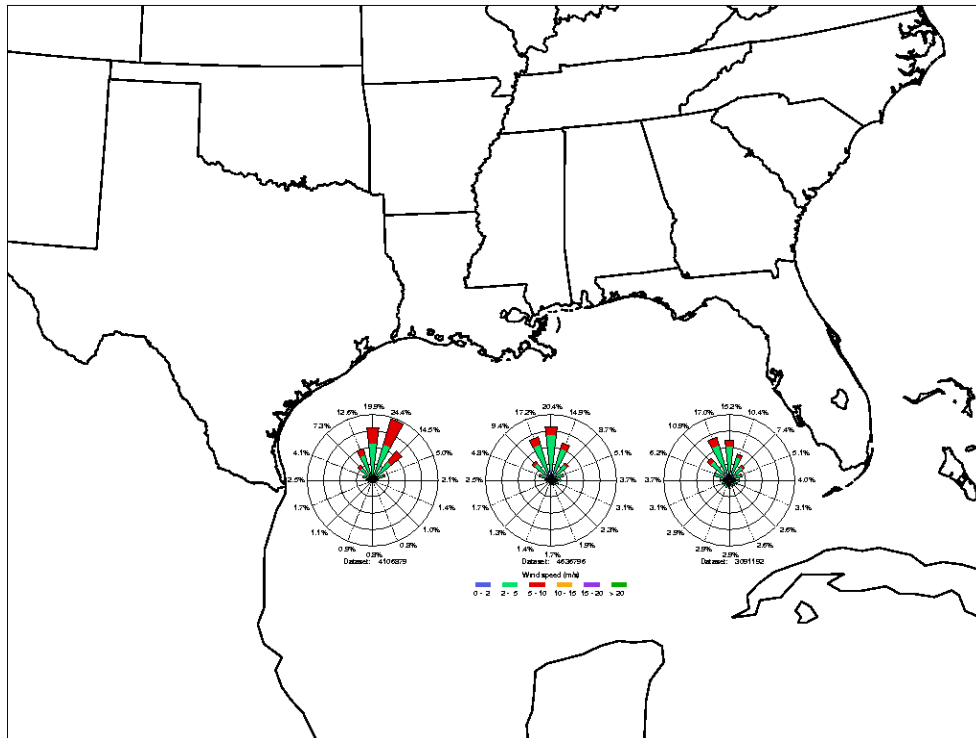


Figure 3-8b. Wind roses based on CALMET outputs for the Gulf of Mexico during summer 2002 (top) and fall 2002 (bottom).

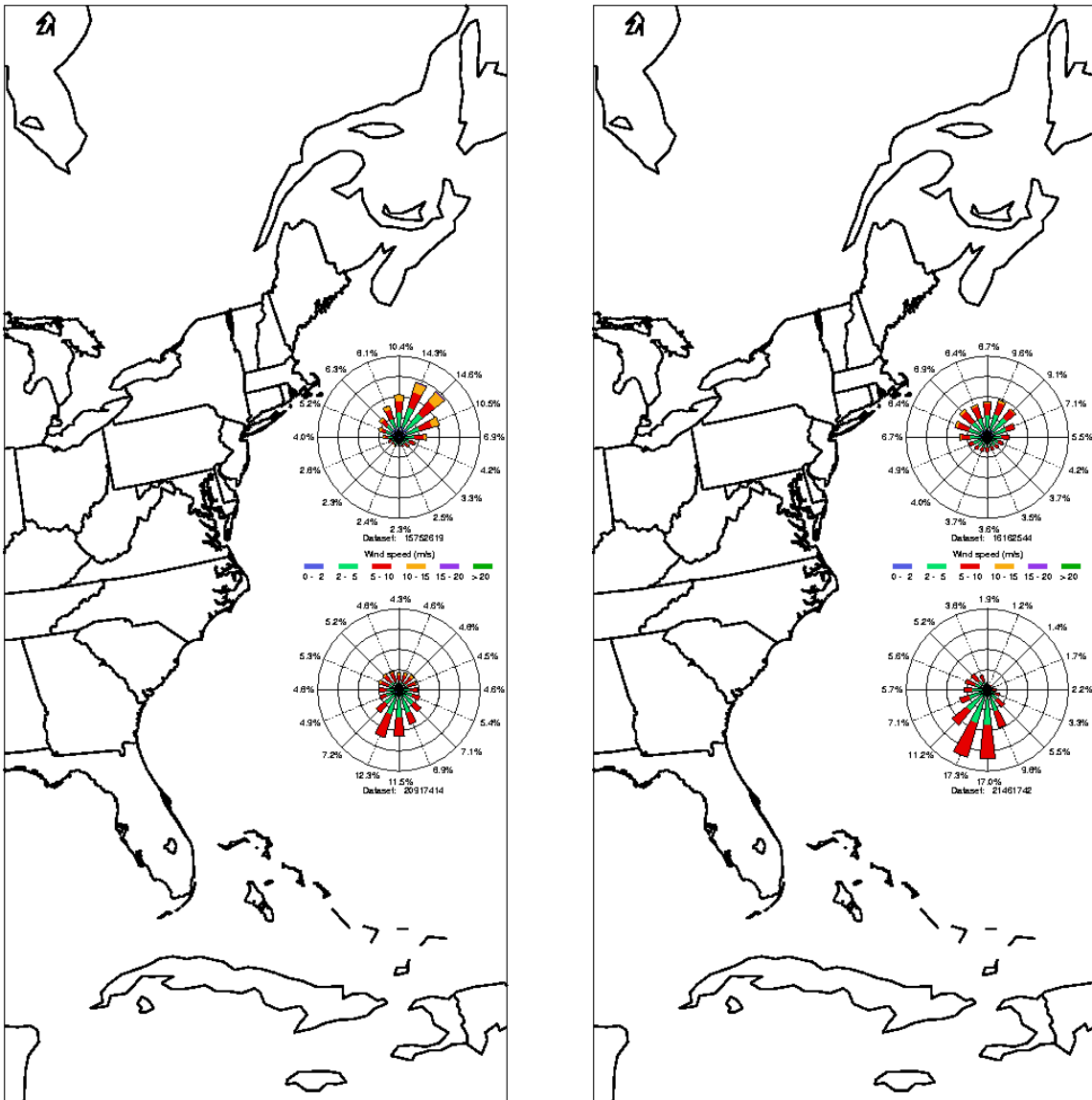


Figure 3-9a. Wind roses based on CALMET outputs for the Atlantic Ocean during winter 2002 (left) and spring 2002 (right).

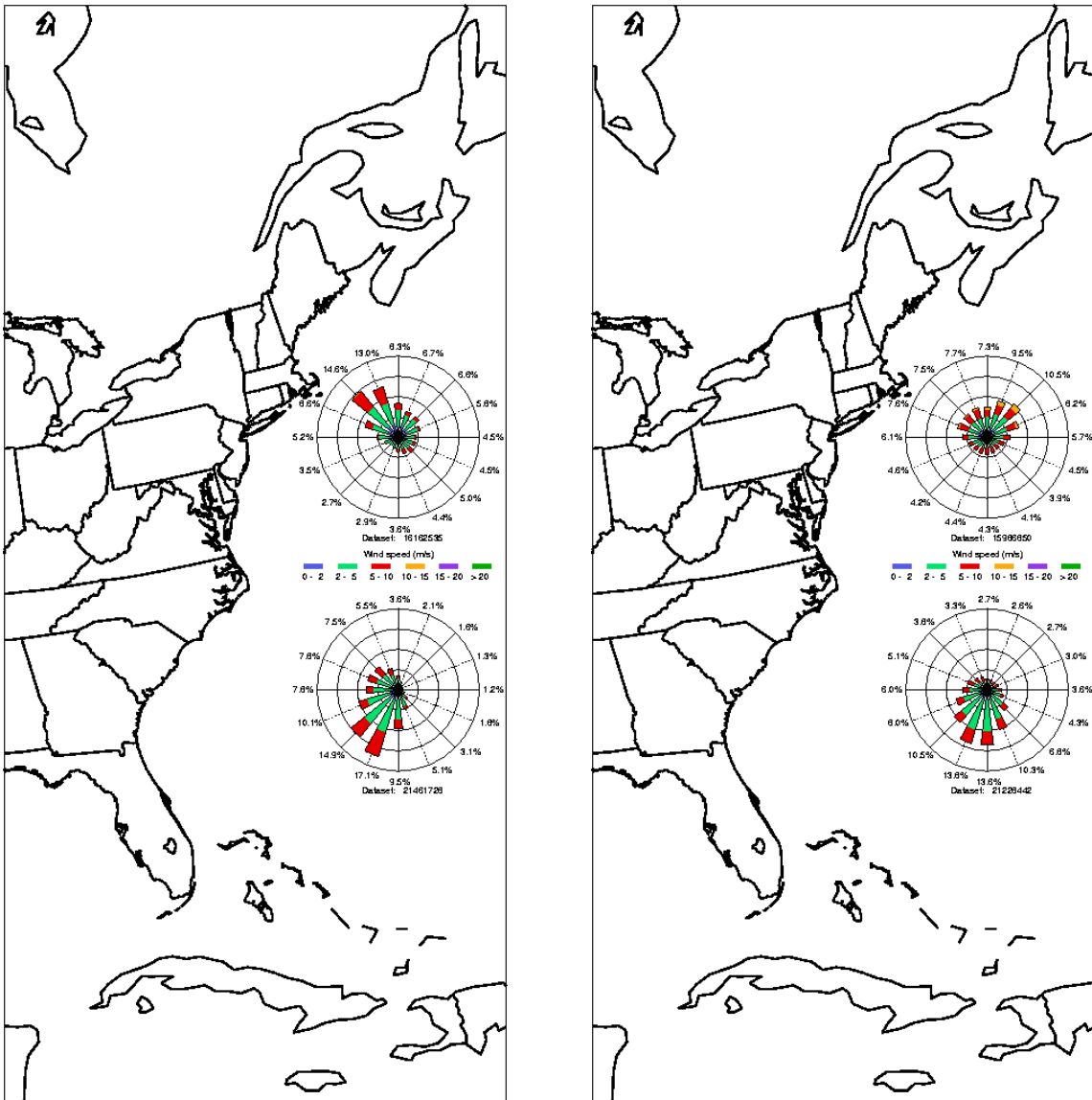


Figure 3-9b. Wind roses based on CALMET outputs for the Atlantic Ocean during summer 2002 (left) and fall 2002 (right).

summer, the winds in the western and central parts of the domain are mostly from the north, but they are variable in direction near the Florida coast (the prevailing wind direction varies from north-north-east in the western part of the domain to north-north-west in the eastern part of the domain). During fall, the winds are more variable with a tendency to be from the west to north-east in the western part of the domain and from the north to north-west in the central and eastern parts of the domain.

In the Atlantic Ocean, winds are mostly from the south to south-west in the southern part of the domain. They are more variable in the northern part of the domain with a prevailing northern trend that evolves from a northeastern direction during winter to a northwestern direction during summer.

3.1.4 CALMET Mixing heights

As mentioned above, the CALMET mixing heights were obtained from the MM5 outputs. They vary spatially and temporally. We illustrate such variability in Figures 3-10 through 3-13 where seasonally-averaged mixing heights are depicted for the southern Pacific coast, northern Pacific coast, gulf of Mexico coast and Atlantic coast, respectively.

Mixing heights are lowest in winter (December – February) and highest in summer (June – August). They are lower over water than over land; they also tend to be greater over the Gulf of Mexico than over the Pacific and Atlantic oceans. Ship emissions were predominantly released after plume rise within the mixing layer.

3.2 Emissions

As described in Section 2.3.2, ship emissions were represented by a set of stationary point sources. The point source emissions information required for the CALPUFF simulations include stack locations, stack characteristics such as stack heights and stack flow rates, and emission rates of SO₂, sulfate, NO and NO₂.

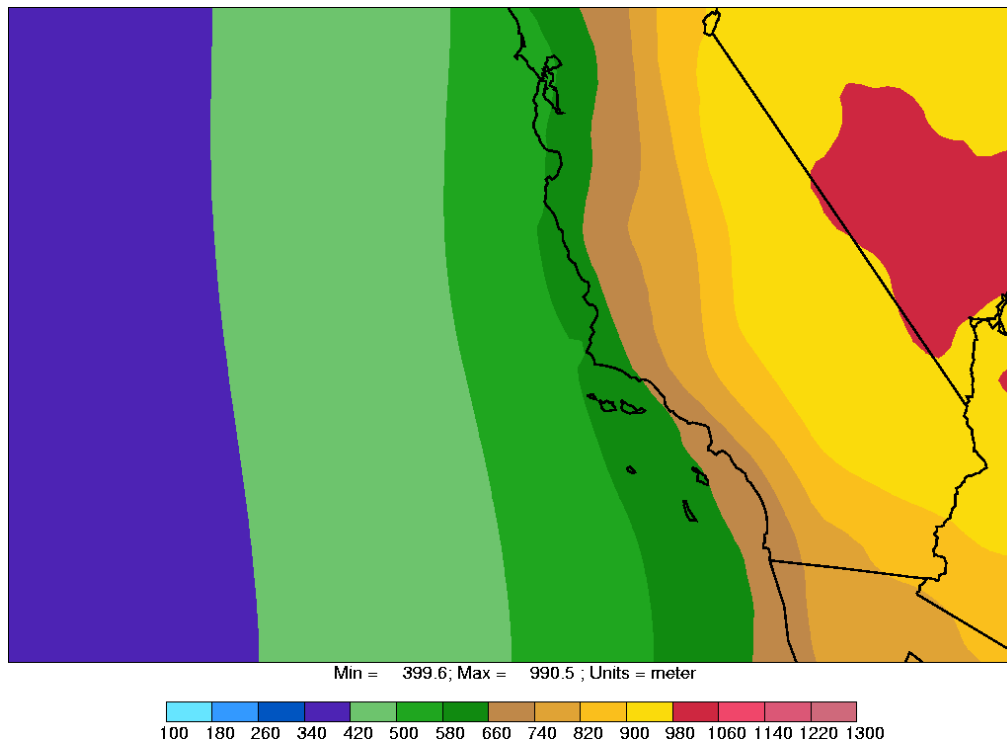
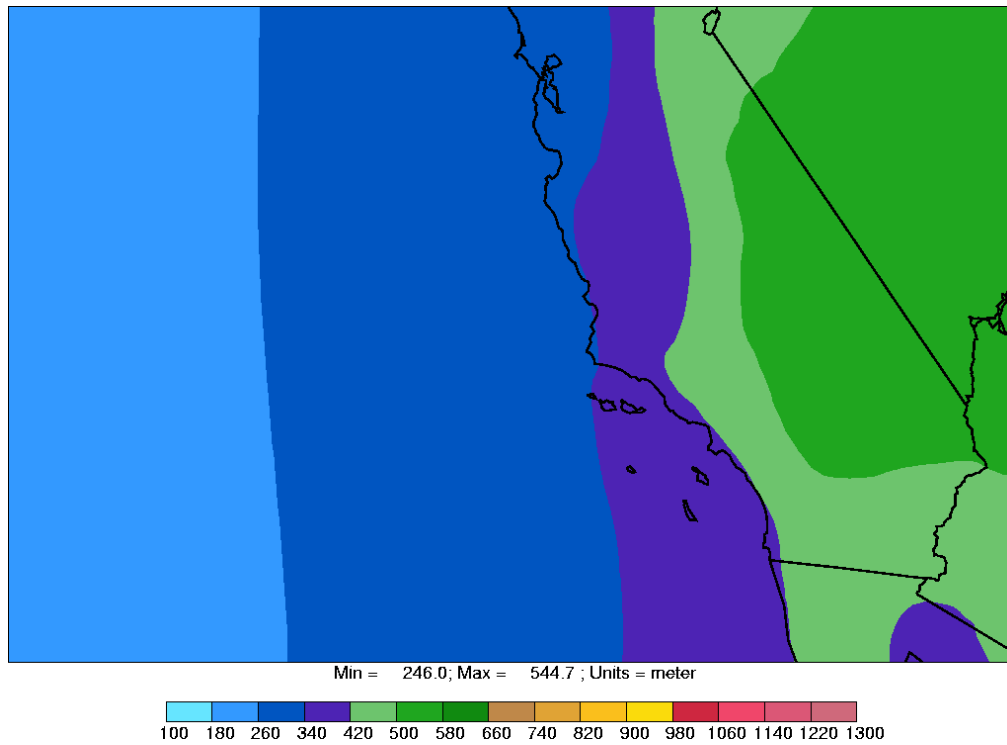


Figure 3-10a. Mixing heights for the southern Pacific Ocean during winter 2002 (top) and spring 2002 (bottom).

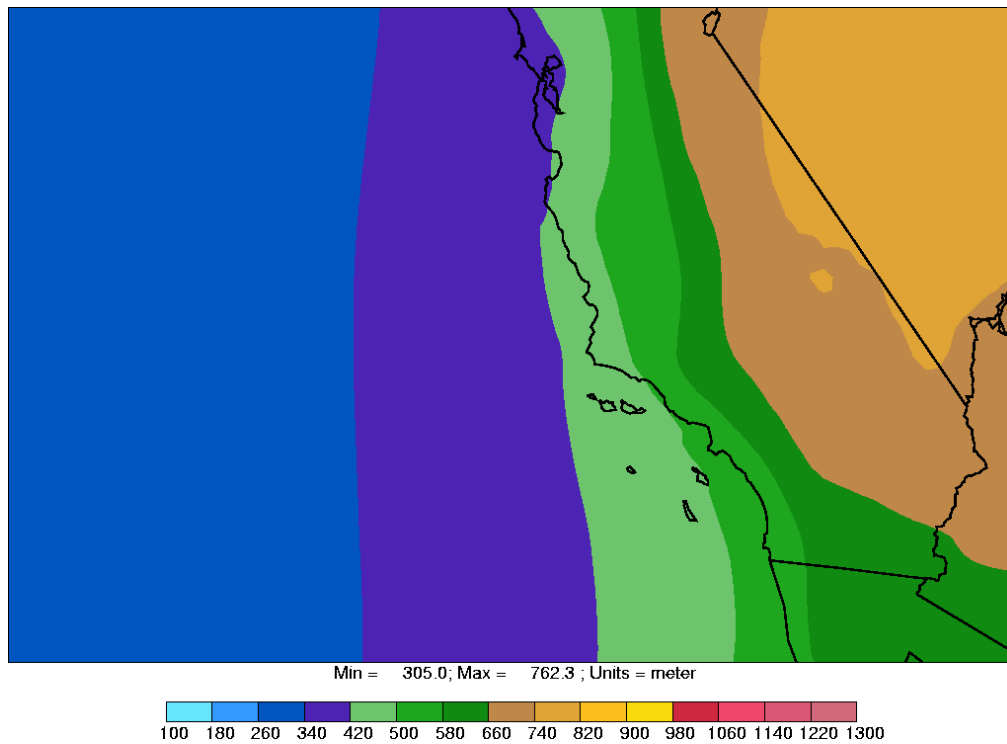
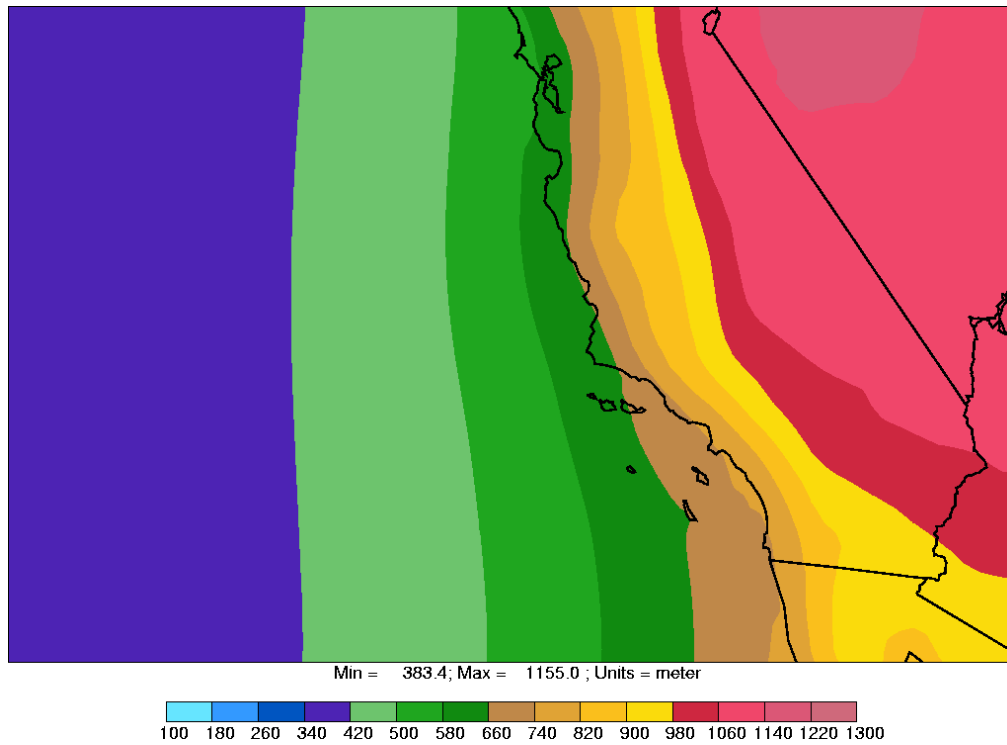


Figure 3-10b. Mixing heights for the southern Pacific Ocean during summer 2002 (top) and fall 2002 (bottom).

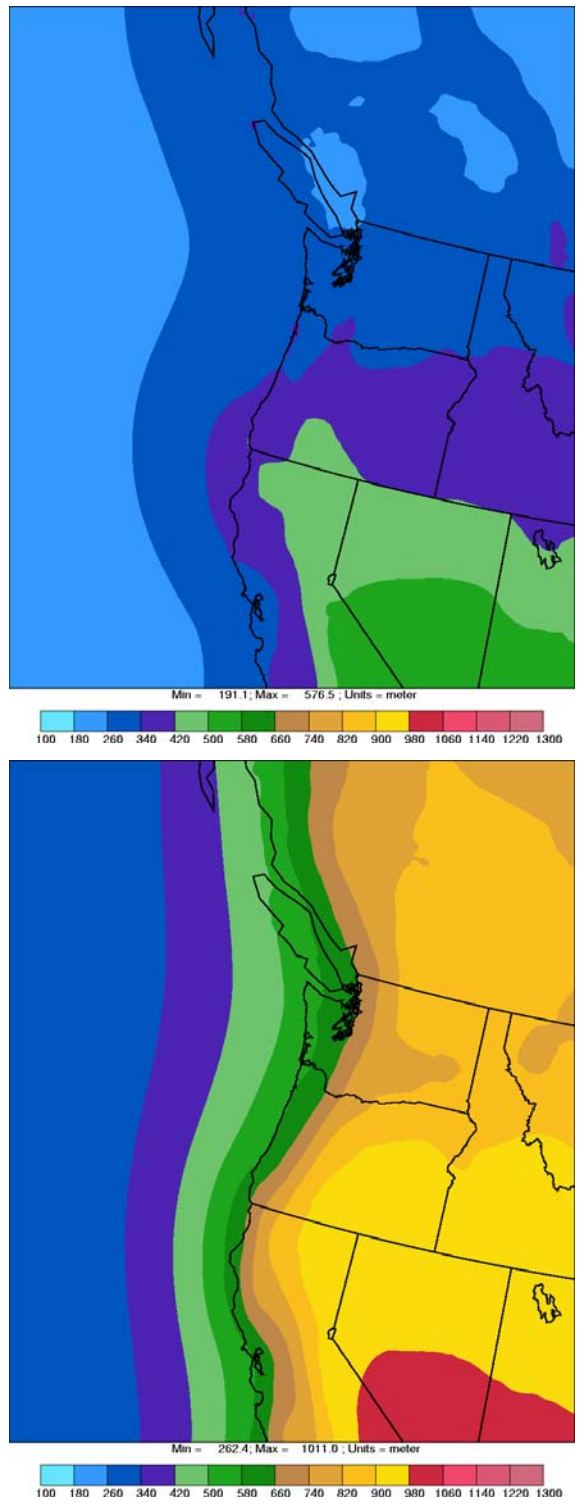


Figure 3-11a. Mixing heights for the northern Pacific Ocean during winter 2002 (top) and spring 2002 (bottom).

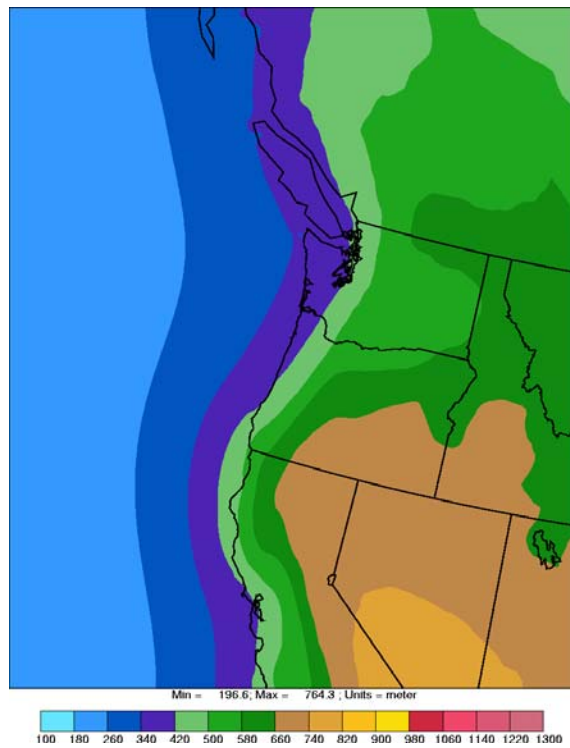
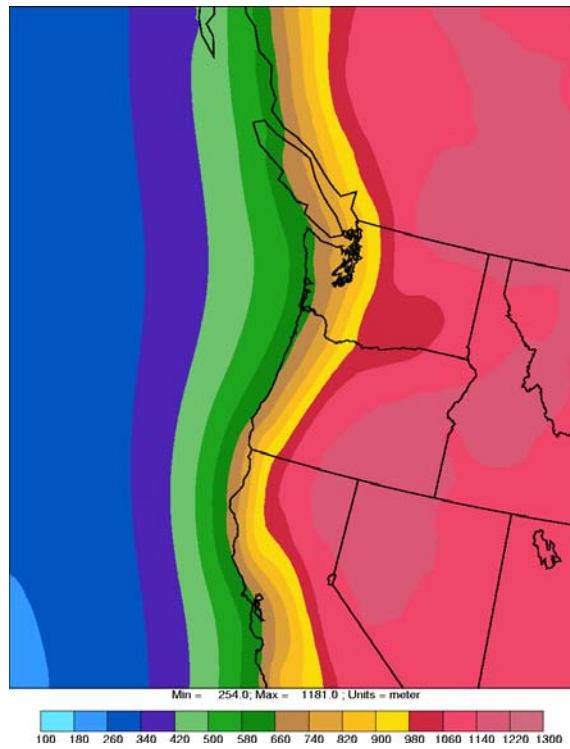


Figure 3-11b. Mixing heights for the northern Pacific Ocean during summer 2002 (top) and fall 2002 (bottom).

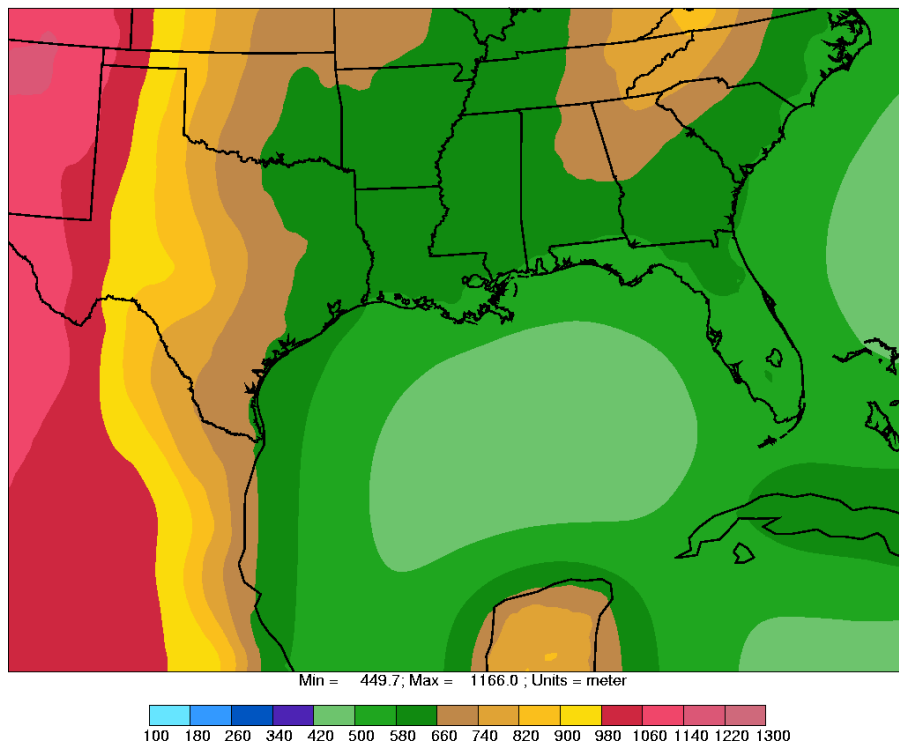
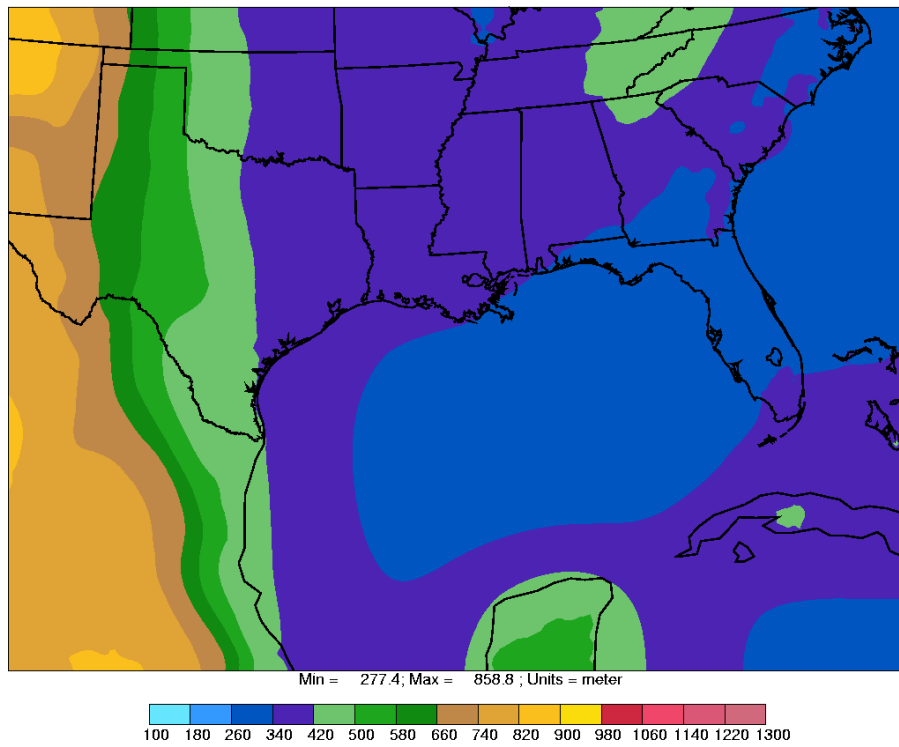


Figure 3-12a. Mixing heights for the Gulf of Mexico during winter 2002 (top) and spring 2002 (bottom).

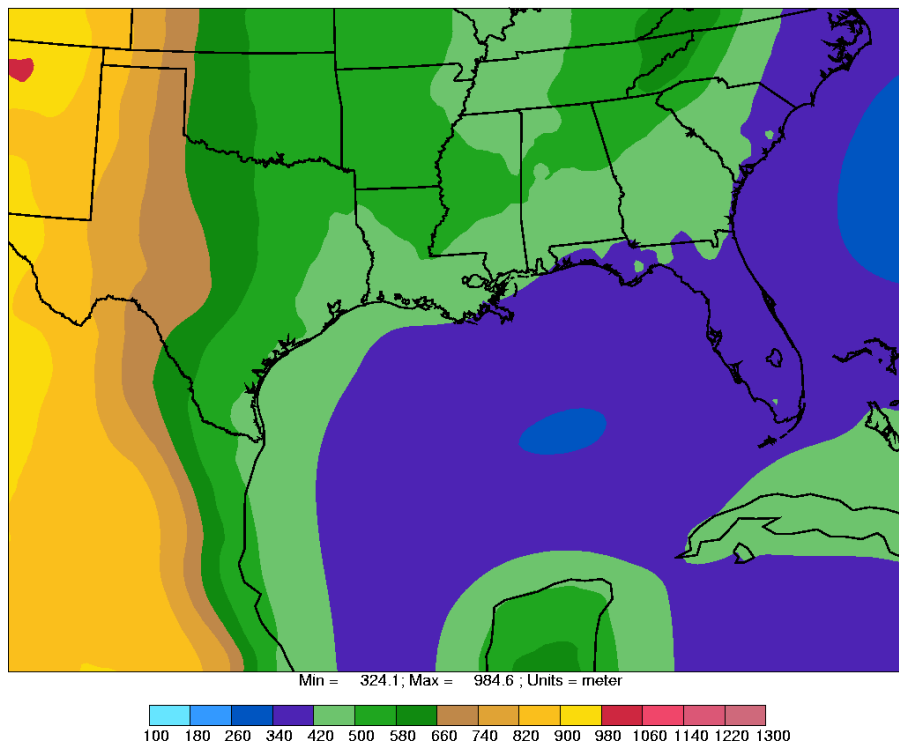
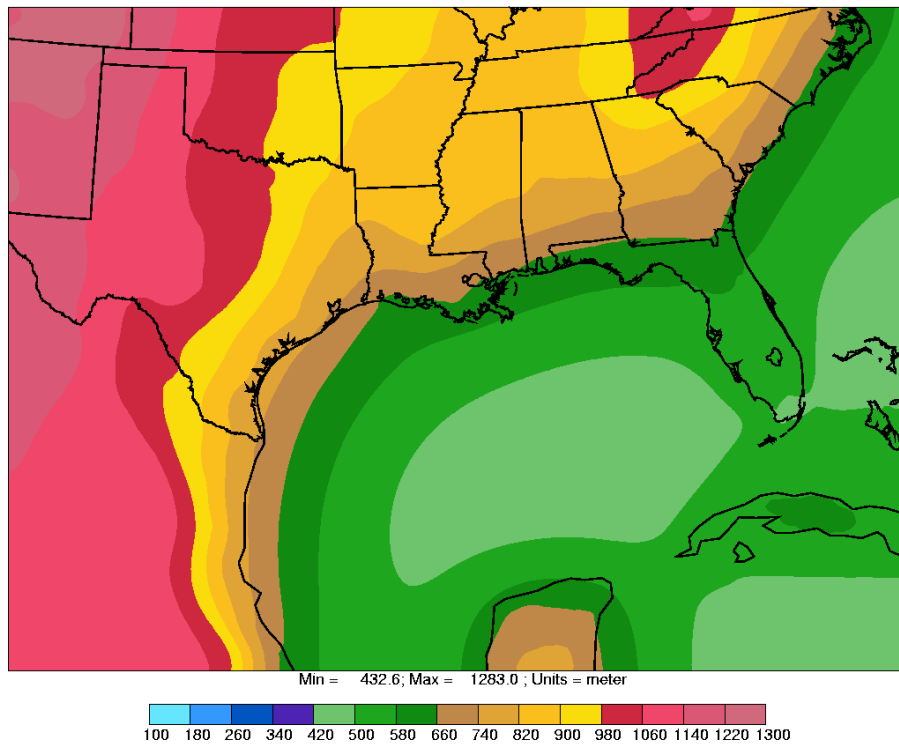


Figure 3-12b. Mixing heights for the Gulf of Mexico during summer 2002 (top) and fall 2002 (bottom).

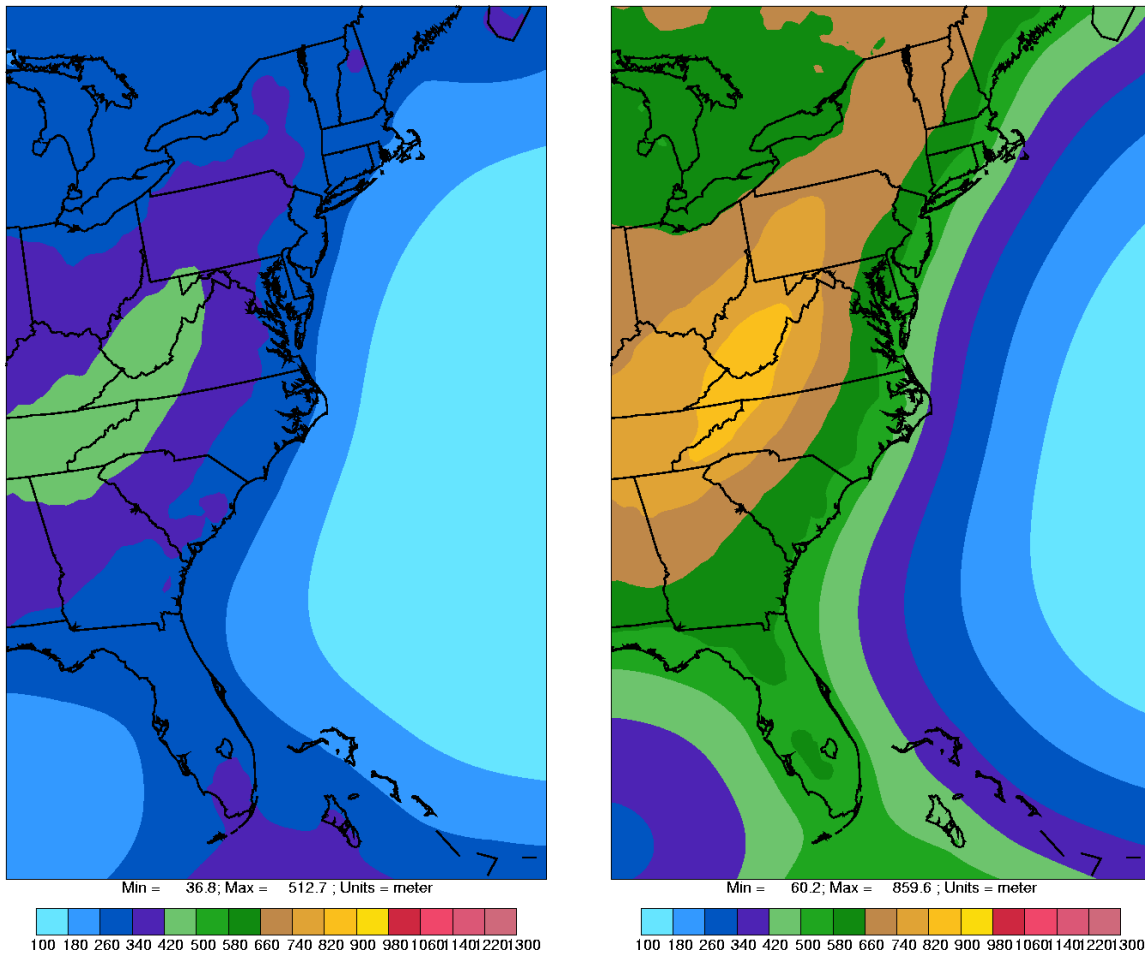


Figure 3-13a. Mixing heights for the Atlantic Ocean during winter 2002 (left) and spring 2002 (right).

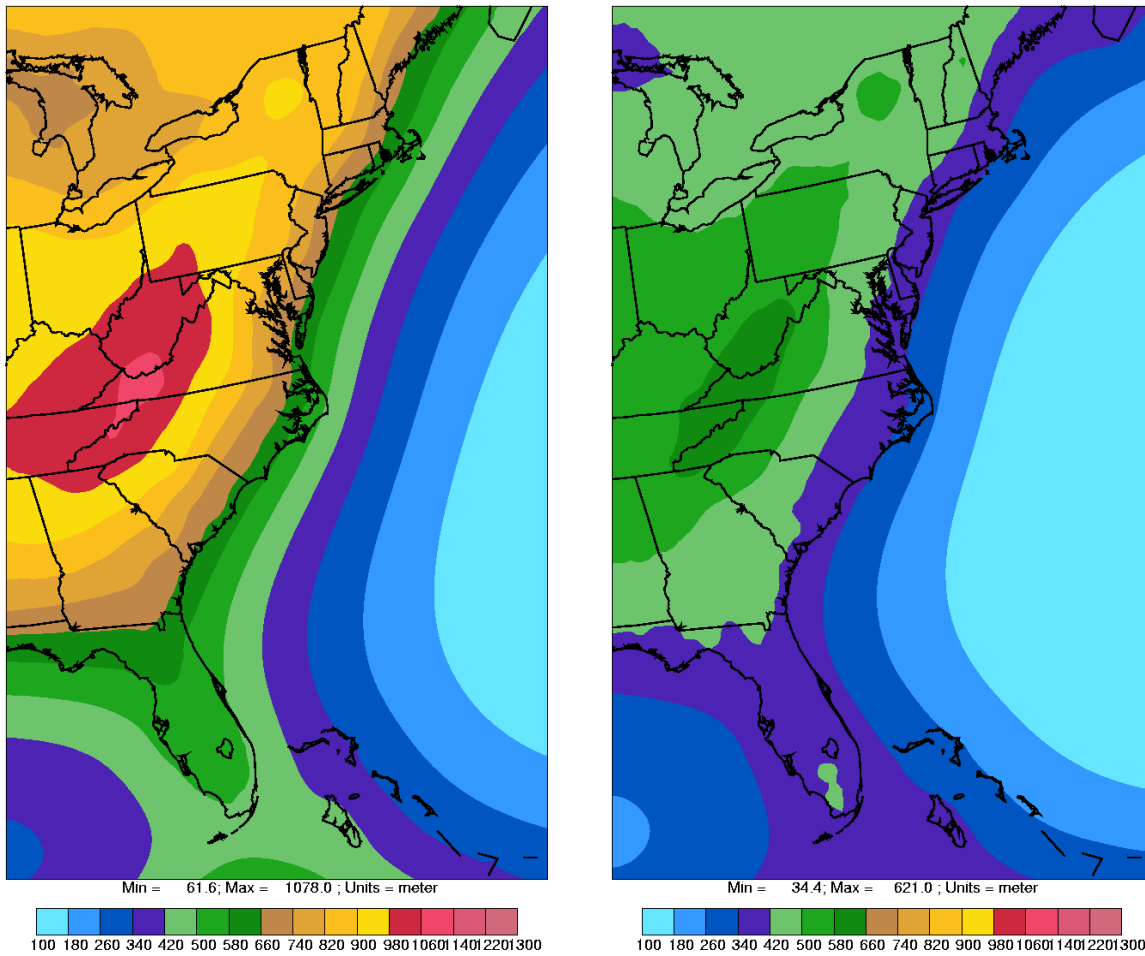


Figure 3-13b. Mixing heights for the Atlantic Ocean during summer 2002 (left) and fall 2002 (right).

3.2.1 Emission rates

Emission factors are needed to estimate the emissions of SO_x (gas-phase SO_2 and particulate-phase sulfate) associated with various ship activities. Based on the review of available emission factors of Seigneur et al. (2005), the most recent EPA emission factors were selected (EPA, 2002). Those emission factors pertain to ships with engines with displacement exceeding 30 liters (so-called Category 3 engines). Emission factors are reported for three different engine types (slow speed, medium speed and steam boiler) for transit modes and hoteling modes. For this study of ships at sea, we are interested in medium speeds for transit modes.

The SO_2 emission factor per unit of work is reported to be 9.56 g/hp-h for a 3% sulfur fuel (i.e., 30,000 ppm) for a ship at slow or medium speed in transit mode. This is equivalent to 12.8 g/kW-h. For a ship within the SECA, we assumed a fuel sulfur content of 15,000 ppm, resulting in an emission factor of 6.4 g/kW-h. For ships at sea outside of the SECA, a fuel sulfur content of 27,000 ppm was assumed. Therefore, the emission factor for such ships was estimated to be 11.52 g/kW-h.

EPA assumes that 2% of sulfur is emitted as primary sulfate PM from Category 3 marine diesel engines. Therefore, we treated 2% of total sulfur emissions as sulfate emissions and the SO_2 emission factor was adjusted down accordingly to maintain the sulfur mass balance. (Note that for the same amount of S, the sulfate emission factor is 1.5 the SO_2 emission factor to account for the different molecular weights of SO_2 and sulfate.)

Therefore, within the SECA, the gas-phase SO_2 and particulate-phase sulfate emission factors are 6.27 g/kW-h and 0.19 g/kW-h, respectively. Outside of the SECA, the gas-phase SO_2 and particulate-phase sulfate emission factors are 11.29 g/kW-h and 0.35 g/kW-h, respectively.

The sulfate emission rates calculated above are consistent with available data on the sulfate fraction of particulate matter (PM) emitted from ship diesel engines. Fleischer et al. (1998) report that 20 to 30% of PM emissions from ship diesel engines are sulfate (for a 3% sulfur fuel content). The EPA (2002) emission factor for PM is 1.3 g/hp-h, i.e.,

1.74 g/kW-h. These values lead to an emission factor for sulfate in the range of 0.31 to 0.47 g/kW-h for a sulfur fuel content of 27,000 ppm. The emission factor of 0.35 g/kW-h calculated above falls within this range.

Based on data from Corbett and Koehler (2003), the power of a typical ship was estimated to be 16,000 kW (Corbett, 2005). It should be noted that there is a wide range of power among various ships, with the largest container ships having power exceeding 65,000 kW.

The gas-phase SO₂ and particulate-phase sulfate emissions per ship are then calculated to be 100,320 g/h and 3,040 g/h, respectively, within the SECA and 180,640 g/h and 5,600 g/h, respectively, outside the SECA

A similar approach was used to calculate the NO and NO₂ emission rates. The NO_x emission factor per unit of work is reported to be 12.38 g/hp-h (as NO₂) for a ship at slow or medium speed in transit mode (EPA, 2002). This is equivalent to 16.6 g/kW-h. For a typical ship with a power of 16,000 kW, the resulting NO_x emission rate is 266,000 g/h (as NO₂). Assuming that 5% of the NO_x emissions are released as NO₂ on a molar basis, the NO and NO₂ emission rates were calculated to be 164,800 g/h and 13,300 g/h, respectively. These emission rates were used for ships within and outside the SECA, i.e., it was assumed that the switch to lower sulfur content fuel within the SECA did not affect the NO_x emission rates.

3.2.2 Stack parameters

These parameters include the locations of the sources and their stack characteristics. As discussed in Section 2.3.2, the ships were placed along the coastline for the target value calculations and at various distances from the coastline for the SECA boundary estimation. In this section, we discuss the spatial density of the ships, i.e., the spacing between each ship. This was determined based on analysis of ship activity data, as described below.

We used the average number, N , of ships in transit along the coast per year and average cruising speed, V (km/h), to calculate the average distance, D (km), between two ships along a shipping lane.

$$D = V * (24 \text{ h/day} * 365 \text{ days/yr}) / N$$

The annual number of ships transiting along the southern California coast was estimated to be 13,000 (ICOADS, 2002). This number includes all ships transiting to and from ports located on the southern Pacific coast as well as ships transiting southward/northward from/to ports located on the northern Pacific coast. It is likely to be an overestimate of the number of ships transiting along the coast because a fraction of those ships will be transiting along shipping lanes that extend from the ports westward into the Pacific Ocean. The cruising speed varies according to ship type. It is about 24 knots for container ships and about 16 knots for tankers. Here, the average ship cruising speed was estimated to be about 20 knots, i.e., 36 km/h (ICOADS, 2002). Thus, the average distance estimated for the southern Pacific coast was calculated as follows.

$$D = 36 * 24 * 365 / 13,000 = 24.3 \text{ km}$$

Based on this analysis, we used a distance of 25 km between ships to calculate ship emissions. The same distance was used for the other coastlines.

The other stack parameters required include stack characteristics such as stack height, stack diameter, stack exhaust velocity, and stack exit temperature. These parameters were obtained for typical container and tanker ship type categories from an ARB report (ARB, 2000). For this study, we used the average values for these two categories (see Table 3-1).

Table 3-1. Stack characteristics.

Stack height	35.3 m
Stack diameter	1.9 m
Exhaust velocity	24.6 m/s
Exhaust temperature	537 K

4. RESULTS

The initial CALPUFF baseline (i.e., ships along the coastline) and SECA boundary simulations for the Southern Pacific, Northern Pacific, and Gulf of Mexico coastlines were conducted using the latest EPA-approved version of CALPUFF. However, after discussions with the CALPUFF developers (Scire, 2006), it was decided that the final simulations would be conducted using the latest BETA-Test version of the model. This version addresses problems reported to the model developers by CALPUFF users. The results presented here are all based on simulations conducted with the beta version of CALPUFF.

Because the objective of the study is to identify upper limits for the off-shore distances at which sea-going ships may switch from cleaner fuel to high-sulfur content fuel, the results are presented in terms of the ratios of the ground-level SO₂ and sulfate concentrations at land-based receptors calculated from the off-shore source simulations to those calculated from the coastline source simulations. This allows us to determine the percentage of receptors at which the emissions from the sea-going ships will lead to air quality impacts that are less than or equal to the target values, i.e., the ground-level SO₂ and sulfate concentrations calculated from the baseline simulation.

Before presenting the results, it is useful to discuss the expected differences between SO₂ and sulfate in terms of the evolution of their downwind concentrations, and how these differences affect the results obtained here. SO₂ and sulfate concentrations will display different behaviors downwind of the ships. SO₂ concentrations will decrease continuously with distance from the source (due to dilution, removal, and conversion to sulfate), whereas sulfate concentrations will first decrease (dilution and removal of primary, i.e., directly emitted sulfate), then increase (formation of secondary sulfate from the oxidation of SO₂) before finally decreasing (dilution and removal exceeding formation).

This behavior of sulfate introduces an additional complication: the sulfate target values at receptors near the coastline will be determined by the directly emitted sulfate, while the target values at larger distances inland will be determined by some combination

of primary and secondary sulfate, with the secondary sulfate component increasing and the primary sulfate component decreasing. Even further inland, both components will decrease as the rate of dilution and removal exceeds the formation of sulfate.

These differences between the behavior of SO₂ and sulfate suggest that the SO₂ concentrations will become smaller than the design values at a smaller distance than the sulfate concentrations will. The SO₂ concentrations due to the higher SO_x emissions from the ships at sea burning higher sulfur fuel will be offset by the dilution and conversion of SO₂ much sooner than the sulfate concentrations since the latter will initially experience an increase from the SO₂ conversion.

In the discussion of the results that follows, we will refer to concentrations calculated from the emissions of coastline sources (i.e., ships within the SECA burning low-sulfur fuel) as the “target” values, and the concentrations due to emissions from ships at sea (i.e., ships outside the SECA burning high-sulfur fuel) as the “design” values. The ratios of the “design” concentrations to the “target” concentrations will be referred to as the “design ratios”.

4.1 Results for the Southern Pacific U.S. Coastline

Figure 4-1 shows the spatial patterns of the design ratios of the ground-level annual average SO₂ concentrations for ships at 125 km from the coastline. While there are large areas where the ratios are less than one, particularly near the southern part of the domain, the ratios are larger than one for the majority of the receptors. This is depicted in Figure 4-2, which shows the cumulative frequency distribution of the design ratios. The design ratios are less than one at about 41% of the receptors.

The spatial distribution of the sulfate design ratios for ships at 125 km from the coastline is shown in Figure 4-3. In contrast to the SO₂ results, the sulfate ratios are less than one over a very small portion of the domain near the southern boundary. From Figure 4-4, we see that the percentage of receptors for which the sulfate design ratios are less than one is only about 4%. These differences between the SO₂ and sulfate results are consistent with our expectations as discussed earlier.

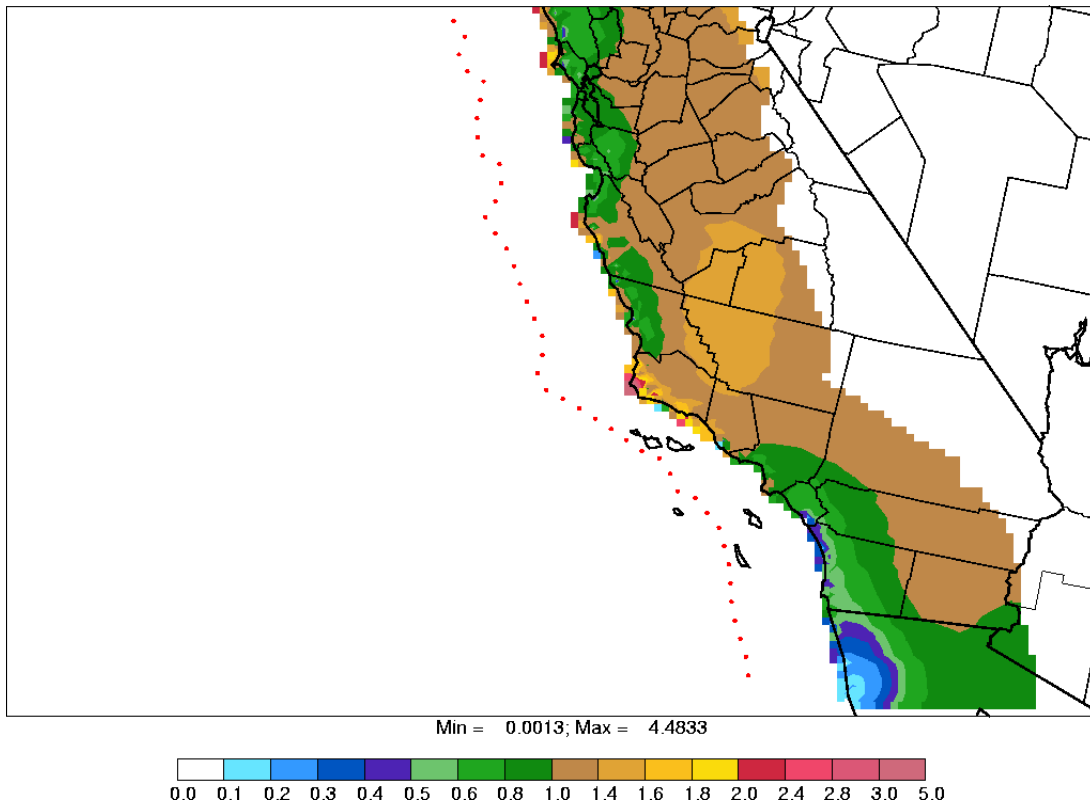


Figure 4-1. Ratios of annual-average SO₂ concentrations due to sea-going ships burning high-sulfur fuel at 125 km from the Southern Pacific U.S. coastline to the concentrations (target values) due to dockside ships at the coastline burning low-sulfur fuel. The red dots represent the locations of the sea-going ships.

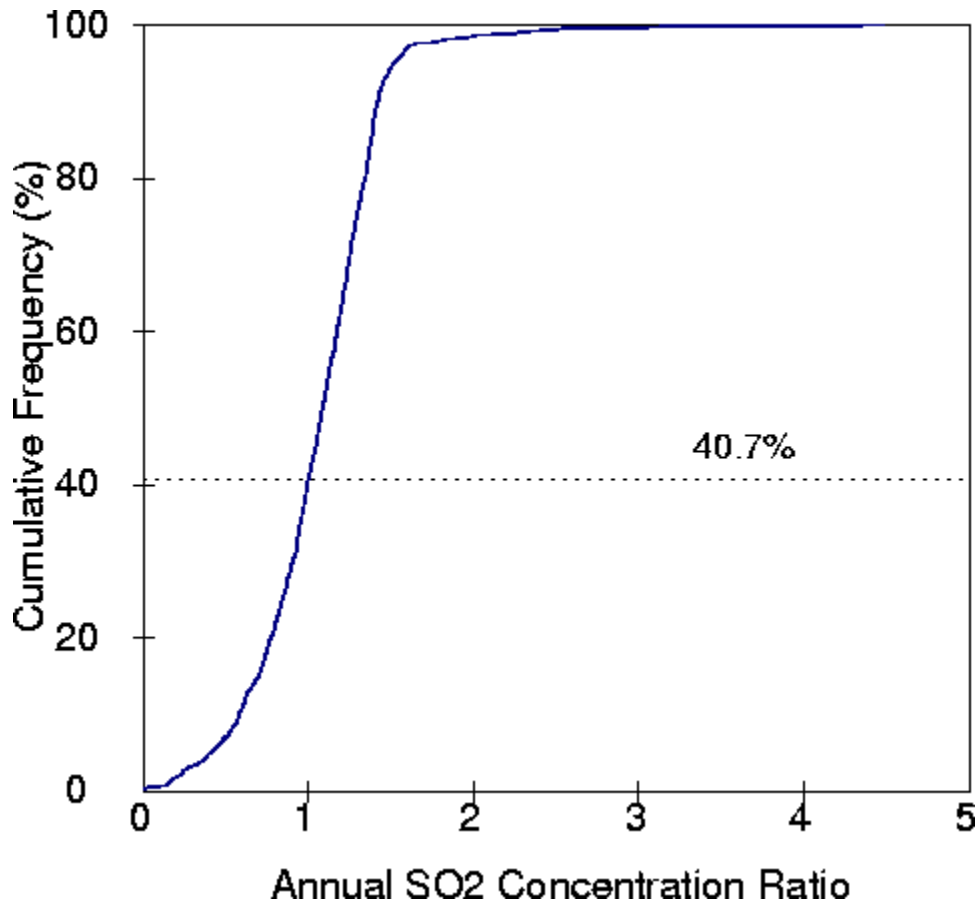


Figure 4-2. Cumulative frequency distribution of design ratios of SO₂ concentrations from ships at 125 km from the Southern Pacific U.S. coastline.

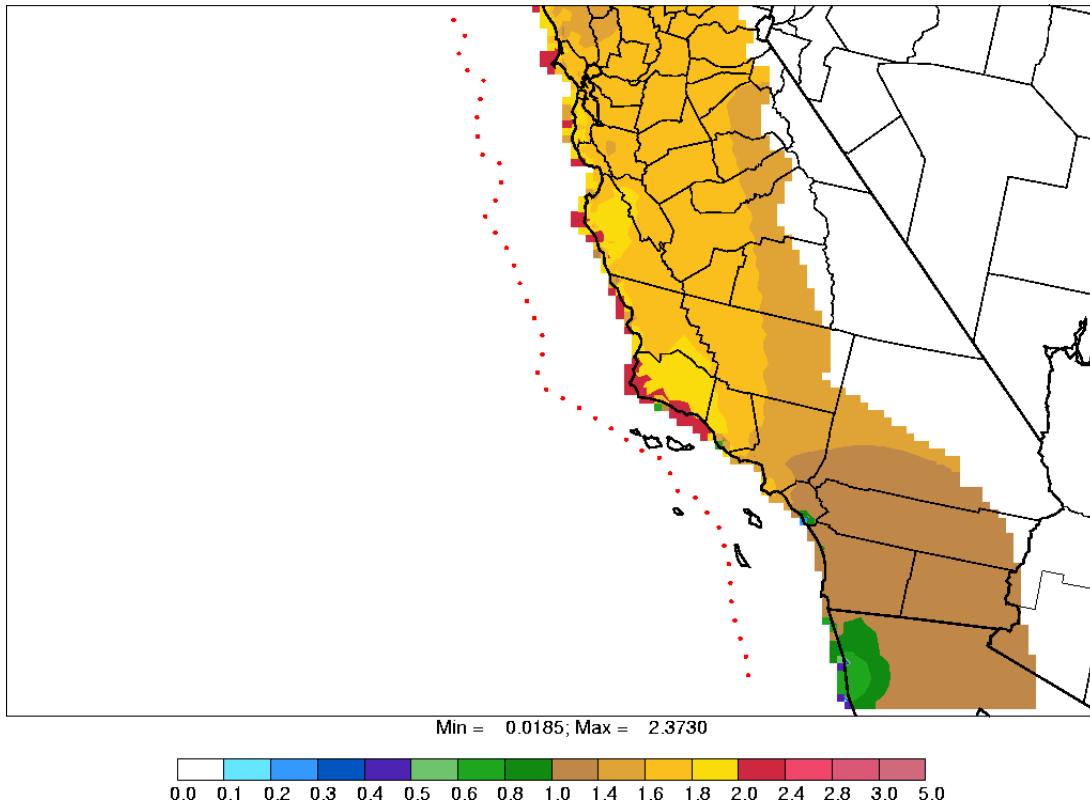


Figure 4-3. Ratios of annual-average sulfate concentrations due to sea-going ships burning high-sulfur fuel at 125 km from the Southern Pacific U.S. coastline to the concentrations (target values) due to dockside ships at the coastline burning low-sulfur fuel. The red dots represent the locations of the sea-going ships.

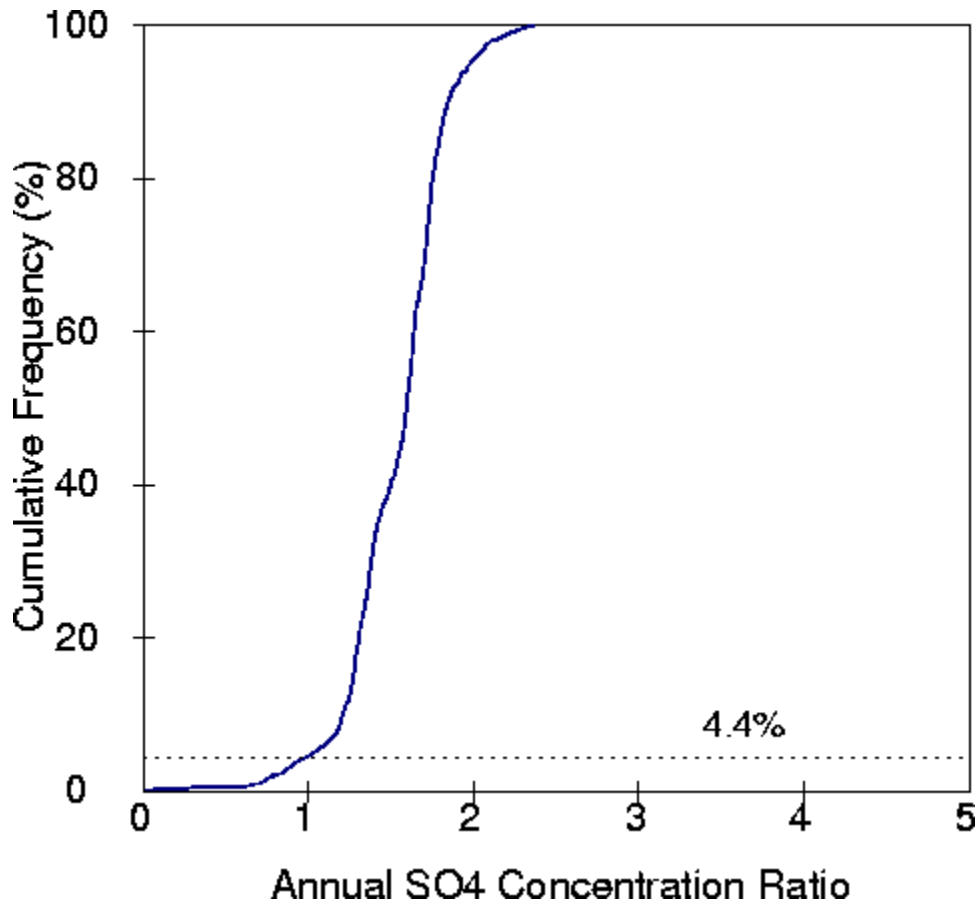


Figure 4-4. Cumulative frequency distribution of design ratios of sulfate concentrations from ships at 125 km from the Southern Pacific U.S. coastline.

The SO₂ results for ships at 250 km from the coastline are shown in Figures 4-5 and 4-6. From Figure 4-5, we see that, except for a small region in the Central Valley of California (Kings county, most of Fresno county, and portions of Tulare and Kern counties) and isolated locations along the coast in Santa Barbara county, most of the receptors have ratios less than one. Figure 4-6 shows that the percentage of receptors that have ratios less than one for ships at 250 km from the coastline is nearly 91%.

For sulfate, even when the ships are at a distance of 250 km, we see from Figure 4-7 that the sulfate design ratios are less than one only near the southern portion of the modeling domain, in Orange and San Diego counties, southern Imperial county, western Riverside county, and a small region of southern Los Angeles county. In the rest of the domain, the design ratios are larger than one, suggesting that increases in downwind sulfate concentrations from the conversion of SO₂ to sulfate are still the determining factors for ship emissions at 250 km. Figure 4-8 shows that the percentage of receptors for which the sulfate design ratios is less than one for ships at 250 km from the coastline is only about 25%.

Figures 4-9 and 4-10 show the SO₂ results for ships at 375 km from the coastline. As seen in Figure 4-9, except for one location along the coastline in Santa Barbara county, all the receptors show design ratios less than one. The cumulative frequency distribution, shown in Figure 4-10, confirms that SO₂ air quality impacts from the ships burning high-sulfur fuel are less than those from coastline ships burning low-sulfur fuel at over 99.99% of the land-based receptors.

Figures 4-11 and 4-12 show that the sulfate results for ships at 375 km from the coastline still show larger air quality impacts than the coastline ships for a large majority of the receptors. From Figure 4-11, a clear north-south gradient is evident. In the region north of Los Angeles county, and including portions of northern Los Angeles county, the sulfate ratios are larger than one. In the region south, all the sulfate ratios are less than one. Figure 4-12 shows that about 42% of the receptors have sulfate ratios less than one.

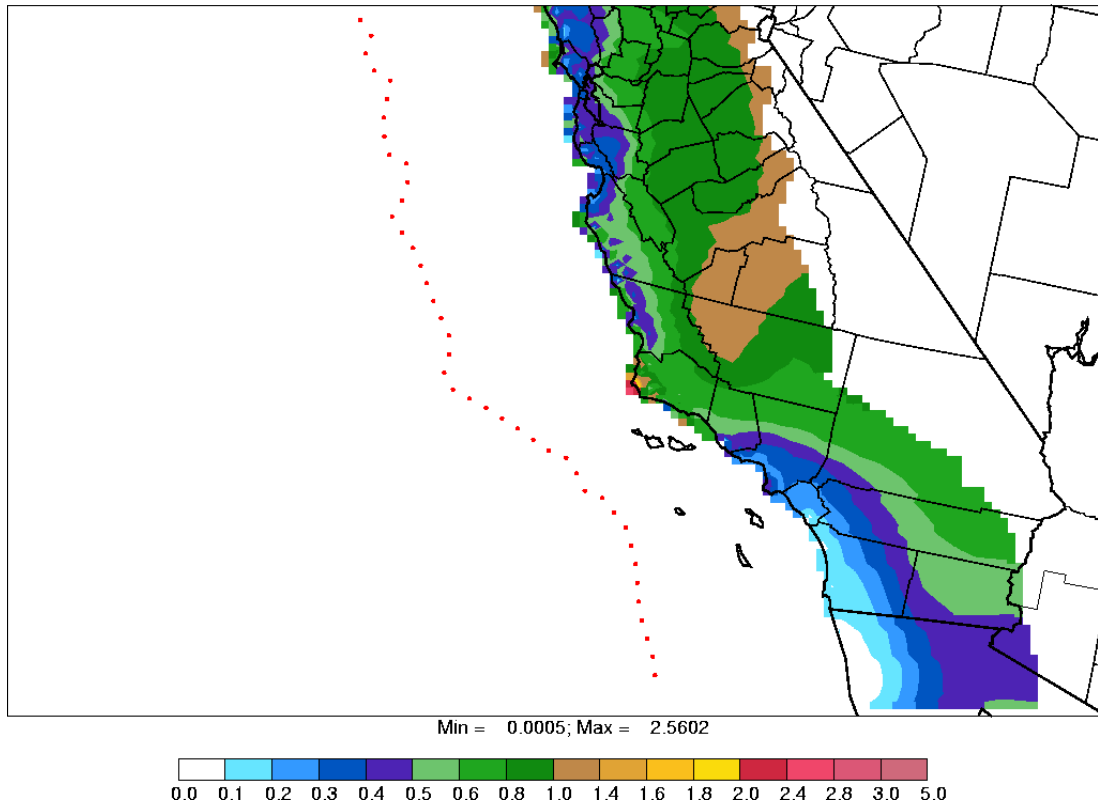


Figure 4-5. Ratios of annual-average SO₂ concentrations due to sea-going ships burning high-sulfur fuel at 250 km from the Southern Pacific U.S. coastline to the concentrations (target values) due to dockside ships at the coastline burning low-sulfur fuel. The red dots represent the locations of the sea-going ships.

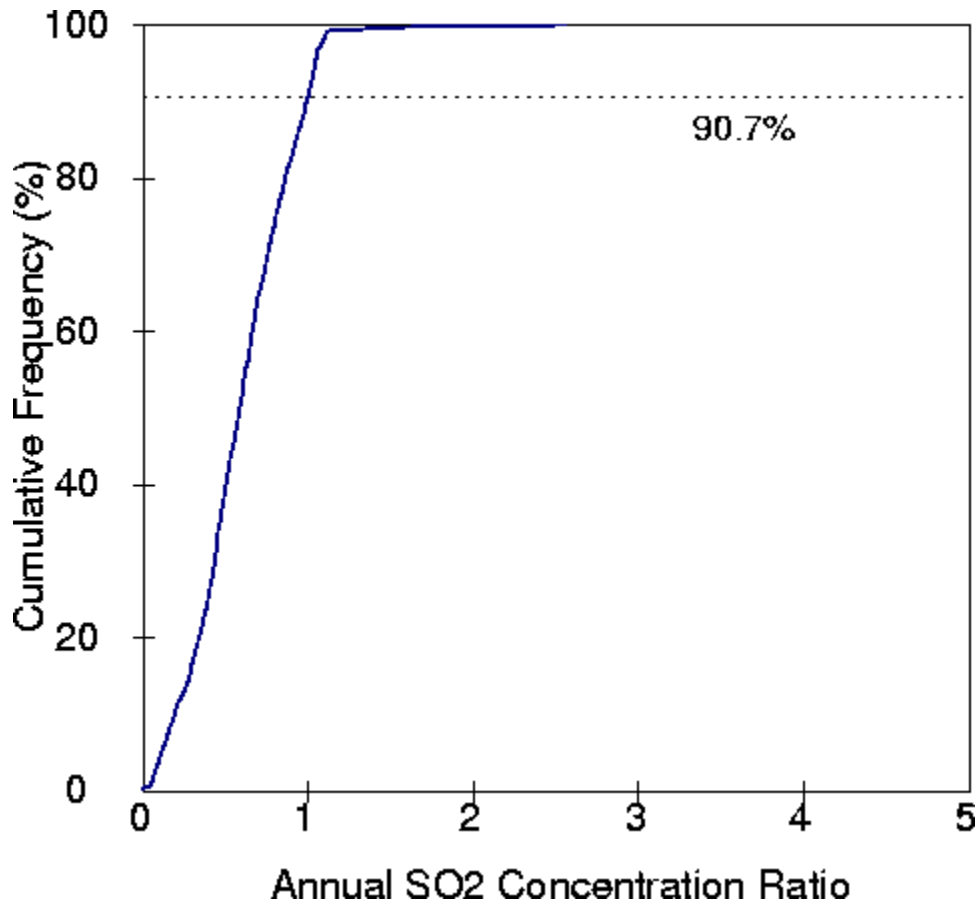


Figure 4-6. Cumulative frequency distribution of design ratios of SO₂ concentrations from ships at 250 km from the Southern Pacific U.S. coastline.

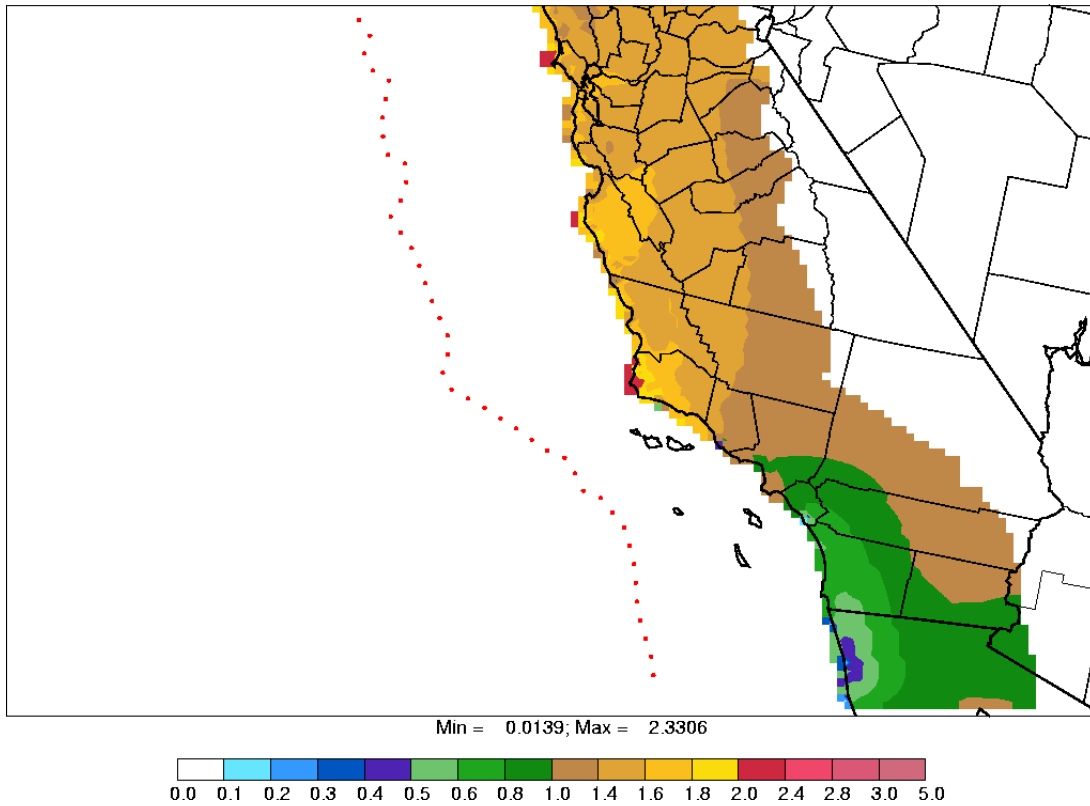


Figure 4-7. Ratios of annual-average sulfate concentrations due to sea-going ships burning high-sulfur fuel at 250 km from the Southern Pacific U.S. coastline to the concentrations (target values) due to dockside ships at the coastline burning low-sulfur fuel. The red dots represent the locations of the sea-going ships.

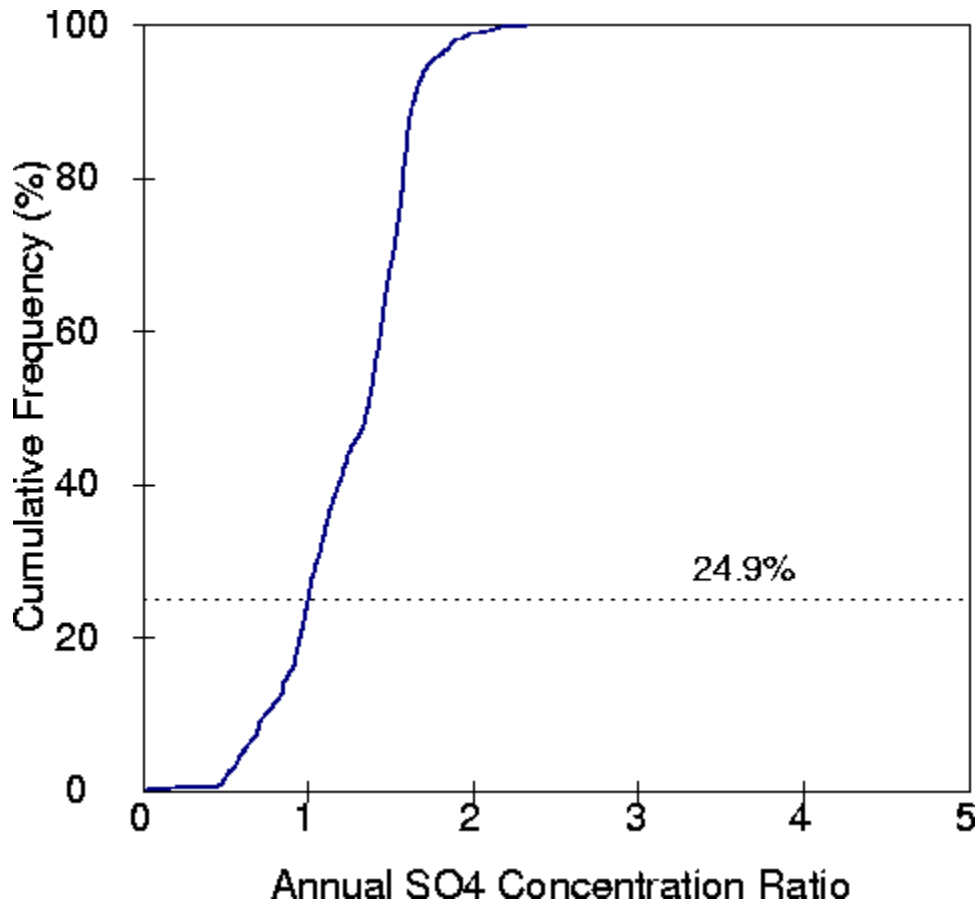


Figure 4-8. Cumulative frequency distribution of design ratios of sulfate concentrations from ships at 250 km from the Southern Pacific U.S. coastline.

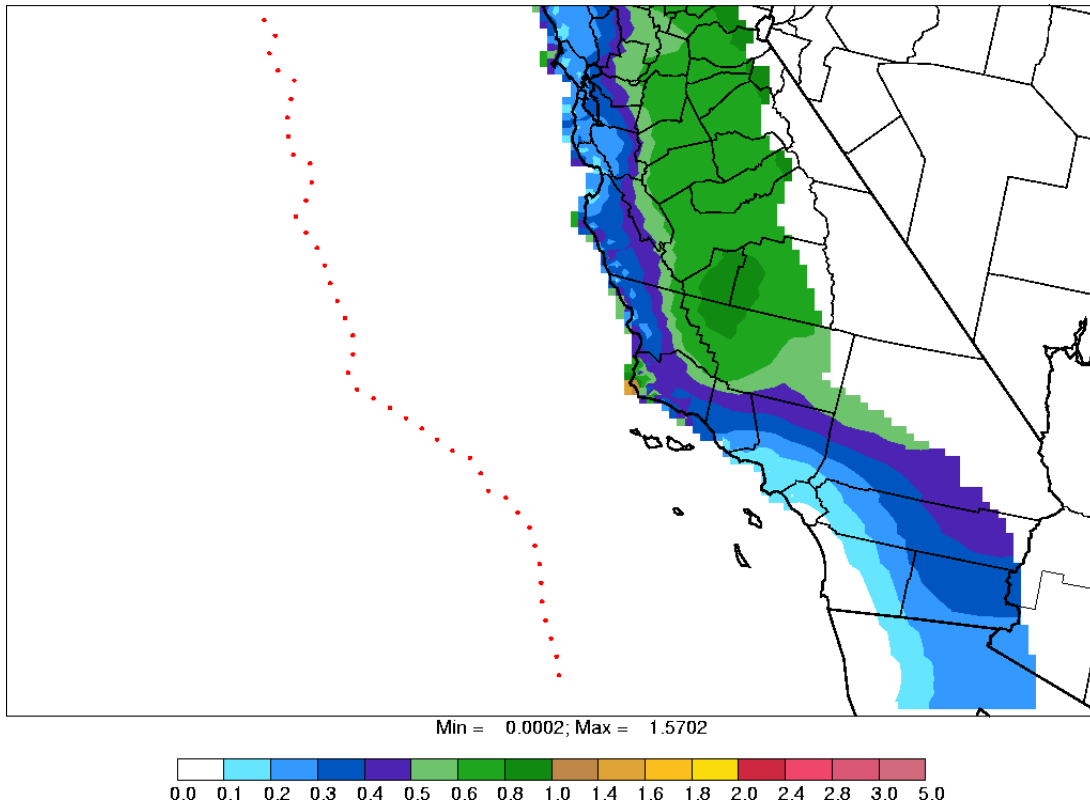


Figure 4-9. Ratios of annual-average SO₂ concentrations due to sea-going ships burning high-sulfur fuel at 375 km from the Southern Pacific U.S. coastline to the concentrations (target values) due to dockside ships at the coastline burning low-sulfur fuel. The red dots represent the locations of the sea-going ships.

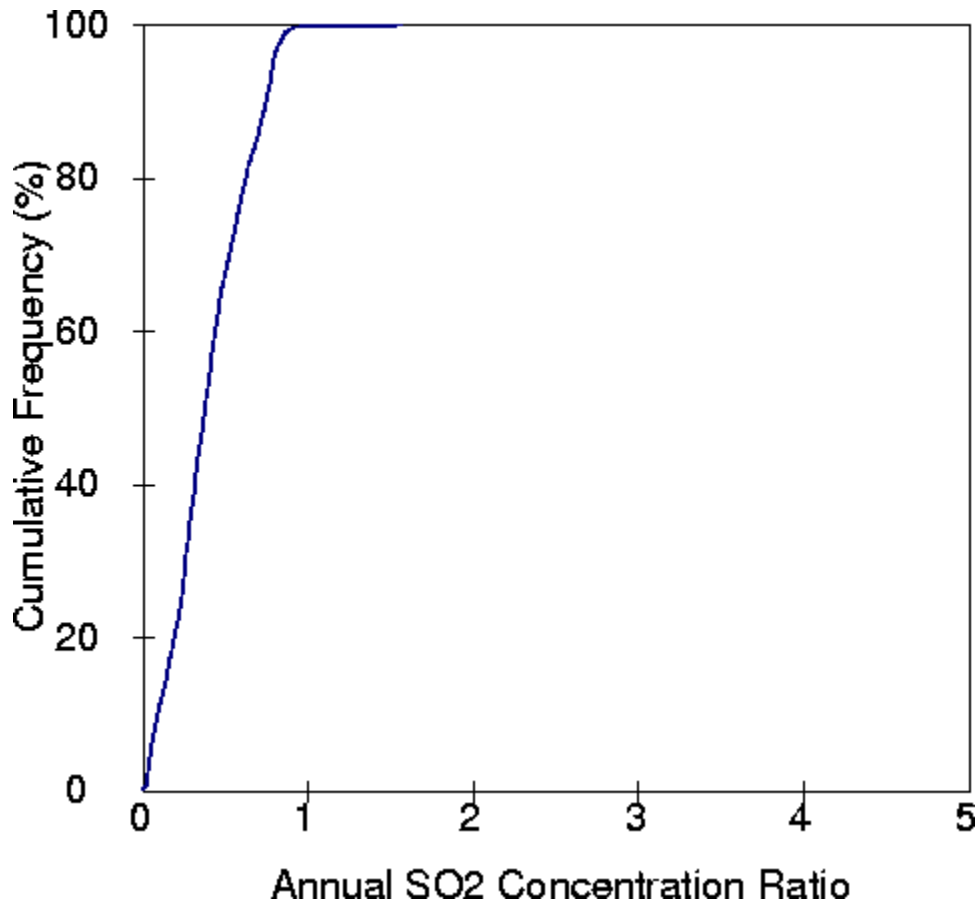


Figure 4-10. Cumulative frequency distribution of design ratios of SO₂ concentrations from ships at 375 km from the Southern Pacific U.S. coastline.

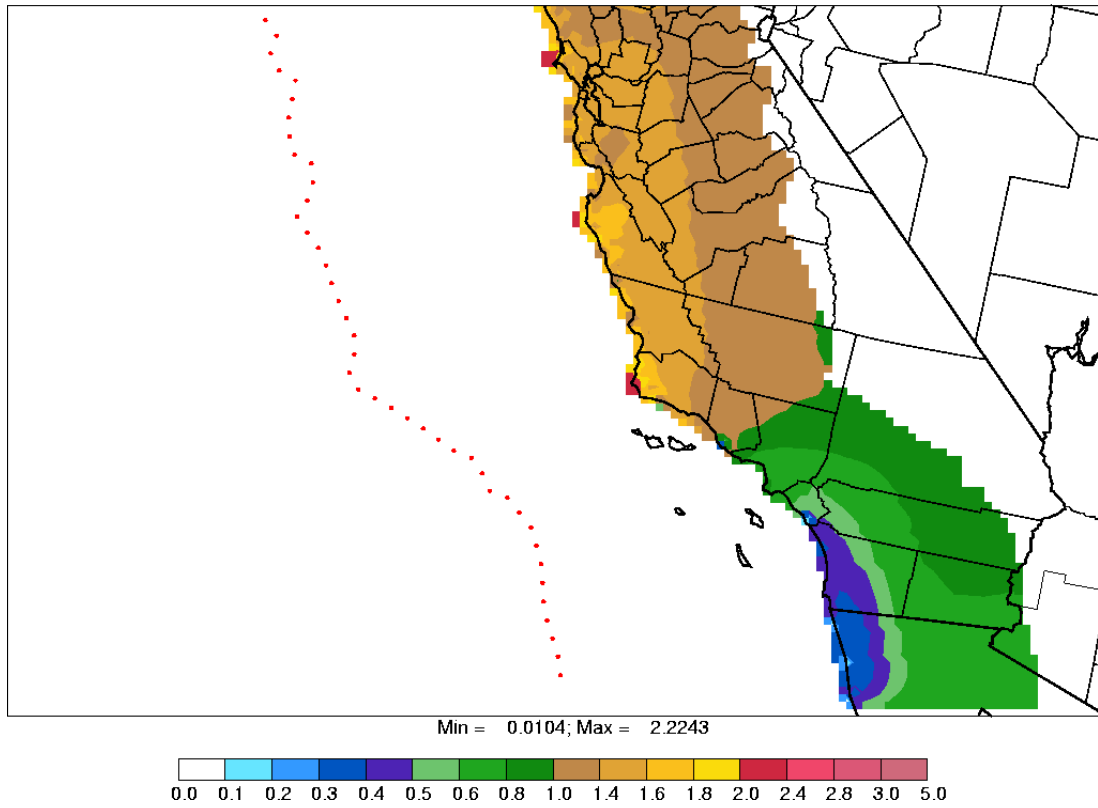


Figure 4-11. Ratios of annual-average sulfate concentrations due to sea-going ships burning high-sulfur fuel at 375 km from the Southern Pacific U.S. coastline to the concentrations (target values) due to dockside ships at the coastline burning low-sulfur fuel. The red dots represent the locations of the sea-going ships.

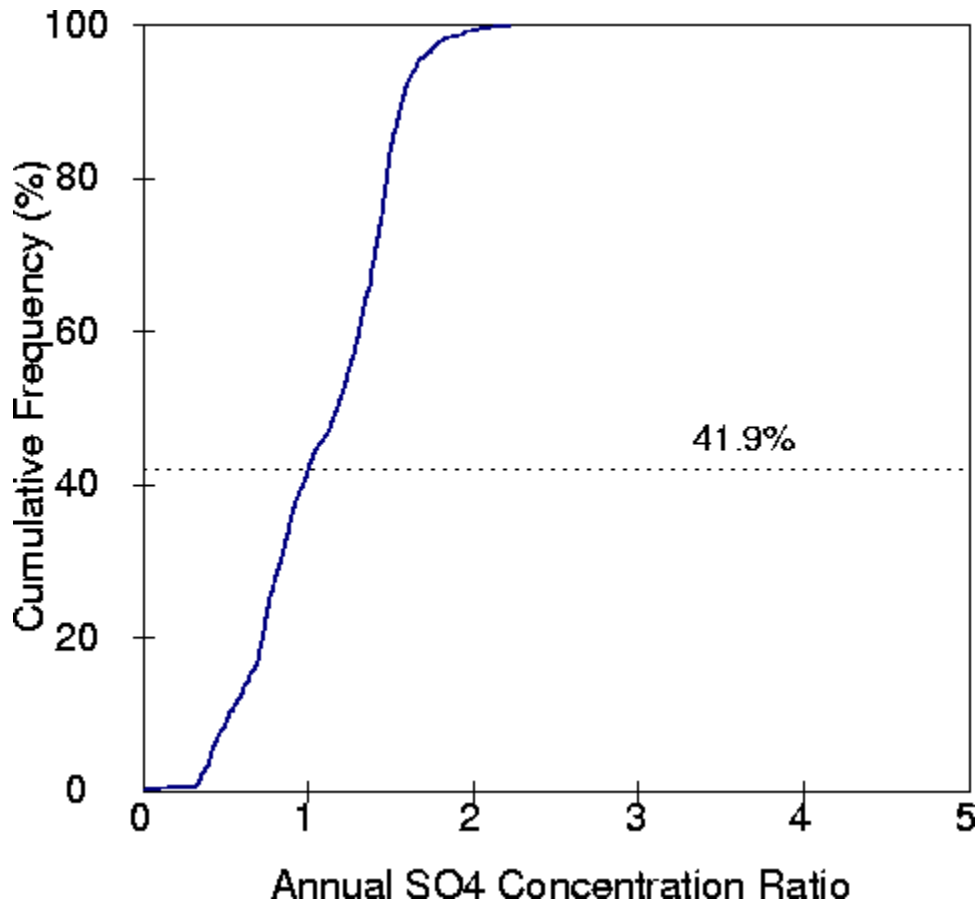


Figure 4-12. Cumulative frequency distribution of design ratios of sulfate concentrations from ships at 375 km from the Southern Pacific U.S. coastline.

The sulfate results for ships at 500 km from the coastline are shown in Figures 4-13 and 4-14 (the corresponding SO₂ results are not shown here since the 375 km results presented earlier show that a distance of 375 km is more than adequate for setting the upper limit of the SECA for SO₂ impacts). The north-south gradient is still evident, as shown in Figure 4-13, but the boundary between the two regions of ratios less than one in the south to ratios larger than one in the north has shifted to the north (to Ventura county in the west and to Kern and Tulare counties in the east). The two regions are approximately equal in area, as confirmed by the cumulative frequency distribution in Figure 4-14.

In these analyses, the Santa Barbara area tends to show higher concentrations of SO₂ and sulfate and, in some cases high concentration/target value ratios. One reason for such high concentrations is that the Santa Barbara area extends westward into the Pacific Ocean and, as a result, receptors near the coast have more ship emission sources in their close vicinity than receptors located in other areas along the coast. All sources will not impact the Santa Barbara receptors simultaneously because such impacts will depend on the wind flow (see Figure 3-6). Nevertheless, the probability of impact from ship emission sources should be higher for the Santa Barbara area than for other areas along the southern Pacific coast because of the design of the source/receptor locations in this screening study. This characteristic of the source/receptor relationship should be kept in mind when interpreting the simulation results. Note that the air quality modeling to be conducted later with the 3-D CMAQ model will locate ship emissions along shipping lanes and, therefore, will provide a more realistic set of source/receptor relationships.

4.2 Results for the Northern Pacific U.S. Coastline

Figures 4-15 and 4-16 show the SO₂ results for ships at 125 km from the Northern Pacific coastline. We see from Figure 4-15 that the regions with ratios less than one are approximately equal in area to the regions with ratios greater than one. As shown in Figure 4-16, the ratios are less than one at about 47% of the receptors. The higher ratios typically occur inland in areas of high elevation (e.g., the Cascade mountain range). The

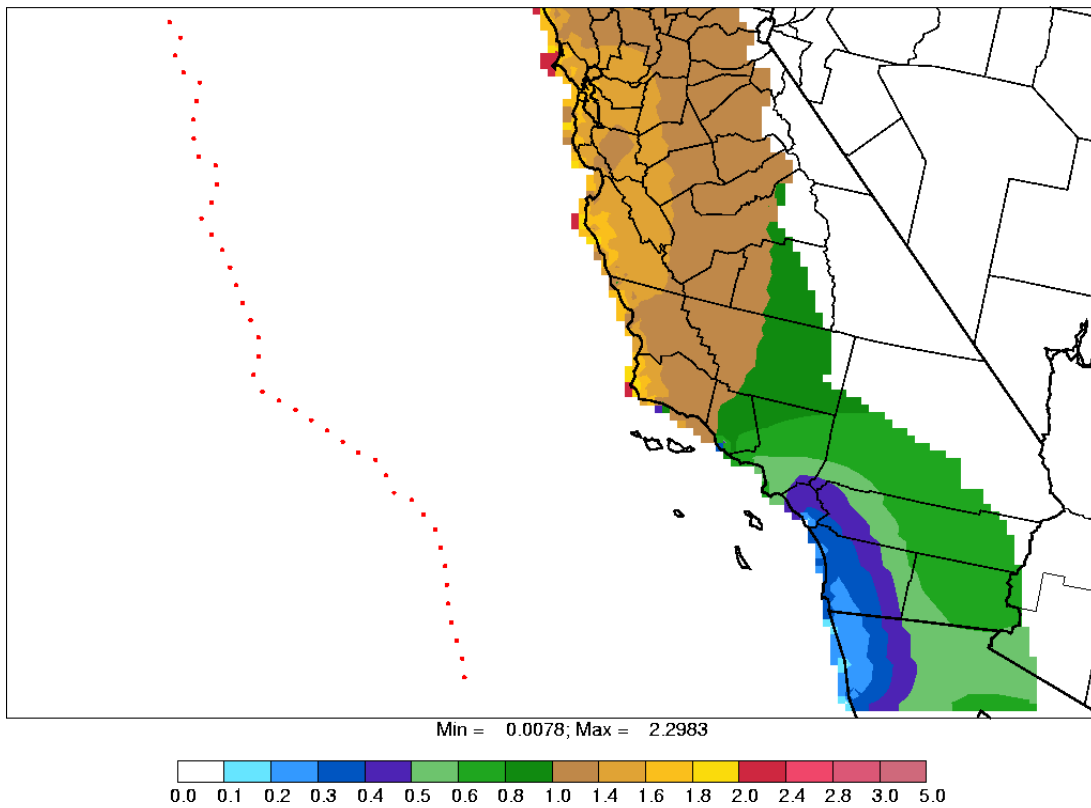


Figure 4-13. Ratios of annual-average sulfate concentrations due to sea-going ships burning high-sulfur fuel at 500 km from the Southern Pacific U.S. coastline to the concentrations (target values) due to dockside ships at the coastline burning low-sulfur fuel. The red dots represent the locations of the sea-going ships.

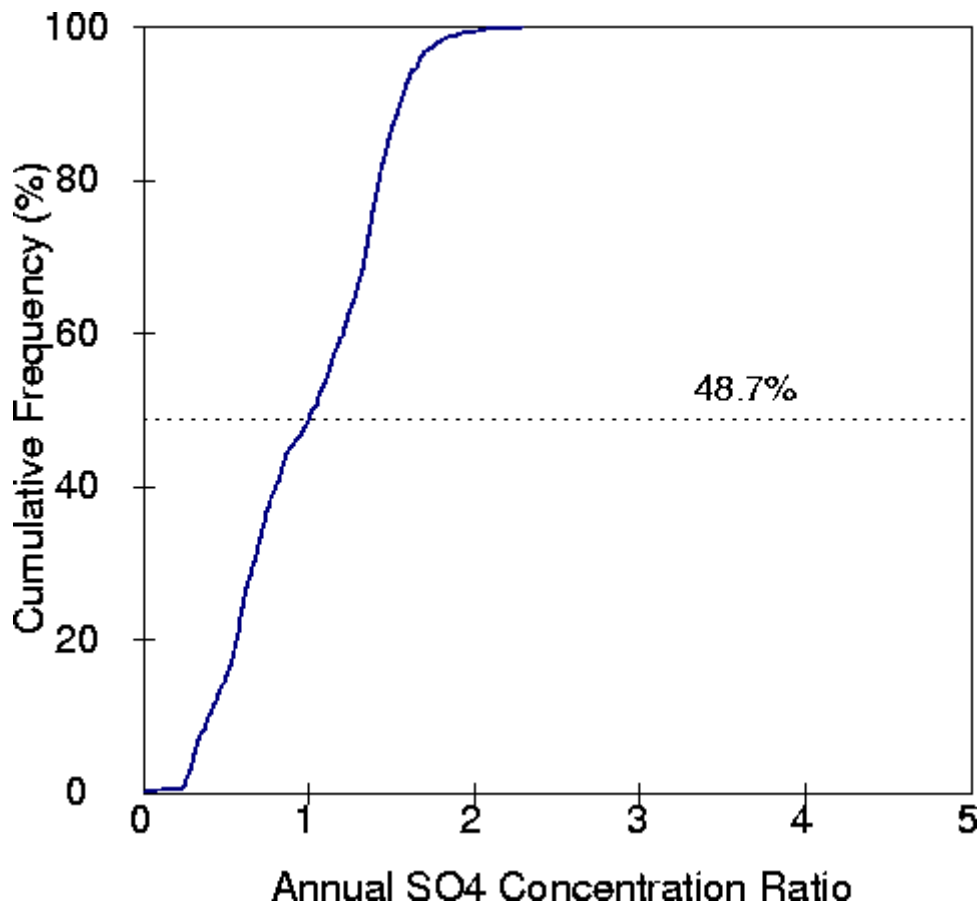


Figure 4-14. Cumulative frequency distribution of design ratios of sulfate concentrations from ships at 500 km from the Southern Pacific U.S. coastline.

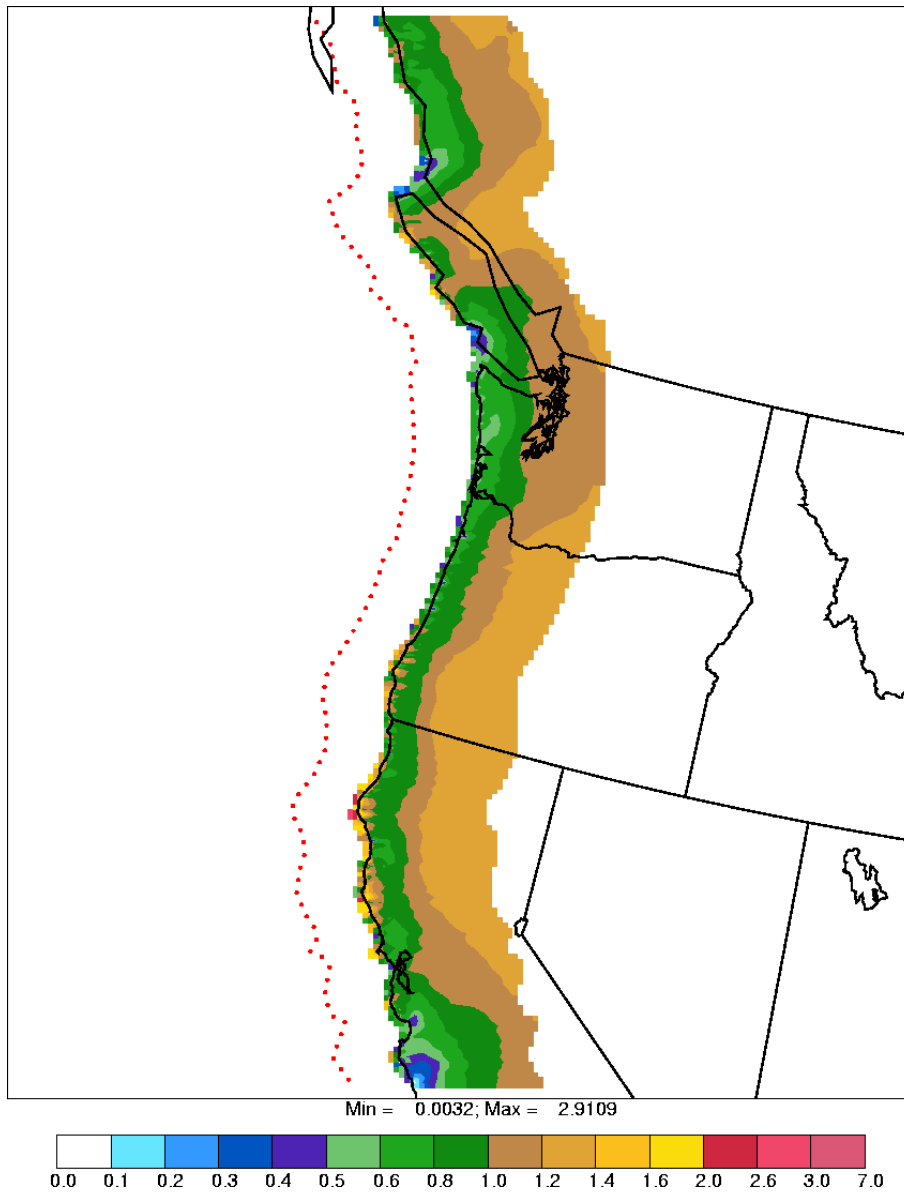


Figure 4-15. Ratios of annual-average SO_2 concentrations due to sea-going ships burning high-sulfur fuel at 125 km from the Northern Pacific U.S. coastline to the concentrations (target values) due to dockside ships at the coastline burning low-sulfur fuel. The red dots represent the locations of the sea-going ships.

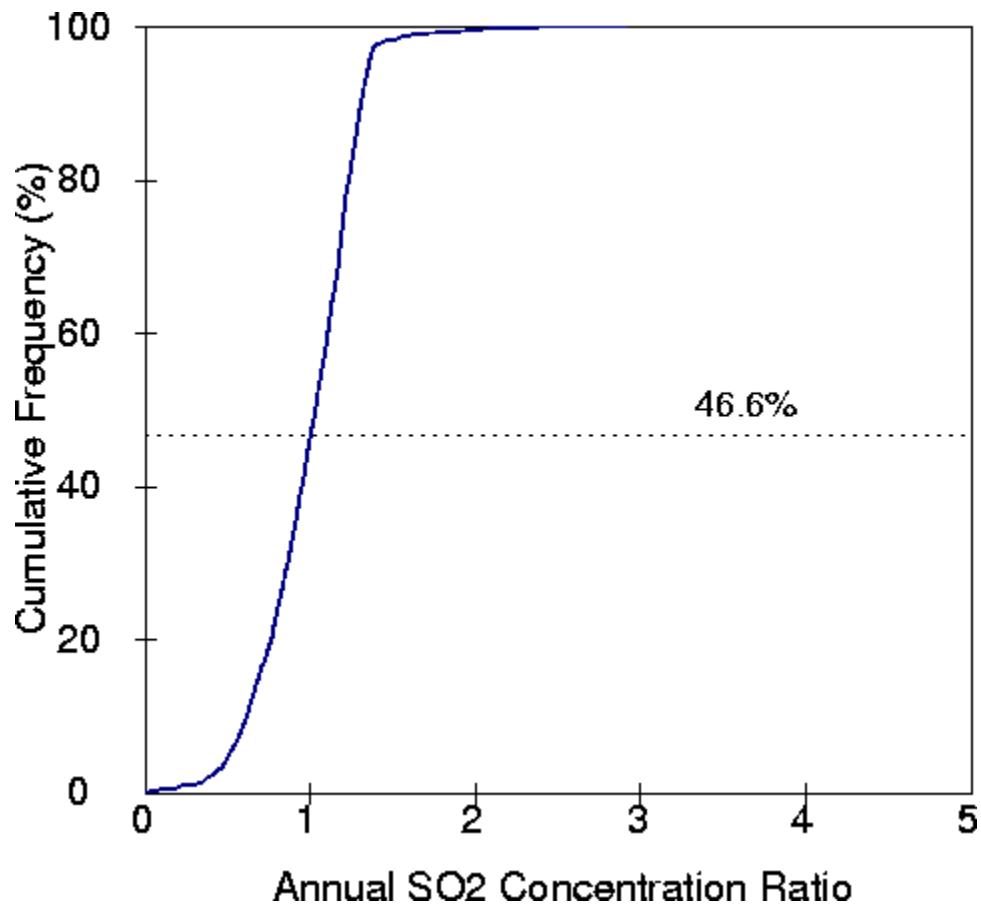


Figure 4-16. Cumulative frequency distribution of design ratios of SO₂ concentrations from ships at 125 km from the Northern Pacific U.S. coastline.

corresponding sulfate results are shown in Figures 4-17 and 4-18. The sulfate ratios are larger than one over the entire domain except for a few isolated locations. Over a large portion of the domain, the ratios range from 1.4 to 1.8. From Figure 4-18, we see that over 99.99% of the receptors have ratios larger than one. The results from the San Francisco Bay Area are similar to those that were obtained for the southern Pacific domain, which suggests that most of the ships impacting this area are within the modeling domains.

At 250 km from the coastline, the SO₂ ratios are less than one at nearly 100% of the receptors, as shown in Figures 4-19 and 4-20. However, sulfate ratios are still larger than one at a majority (nearly 96%) of the receptors, as shown in Figures 4-21 and 4-22.

The SO₂ ratios for ships at 375 km and 500 km from the North Pacific U.S. coastline are less than one at all the receptors and are not shown here. Figure 4-23 shows the spatial distribution of the sulfate ratios for ships at 375 km from the coastline, while Figure 4-24 shows the cumulative frequency distribution of the ratios. From Figure 4-24, we see that only about 20% of the receptors show ratios less than one. However, over a very large part of the domain, the ratios larger than one are usually in the range of 1 to 1.4, as shown in Figure 4-23. The largest ratios, in the range of 1.4 to 1.8, are concentrated in the western parts of southern Oregon and northern California, near the boundary between the two states. This area is in the center of the domain and is, therefore, exposed to the ship emissions located west and southwest from its coastline (see wind roses in Figure 3-7).

The sulfate results for ships at 500 km from the North Pacific U.S. coastline are shown in Figures 4-25 and 4-26. At a majority (56%) of the receptors, the ratios are less than one for ships at this distance. The largest ratios are again near the boundary region between California and Oregon. The results for the San Francisco Bay Area are significantly lower than those obtained for the southern Pacific domain because, at that distance, most of the ships that impact this area are located southwest of this area (see windroses in Figures 3-6 and 3-7).

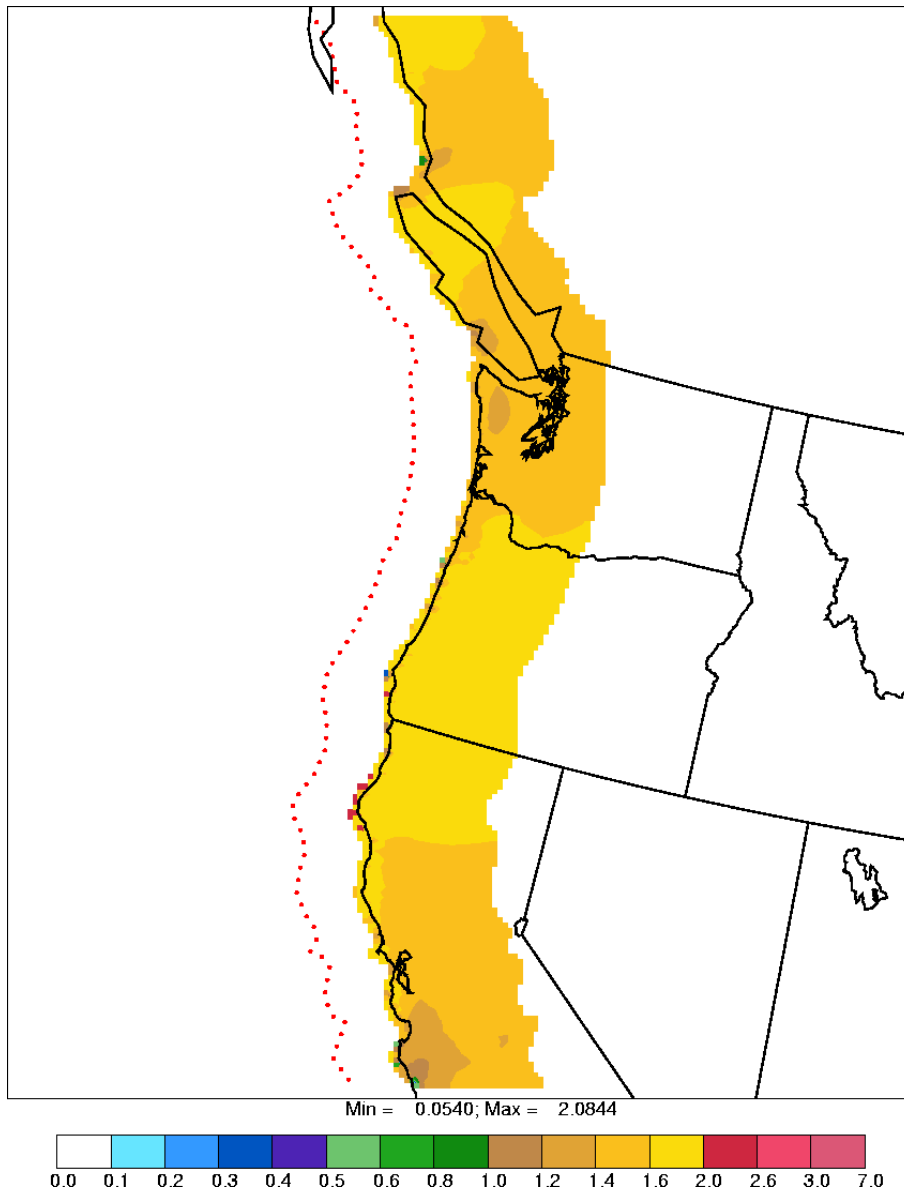


Figure 4-17. Ratios of annual-average sulfate concentrations due to sea-going ships burning high-sulfur fuel at 125 km from the Northern Pacific U.S. coastline to the concentrations (target values) due to dockside ships at the coastline burning low-sulfur fuel. The red dots represent the locations of the sea-going ships.

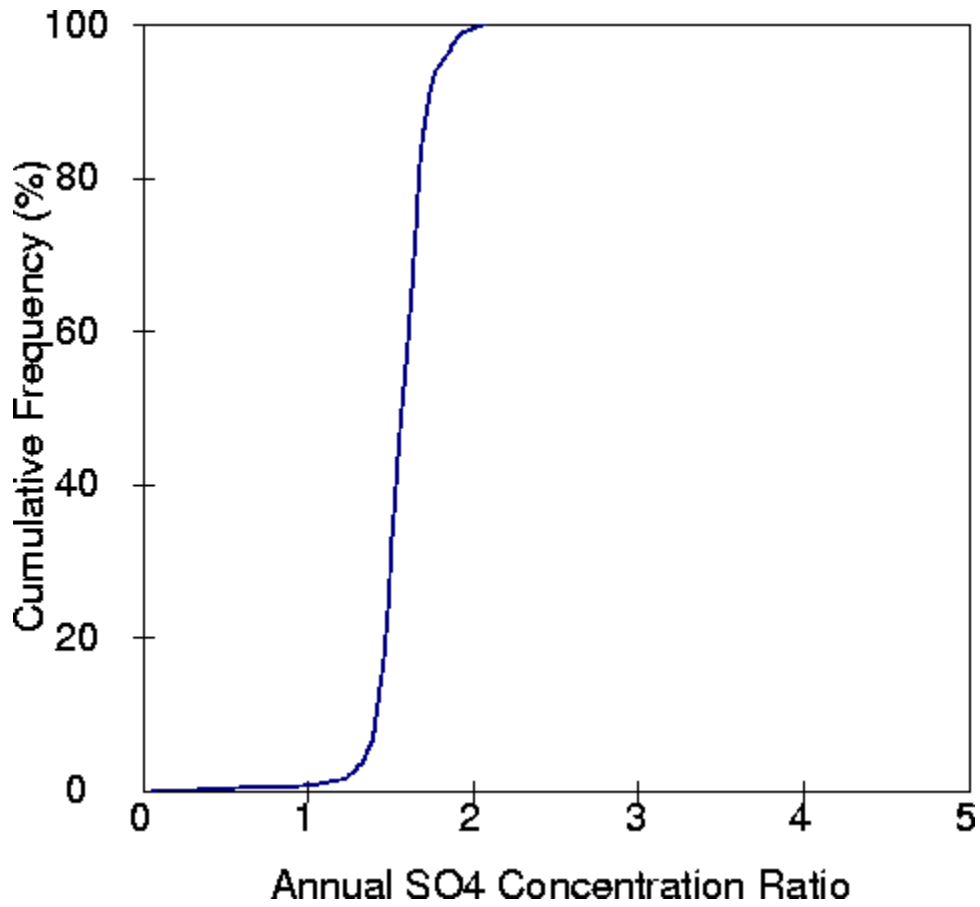


Figure 4-18. Cumulative frequency distribution of design ratios of sulfate concentrations from ships at 125 km from the Northern Pacific U.S. coastline.

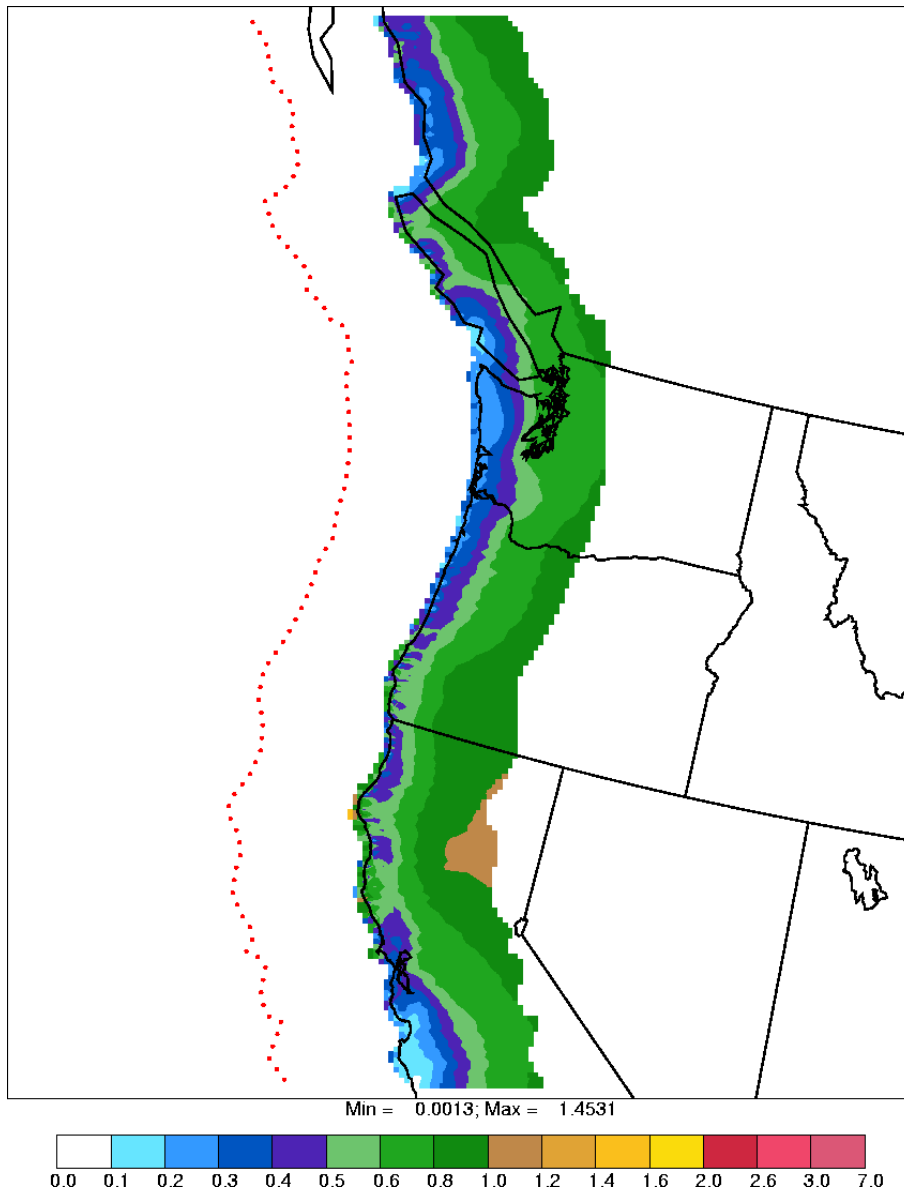


Figure 4-19. Ratios of annual-average SO_2 concentrations due to sea-going ships burning high-sulfur fuel at 250 km from the Northern Pacific U.S. coastline to the concentrations (target values) due to dockside ships at the coastline burning low-sulfur fuel. The red dots represent the locations of the sea-going ships.

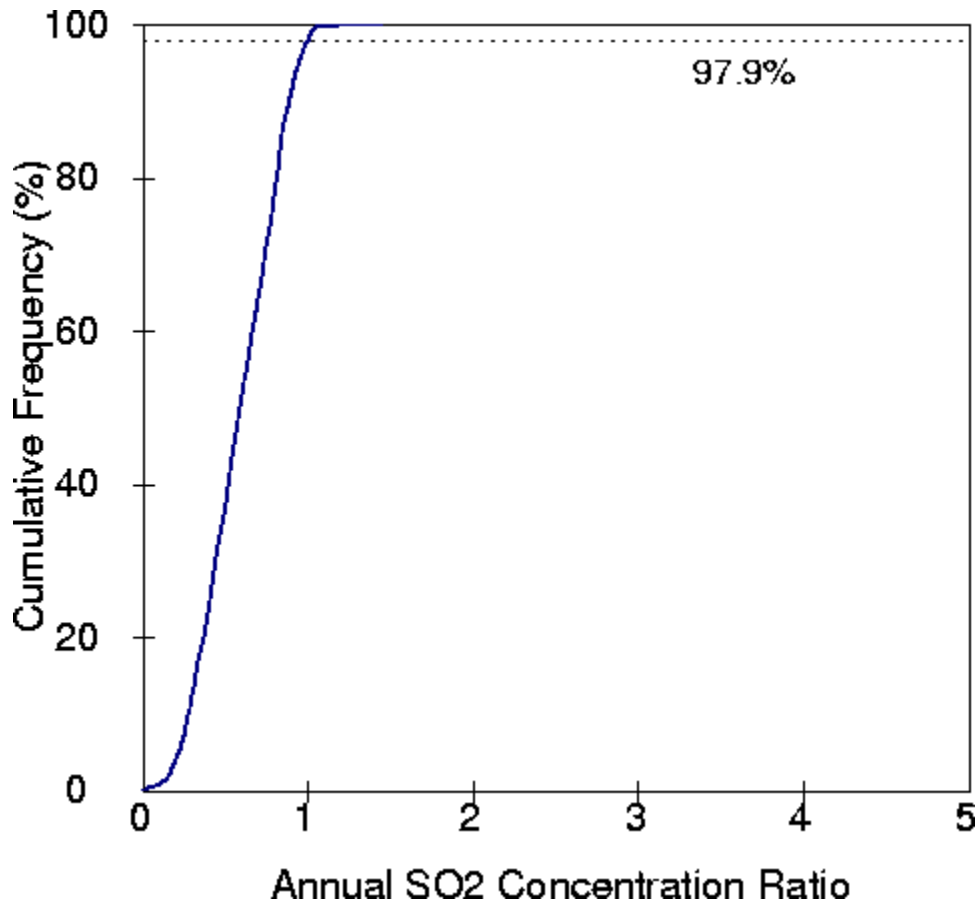


Figure 4-20. Cumulative frequency distribution of design ratios of SO₂ concentrations from ships at 250 km from the Northern Pacific U.S. coastline.

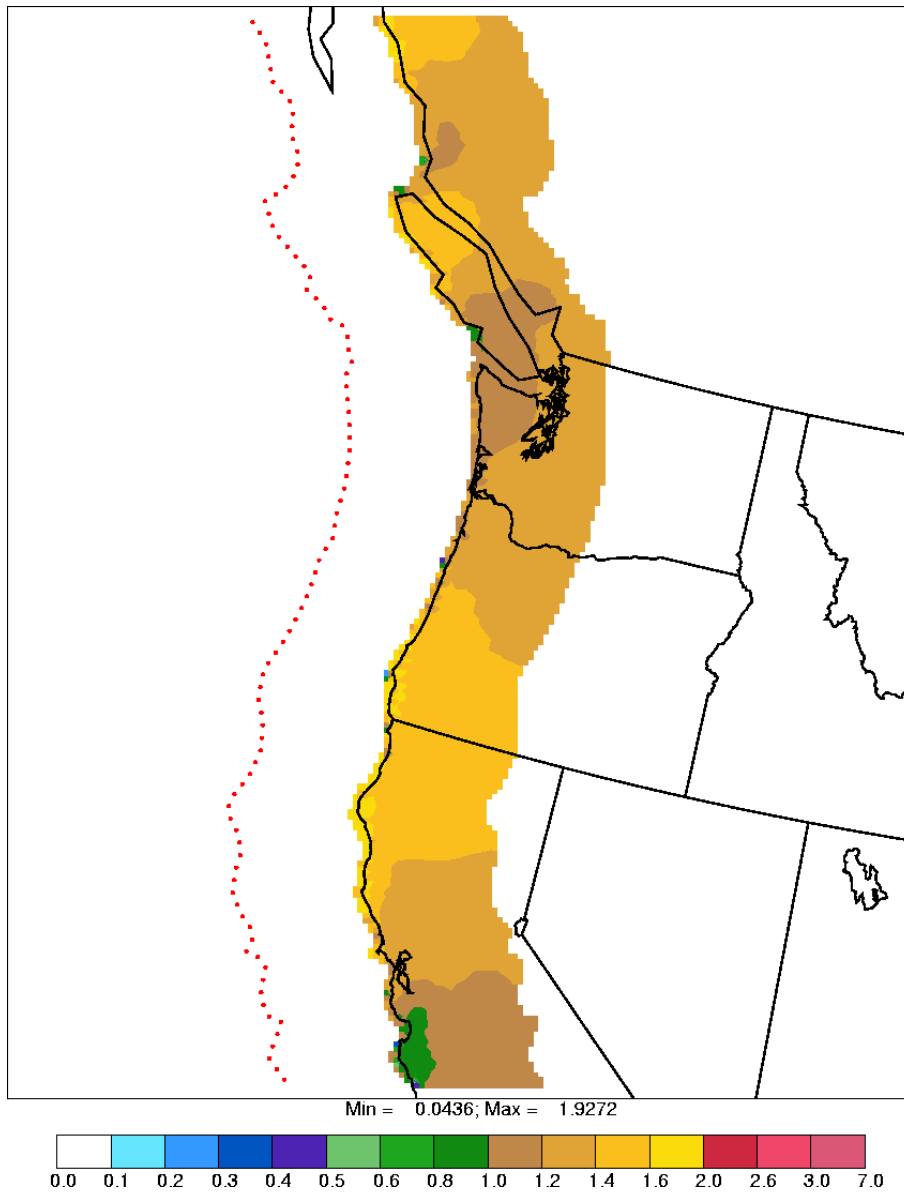


Figure 4-21. Ratios of annual-average sulfate concentrations due to sea-going ships burning high-sulfur fuel at 250 km from the Northern Pacific U.S. coastline to the concentrations (target values) due to dockside ships at the coastline burning low-sulfur fuel. The red dots represent the locations of the sea-going ships.

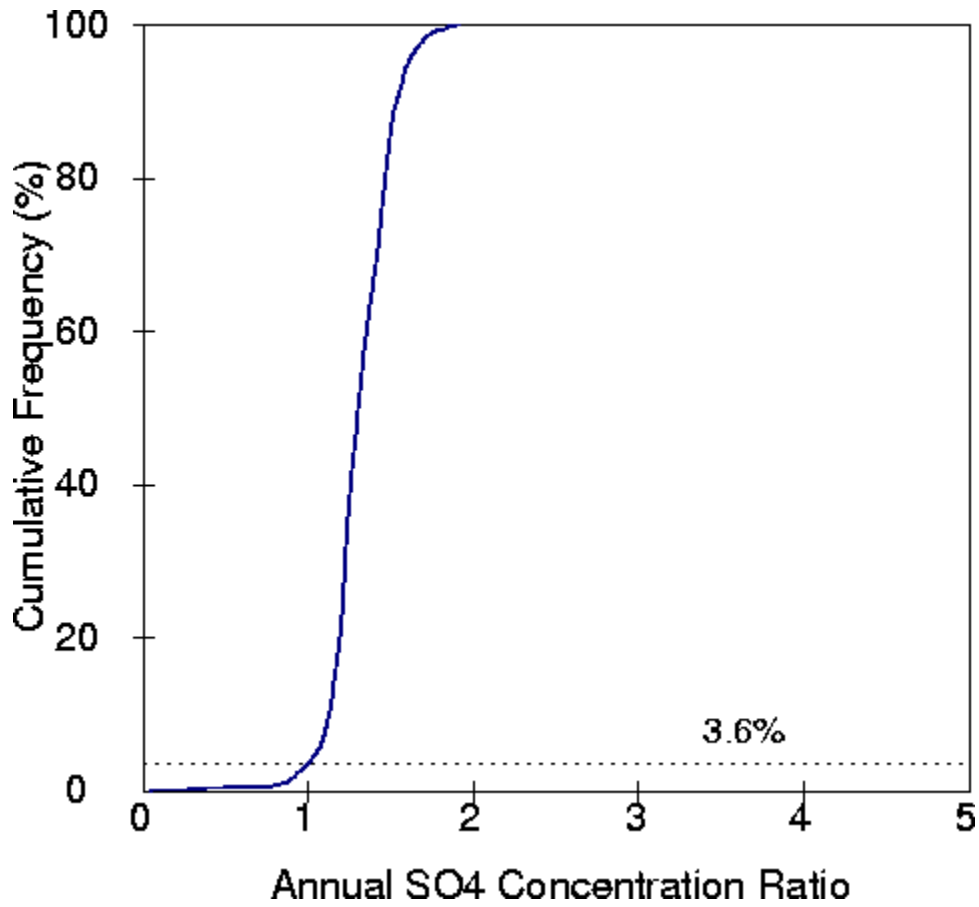


Figure 4-22. Cumulative frequency distribution of design ratios of sulfate concentrations from ships at 250 km from the Northern Pacific U.S. coastline.

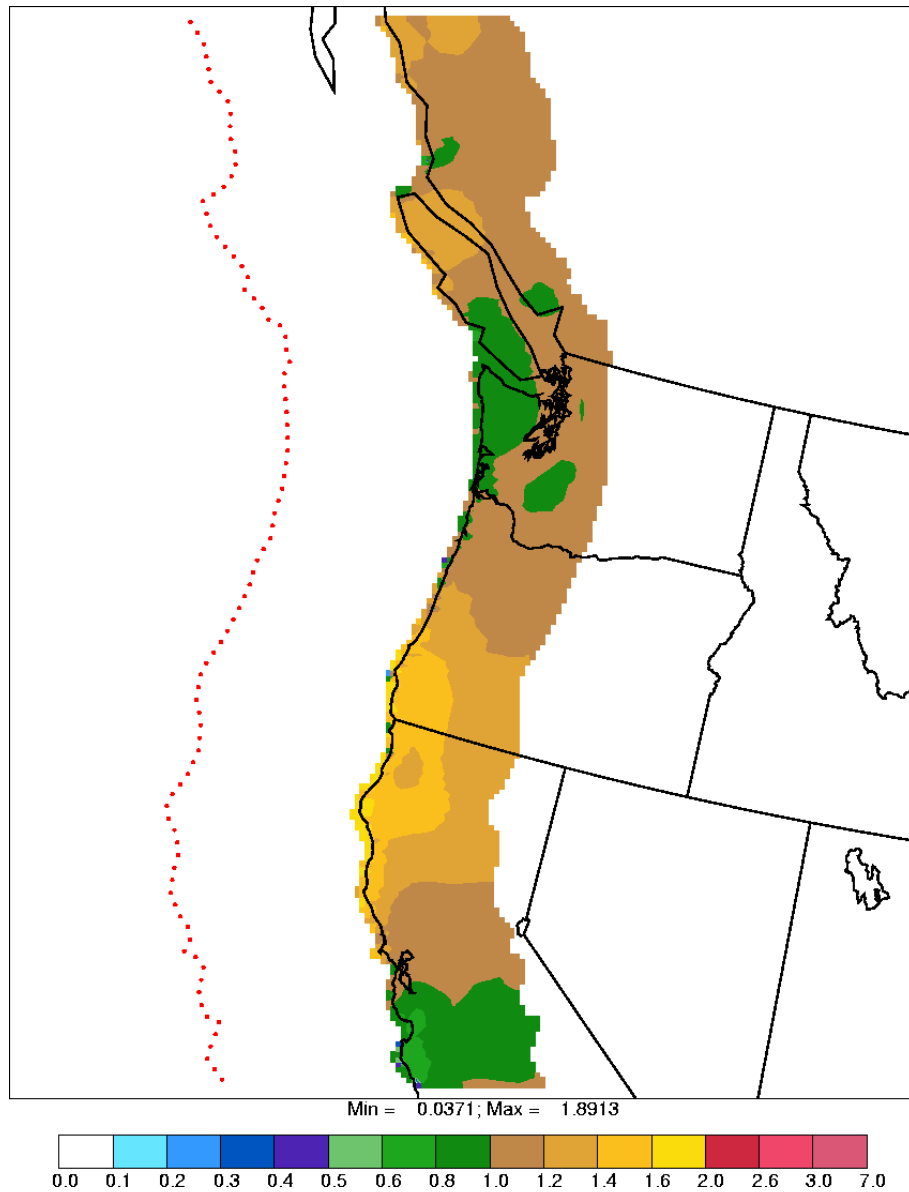


Figure 4-23. Ratios of annual-average sulfate concentrations due to sea-going ships burning high-sulfur fuel at 375 km from the Northern Pacific U.S. coastline to the concentrations (target values) due to dockside ships at the coastline burning low-sulfur fuel. The red dots represent the locations of the sea-going ships.

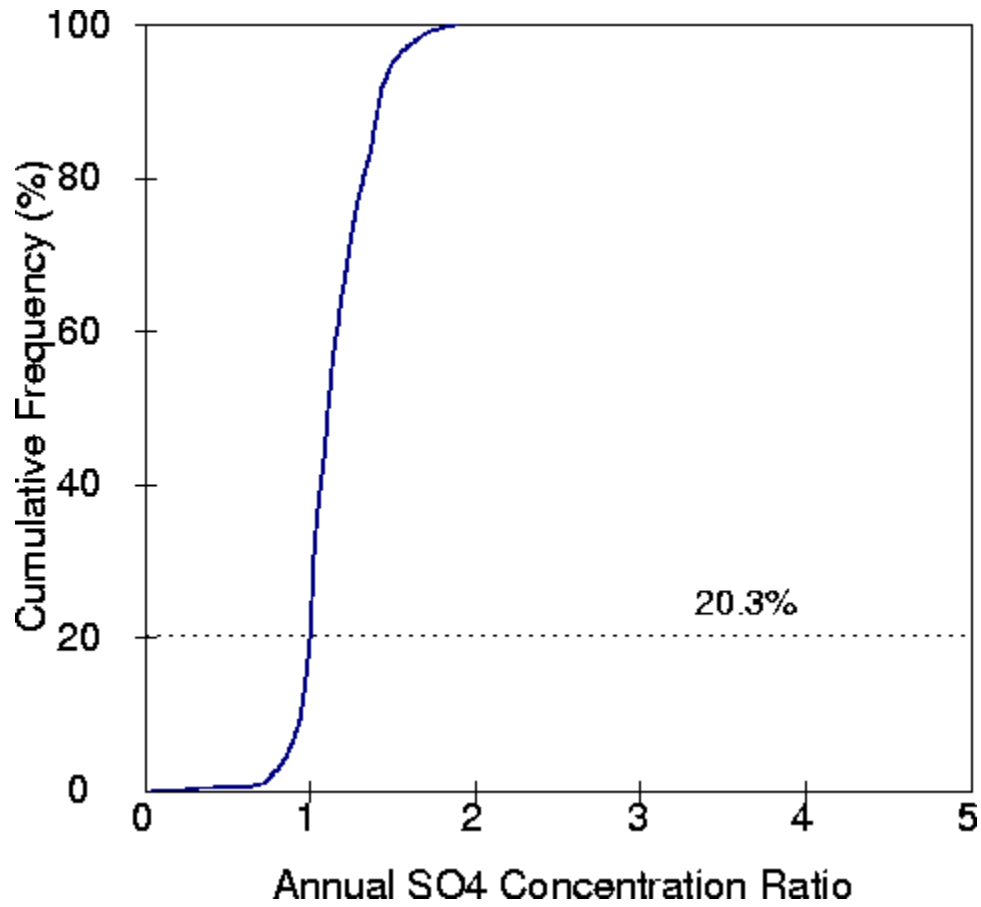


Figure 4-24. Cumulative frequency distribution of design ratios of sulfate concentrations from ships at 375 km from the Northern Pacific U.S. coastline.

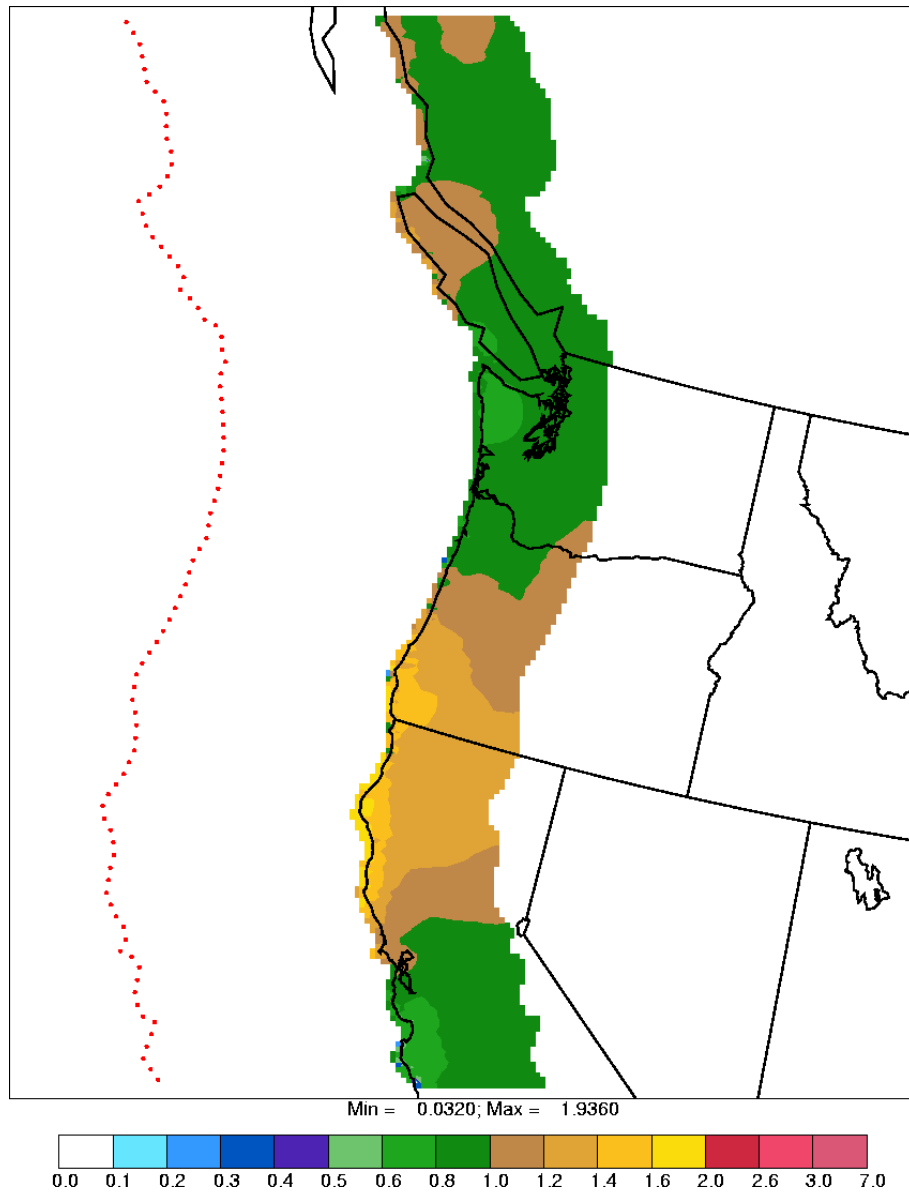


Figure 4-25. Ratios of annual-average sulfate concentrations due to sea-going ships burning high-sulfur fuel at 500 km from the Northern Pacific U.S. coastline to the concentrations (target values) due to dockside ships at the coastline burning low-sulfur fuel. The red dots represent the locations of the sea-going ships.

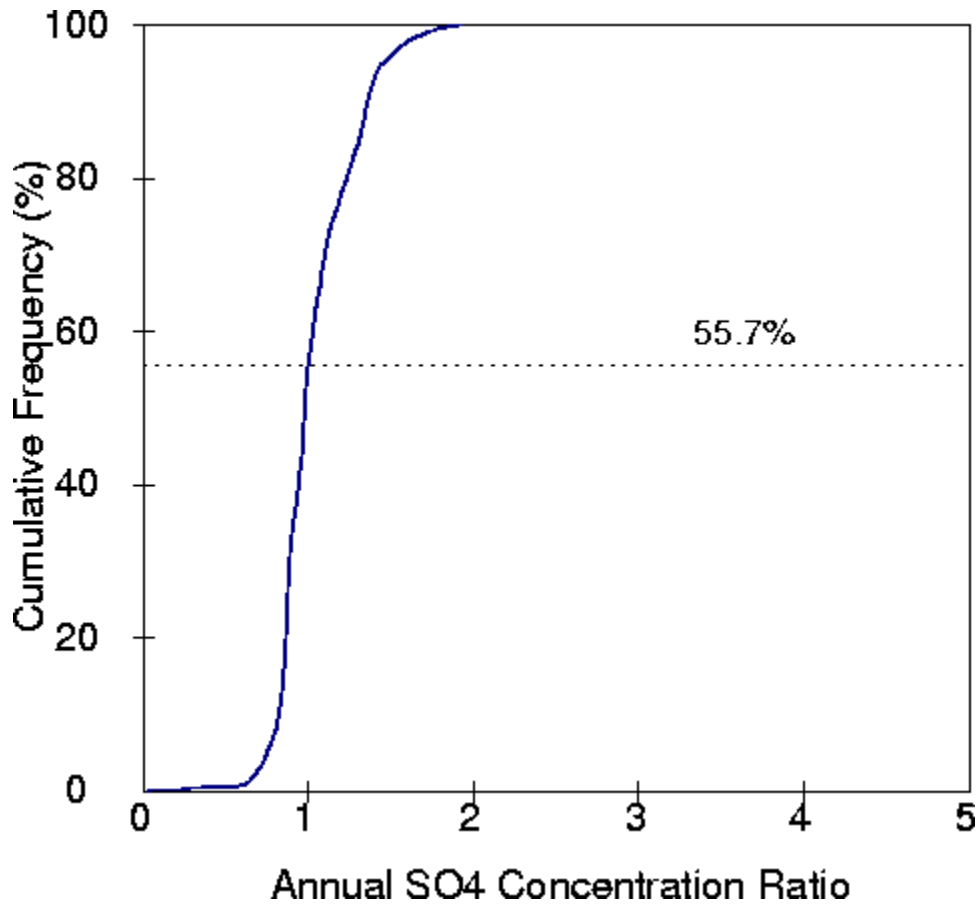


Figure 4-26. Cumulative frequency distribution of design ratios of sulfate concentrations from ships at 500 km from the Northern Pacific U.S. coastline.

4.3 Results for the Gulf of Mexico Coastline

The results for the Gulf of Mexico coastline are quite different from the two coastlines on the West Coast. The relative air quality impacts at land-based receptors from ships at sea are generally lower for the Gulf of Mexico than for the Pacific Ocean even for ships located at 125 km from the coastline. The SO₂ results for ships at 125 km from the Gulf of Mexico coastline are shown in Figures 4-27 and 4-28. From Figure 4-27, we see that the SO₂ ratios are less than one over most of the receptor network, except in southern Florida. The ratios are larger than one at only about 16% of the receptors, as shown in Figure 4-28. The larger values simulated in Florida result in part from the design of the “shipping lane” that is located 125 km south of the coastline but, in the case of Florida, closer from a coastline located directly east from the ships. Therefore, the fraction of receptors that have ratios below one should be seen as a lower limit.

The sulfate results for ships at 125 km from the Gulf of Mexico coastline, shown in Figures 4-29 and 4-30, are also different from the sulfate results for the Pacific Ocean coastlines. Nearly 40% of the receptors have sulfate ratios less than one. Ratios larger than one are seen in Florida, Georgia, Alabama, and portions of Mississippi and Louisiana, as well as at the tip of southern Texas near the border with Mexico.

The SO₂ results for ships at 250 km from the Gulf of Mexico coastline are shown in Figures 4-31 and 4-32. We see from Figure 4-31 that, except for a small region in southern Florida, the ratios at all the receptors are less than one. The percentage of receptors with ratios less than one is over 98%, as shown in Figure 4-32. Figures 4-33 and 4-34 show the 250 km results for sulfate. We see from Figure 4-33 that the region with sulfate ratios larger than one is confined to most of Florida and southern Georgia. Figure 4-34 shows that only 28% of the receptors have sulfate ratios larger than one.

We only show the sulfate results for the 375 km and 500 km distances from the Gulf of Mexico coastline, since all receptors satisfy the criterion of SO₂ ratios less than one at these distances. Figure 4-35 shows the spatial pattern of sulfate ratios for ships at 375 km from the coastline. Ratios larger than one are only seen in Florida and small areas of southern Georgia. From Figure 4-36, we see that over 80% of the receptors show sulfate ratios less than one.

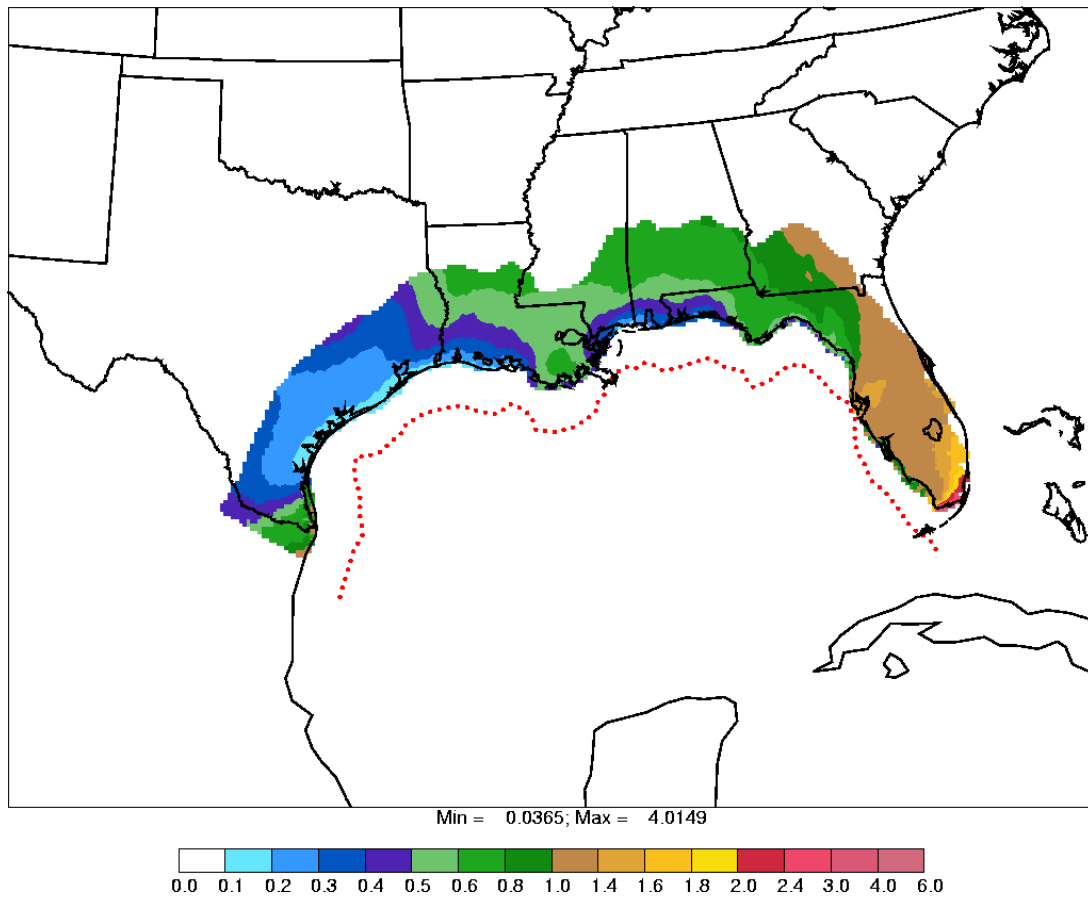


Figure 4-27. Ratios of annual-average SO₂ concentrations due to sea-going ships burning high-sulfur fuel at 125 km from the Gulf of Mexico coastline to the concentrations (target values) due to dockside ships at the coastline burning low-sulfur fuel. The red dots represent the locations of the sea-going ships.

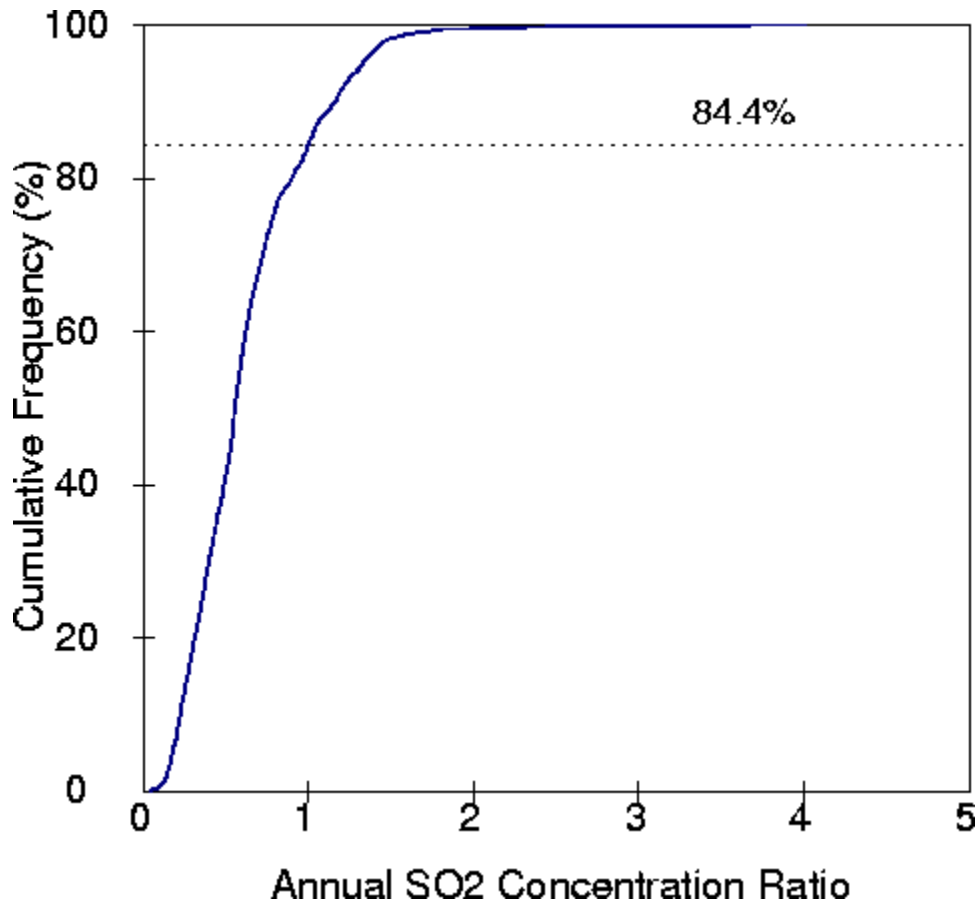


Figure 4-28. Cumulative frequency distribution of design ratios of SO₂ concentrations from ships at 125 km from the Gulf of Mexico coastline.

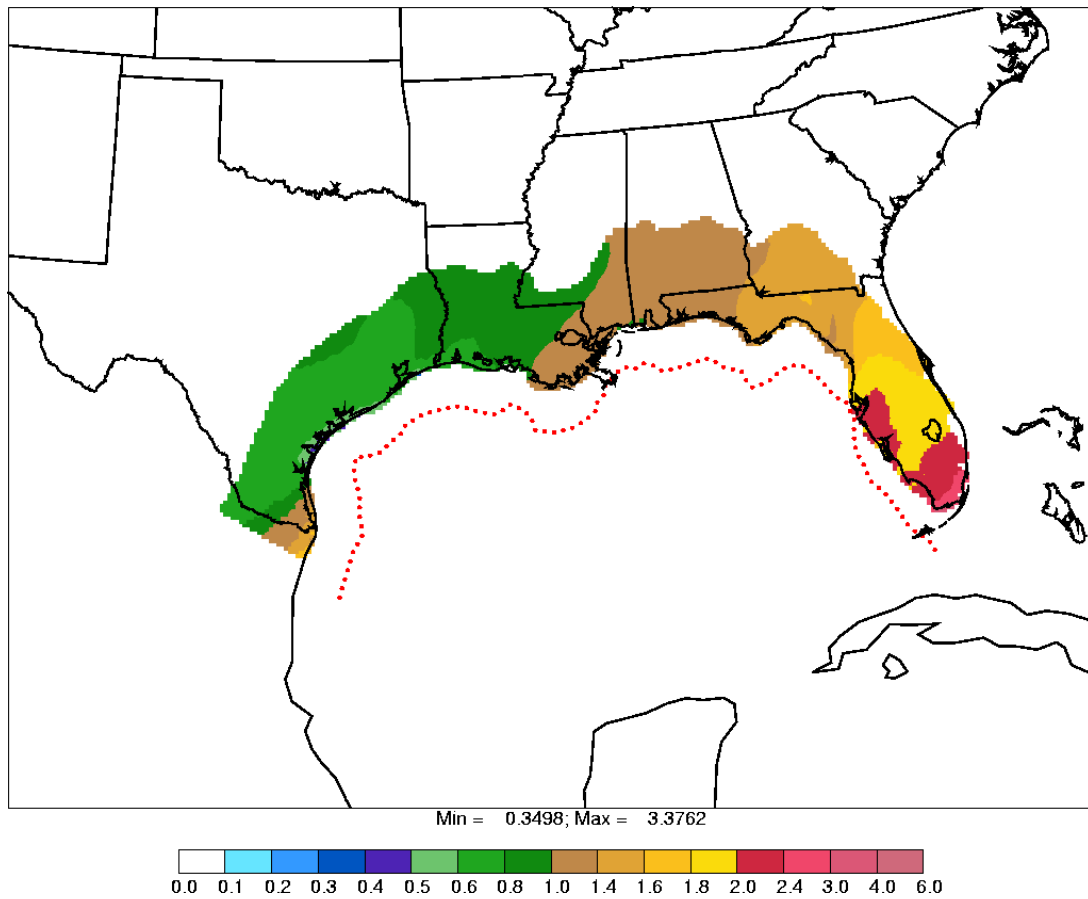


Figure 4-29. Ratios of annual-average sulfate concentrations due to sea-going ships burning high-sulfur fuel at 125 km from the Gulf of Mexico coastline to the concentrations (target values) due to dockside ships at the coastline burning low-sulfur fuel. The red dots represent the locations of the sea-going ships.

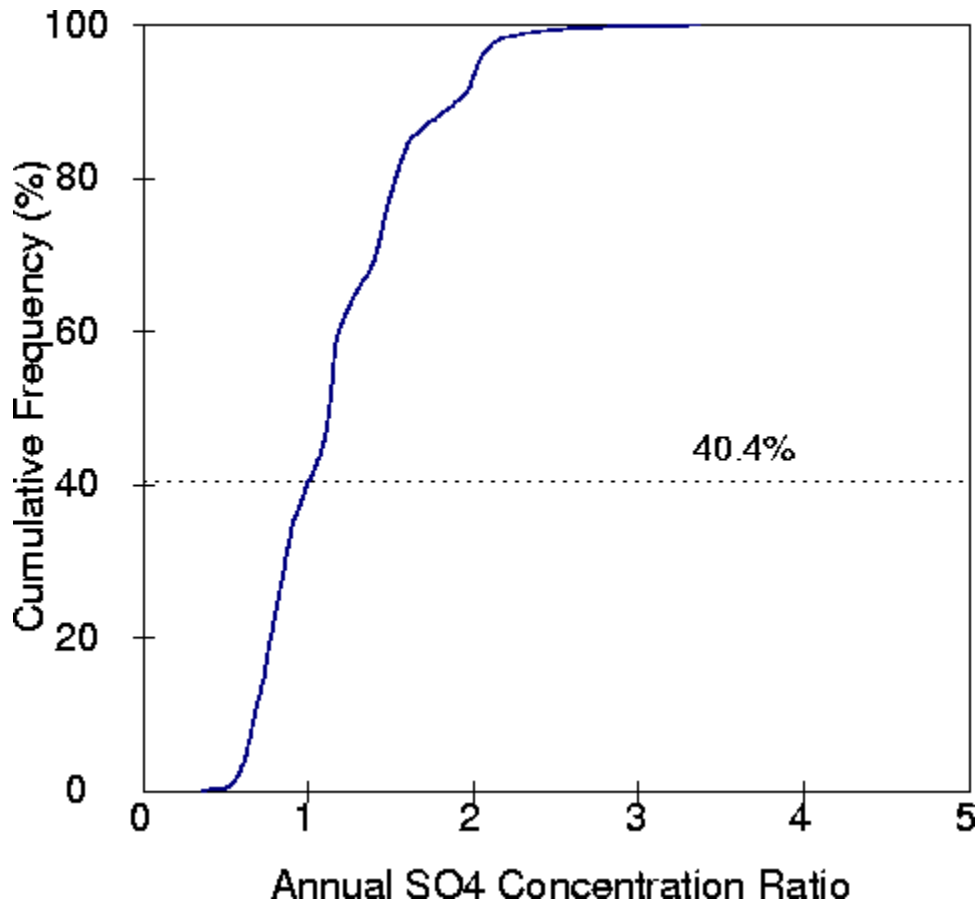


Figure 4-30. Cumulative frequency distribution of design ratios of sulfate concentrations from ships at 125 km from the Gulf of Mexico coastline.

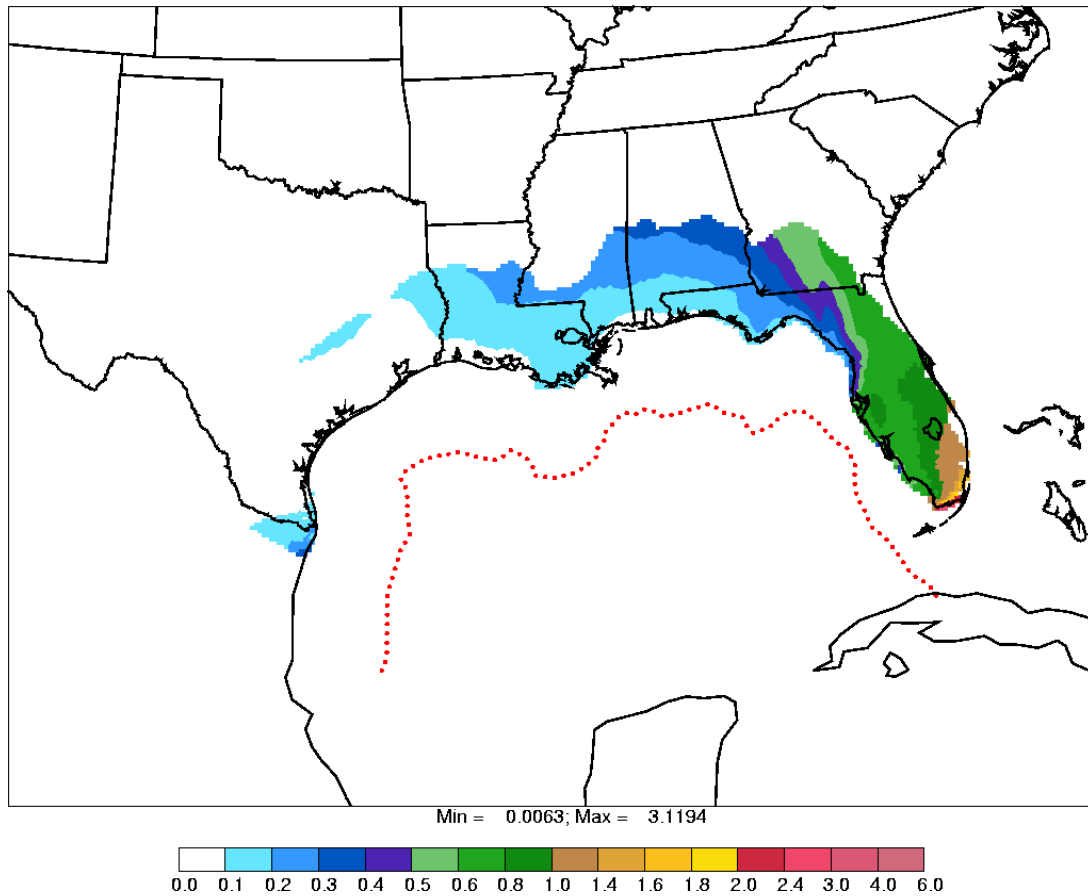


Figure 4-31. Ratios of annual-average SO_2 concentrations due to sea-going ships burning high-sulfur fuel at 250 km from the Gulf of Mexico coastline to the concentrations (target values) due to dockside ships at the coastline burning low-sulfur fuel. The red dots represent the locations of the sea-going ships.

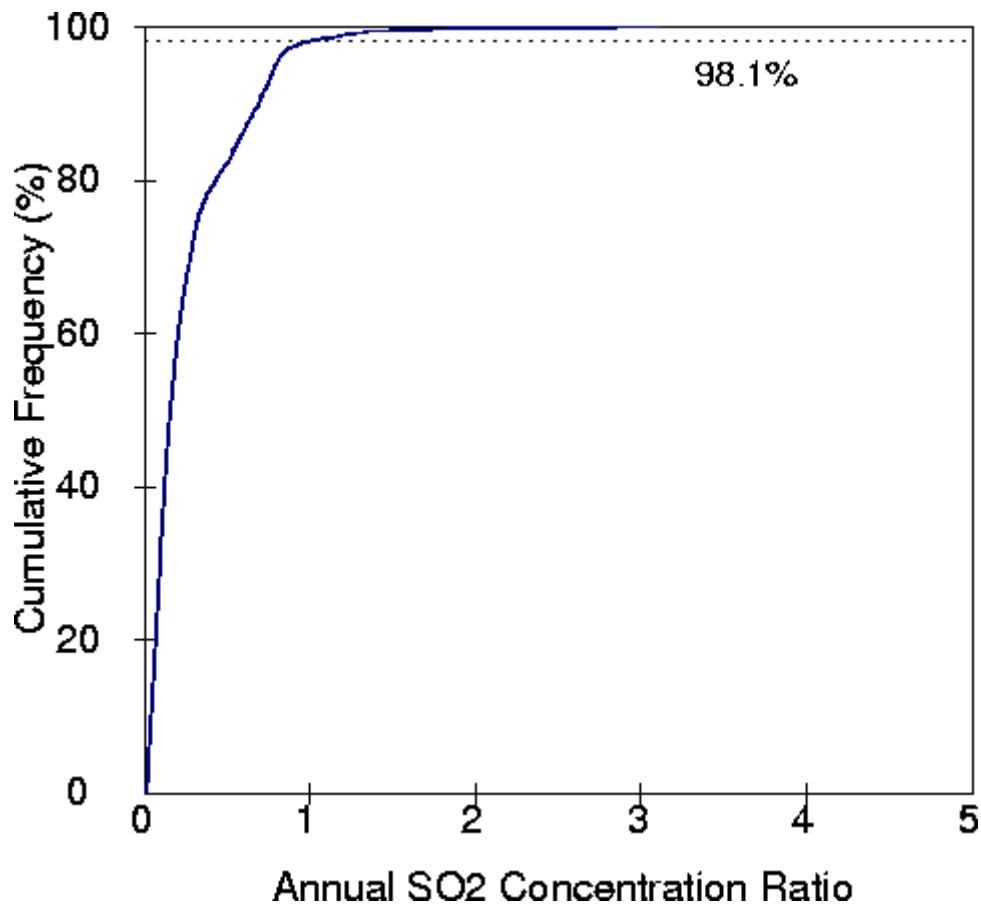


Figure 4-32. Cumulative frequency distribution of design ratios of SO₂ concentrations from ships at 250 km from the Gulf of Mexico coastline.

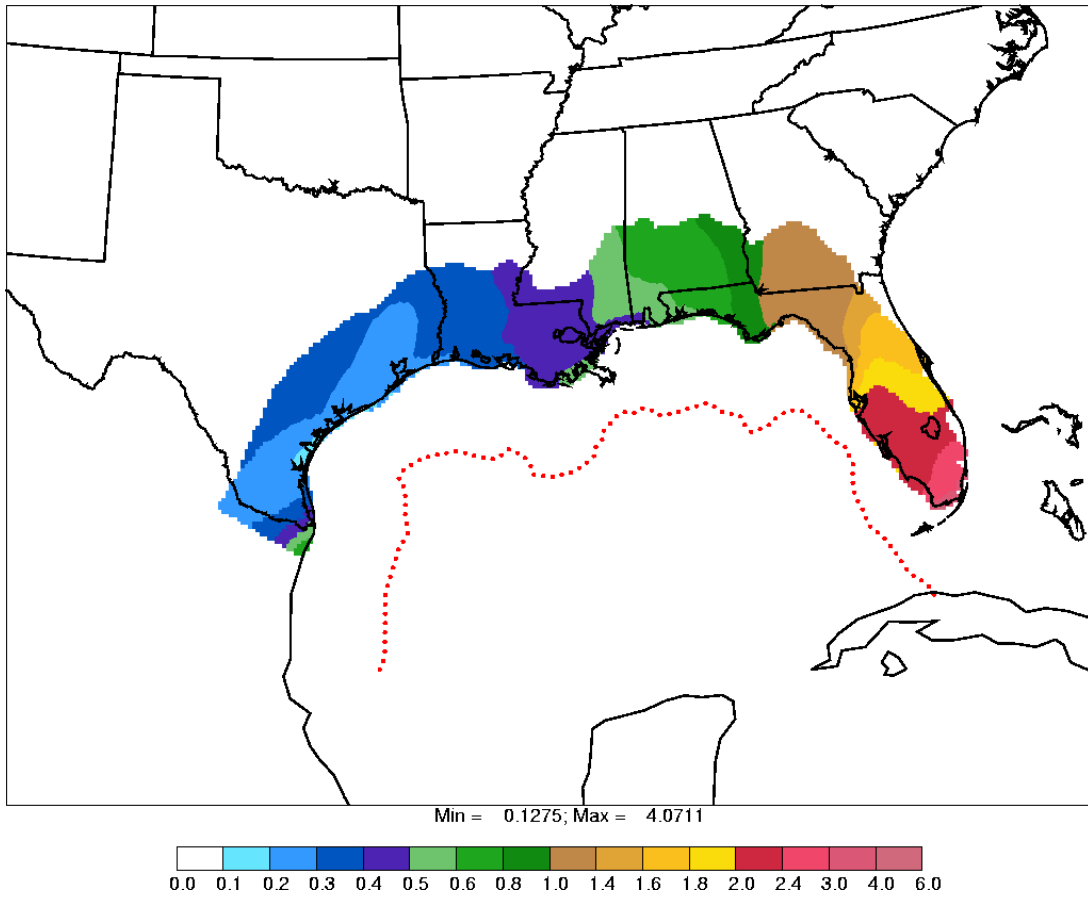


Figure 4-33. Ratios of annual-average sulfate concentrations due to sea-going ships burning high-sulfur fuel at 250 km from the Gulf of Mexico coastline to the concentrations (target values) due to dockside ships at the coastline burning low-sulfur fuel. The red dots represent the locations of the sea-going ships.

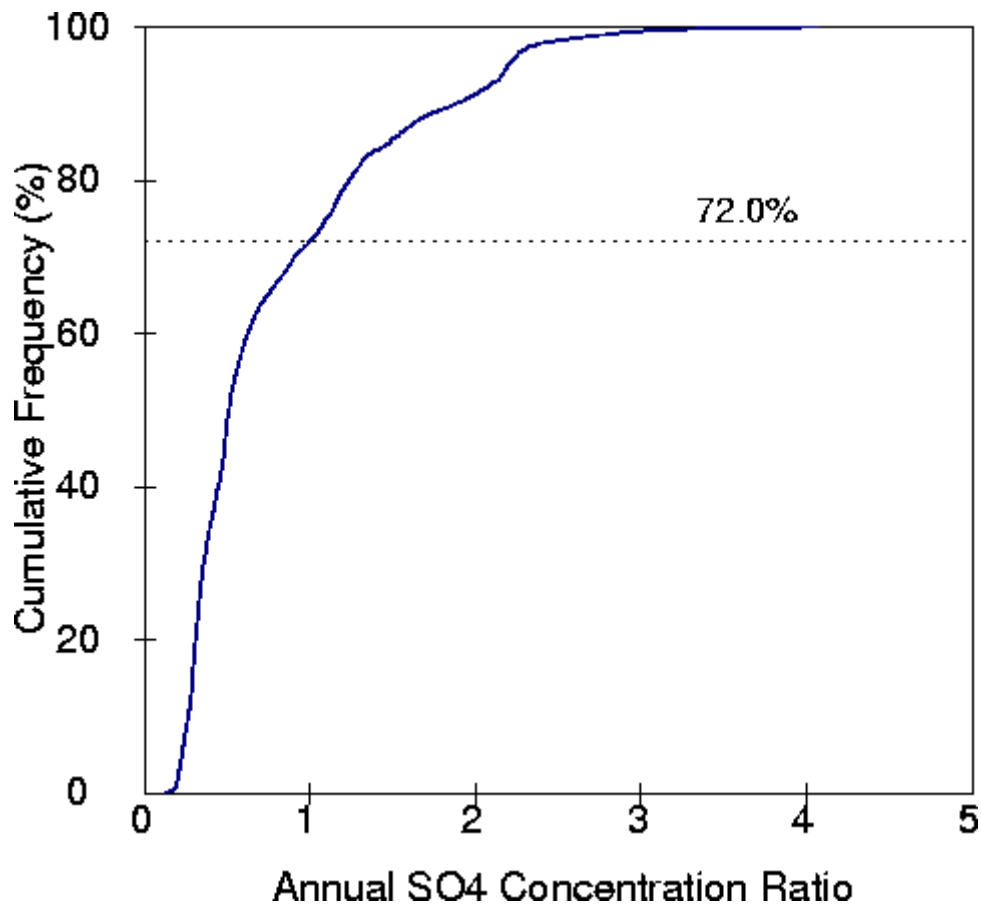


Figure 4-34. Cumulative frequency distribution of design ratios of sulfate concentrations from ships at 250 km from the Gulf of Mexico coastline.

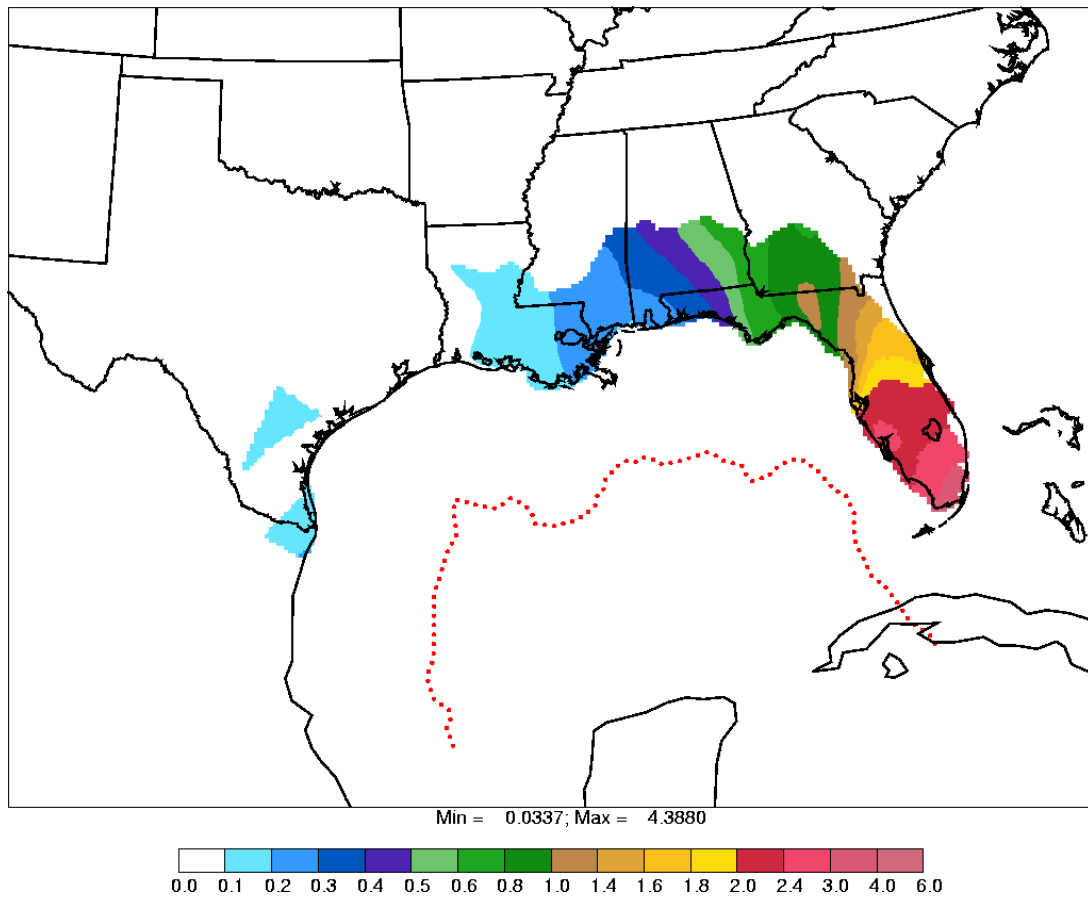


Figure 4-35. Ratios of annual-average sulfate concentrations due to sea-going ships burning high-sulfur fuel at 375 km from the Gulf of Mexico coastline to the concentrations (target values) due to dockside ships at the coastline burning low-sulfur fuel. The red dots represent the locations of the sea-going ships.

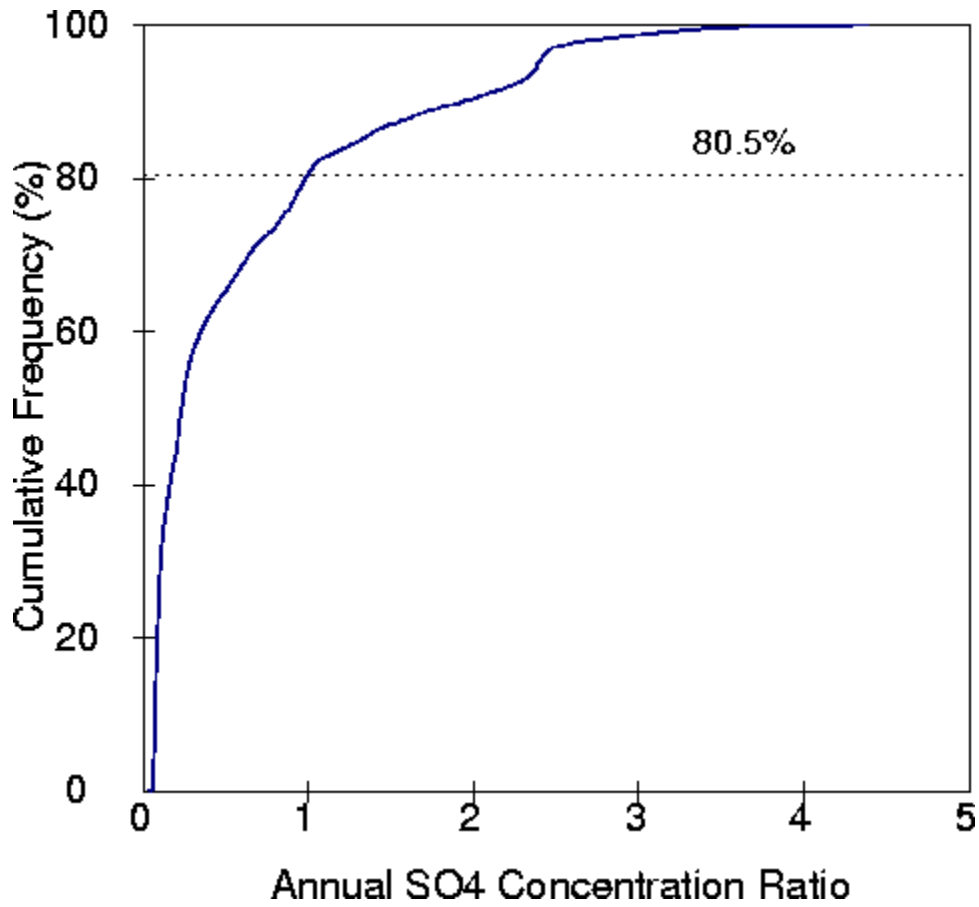


Figure 4-36. Cumulative frequency distribution of design ratios of sulfate concentrations from ships at 375 km from the Gulf of Mexico coastline.

The sulfate results for ships at 500 km from the Gulf of Mexico coastline are qualitatively similar to the 375 km distance results, as shown in Figures 4-37 and 4-38. For the 500 km scenario, sulfate ratios are larger than one only in Florida, as shown in Figure 4-37. Figure 4-38 shows that the percentage of receptors with sulfate ratios less than one increases only marginally (by about 3.5%) when the ships are placed at 500 km instead of 375 km.

4.4 Results for the Atlantic Ocean Coastline

Figure 4-39 shows the spatial distribution of annual-average SO₂ ratios for ships at 125 km from the Atlantic Ocean coastline, while Figure 4-40 shows the cumulative frequency distribution of the ratios. As in the case of the Gulf of Mexico coastline, the SO₂ ratios are less than one for a majority of the receptors at the 125 km distance. From Figure 4-39, we see that the ratios are larger than one only in southern Georgia, most of North Carolina, and portions of Connecticut and Massachusetts. The percentage of receptors with SO₂ ratios less than one is nearly 87%, as shown in Figure 4-40. In contrast, the 125 km sulfate results for the Atlantic Ocean show that the ratios are larger than one for almost the entire domain, as shown in Figures 4-41 and 4-42.

The SO₂ results for ships at 250 km from the Atlantic Ocean coastline are shown in Figures 4-43 and 4-44. At this distance, the SO₂ ratios are less than one throughout the domain. Figures 4-45 and 4-46 show the corresponding results for sulfate. We see from Figure 4-45 that sulfate ratios are less than one in the southeastern U.S. (Florida, Georgia, and South Carolina) and some of the New England states, such as Vermont, New Hampshire and Maine. The ratios are larger than one in most of North Carolina, eastern Virginia, eastern Pennsylvania, New Jersey, southern New York, Connecticut, Rhode Island, and southern Massachusetts. Figure 4-46 shows that the sulfate ratios are less than one at nearly 58% of the receptors.

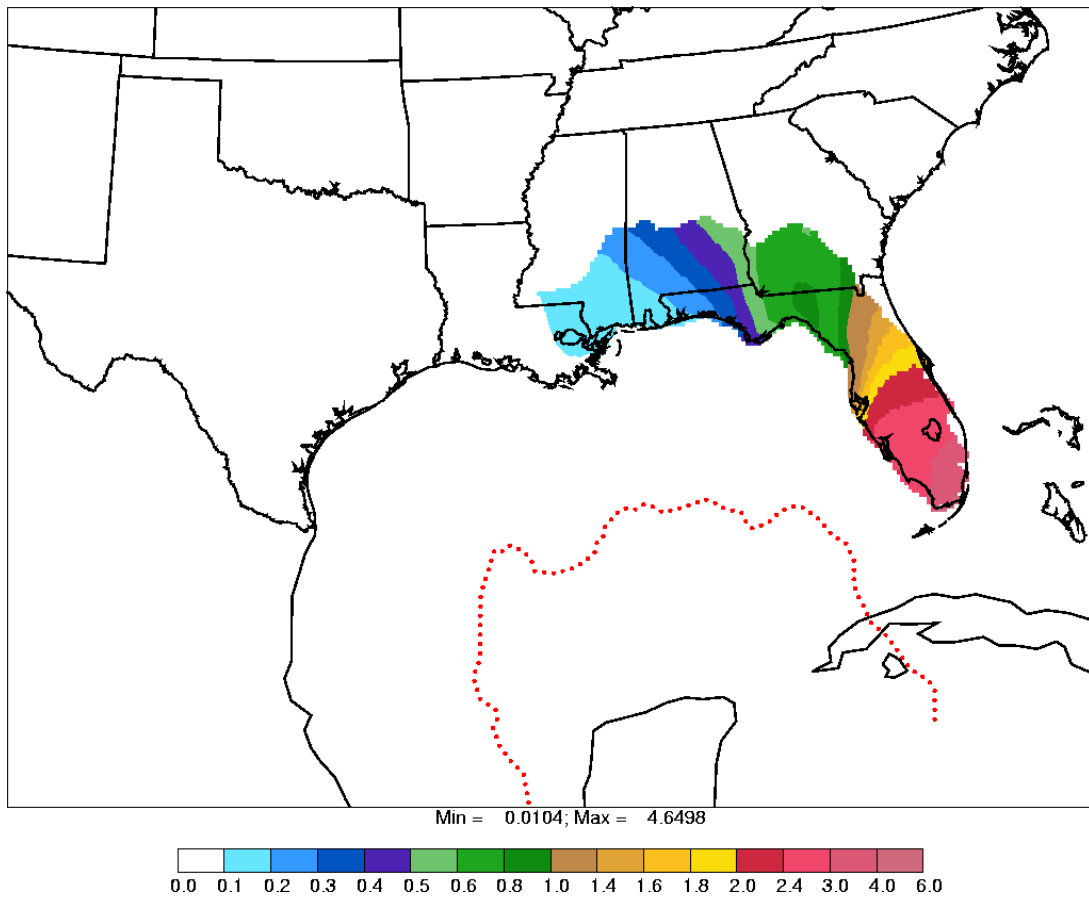


Figure 4-37. Ratios of annual-average sulfate concentrations due to sea-going ships burning high-sulfur fuel at 500 km from the Gulf of Mexico coastline to the concentrations (target values) due to dockside ships at the coastline burning low-sulfur fuel. The red dots represent the locations of the sea-going ships.

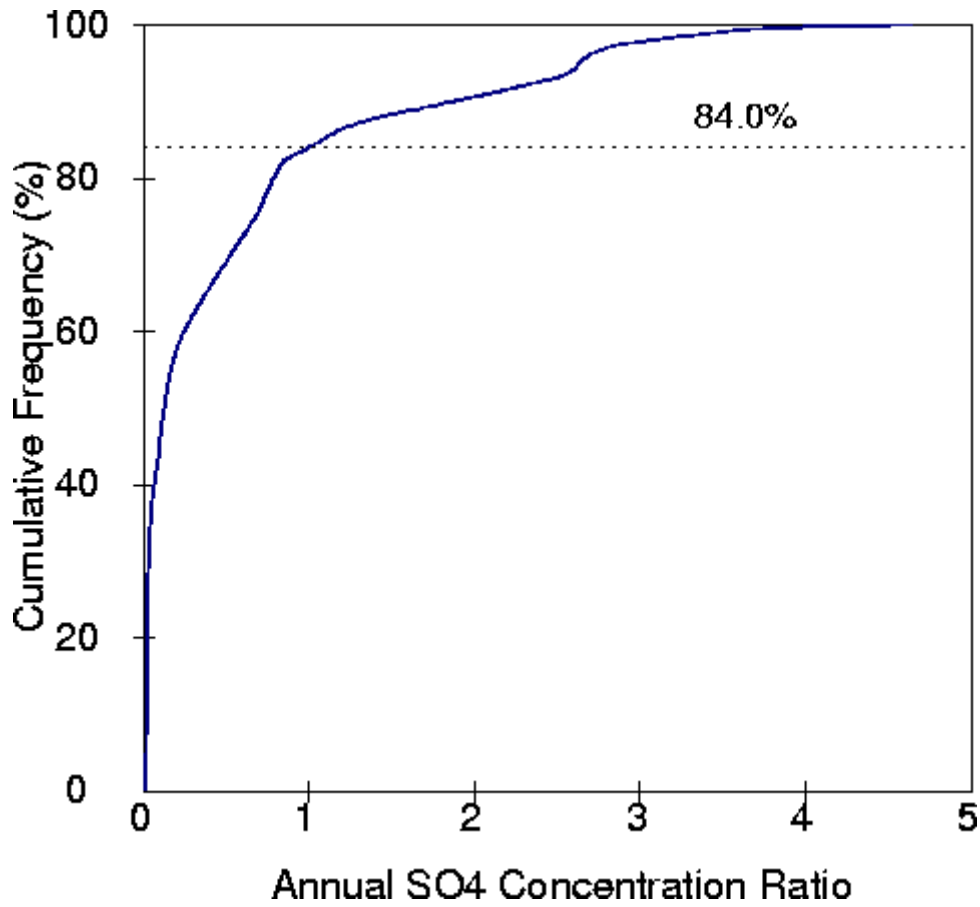


Figure 4-38. Cumulative frequency distribution of design ratios of sulfate concentrations from ships at 500 km from the Gulf of Mexico coastline.

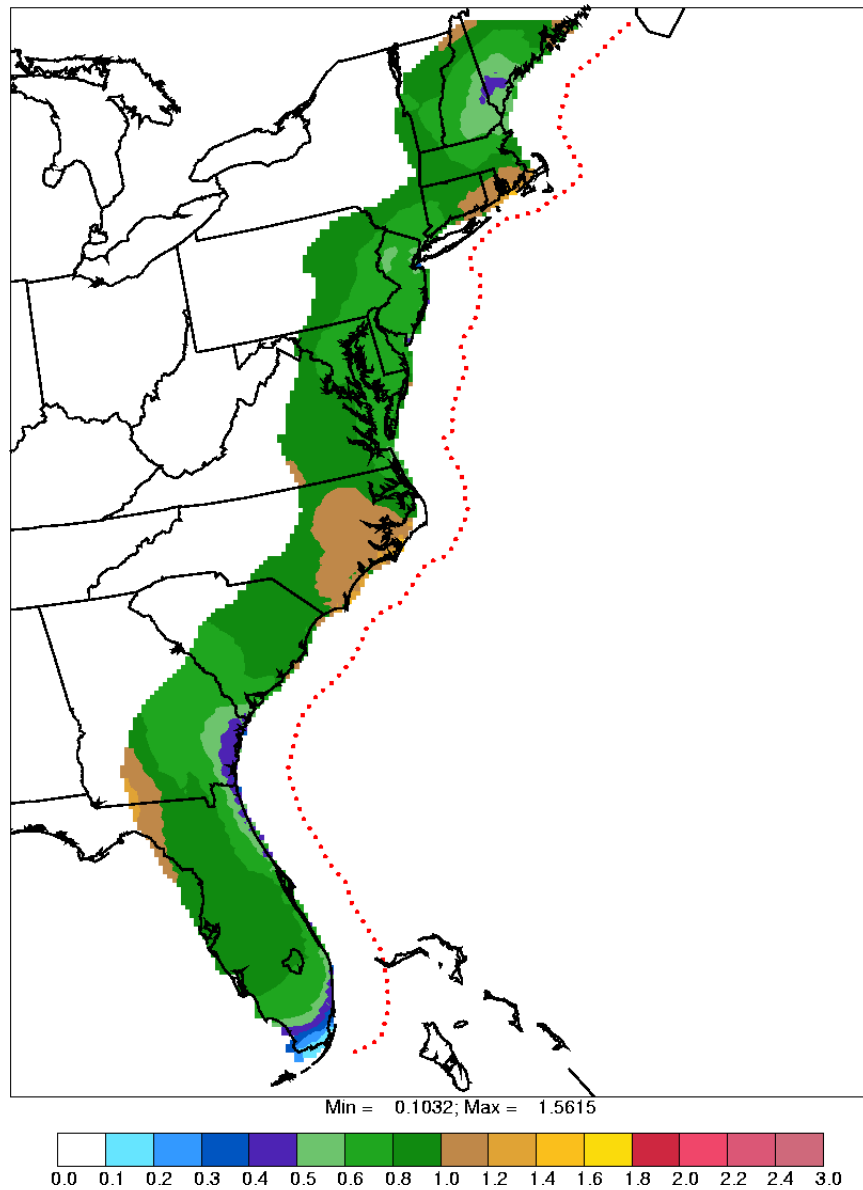


Figure 4-39. Ratios of annual-average SO₂ concentrations due to sea-going ships burning high-sulfur fuel at 125 km from the Atlantic Ocean coastline to the concentrations (target values) due to dockside ships at the coastline burning low-sulfur fuel. The red dots represent the locations of the sea-going ships.

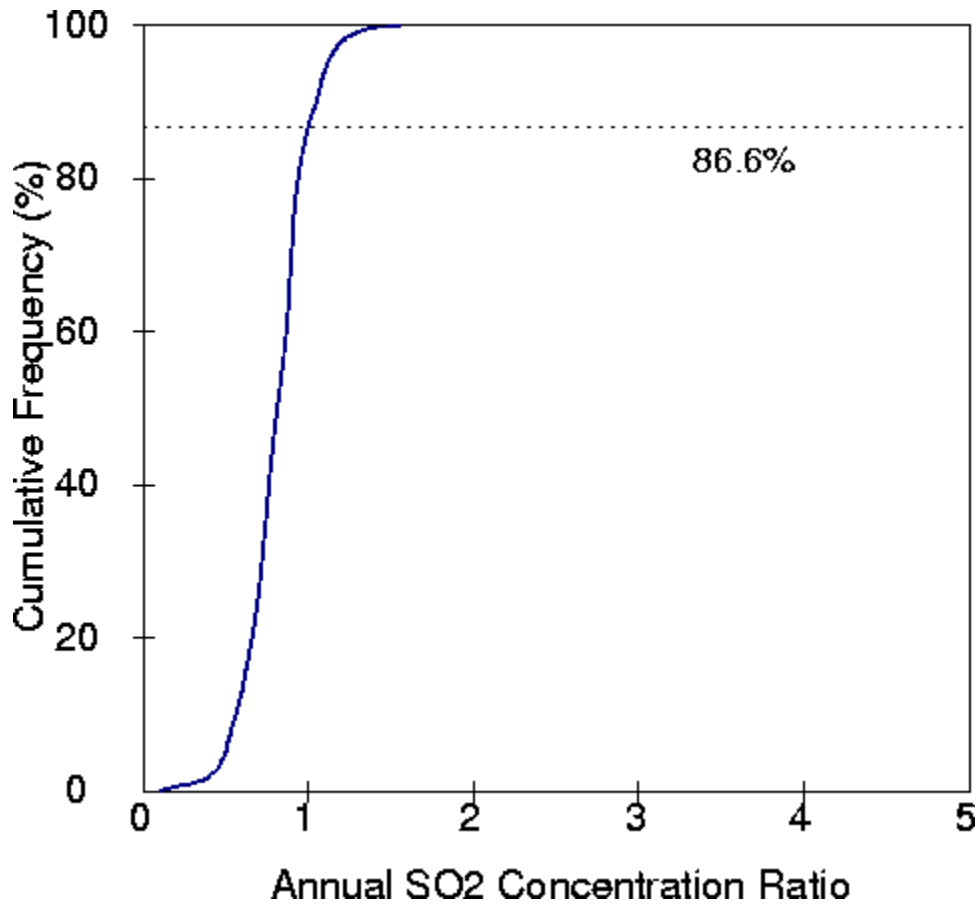


Figure 4-40. Cumulative frequency distribution of design ratios of SO₂ concentrations from ships at 125 km from the Atlantic Ocean coastline.

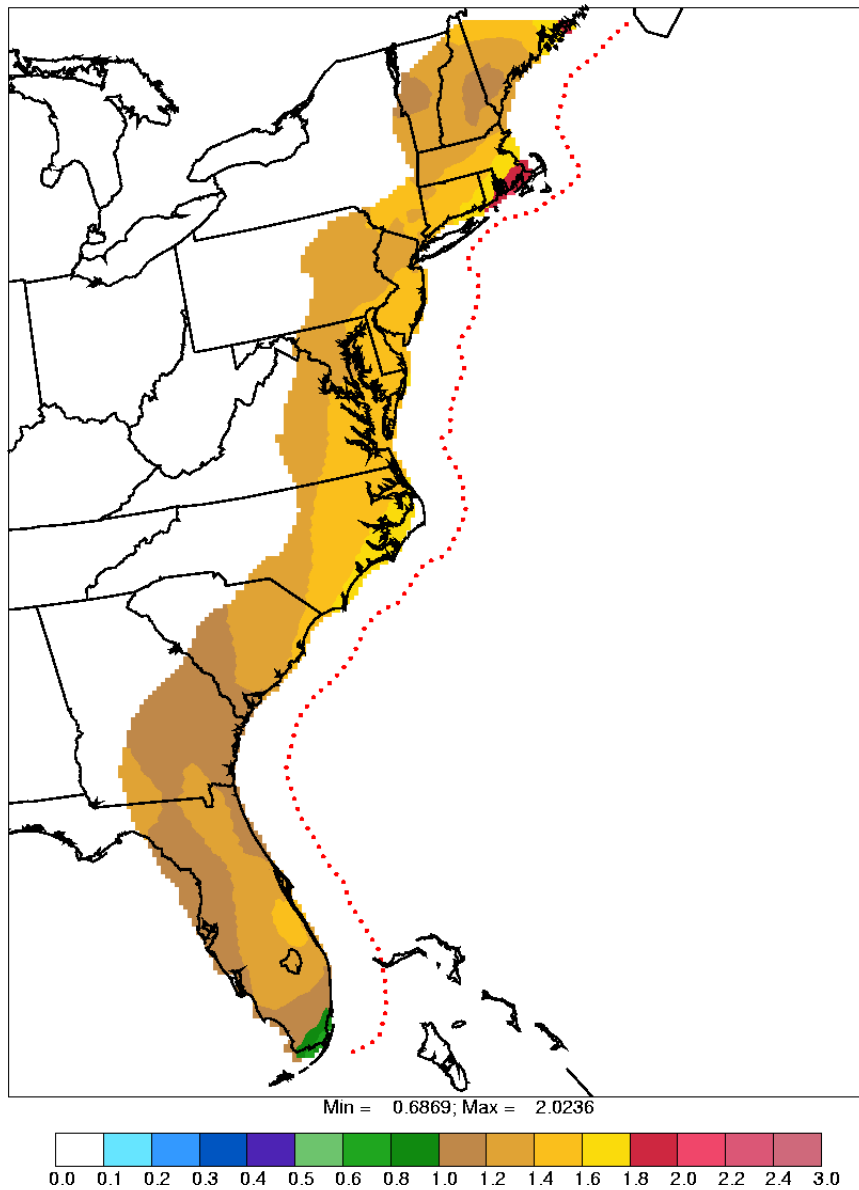


Figure 4-41. Ratios of annual-average sulfate concentrations due to sea-going ships burning high-sulfur fuel at 125 km from the Atlantic Ocean coastline to the concentrations (target values) due to dockside ships at the coastline burning low-sulfur fuel. The red dots represent the locations of the sea-going ships.

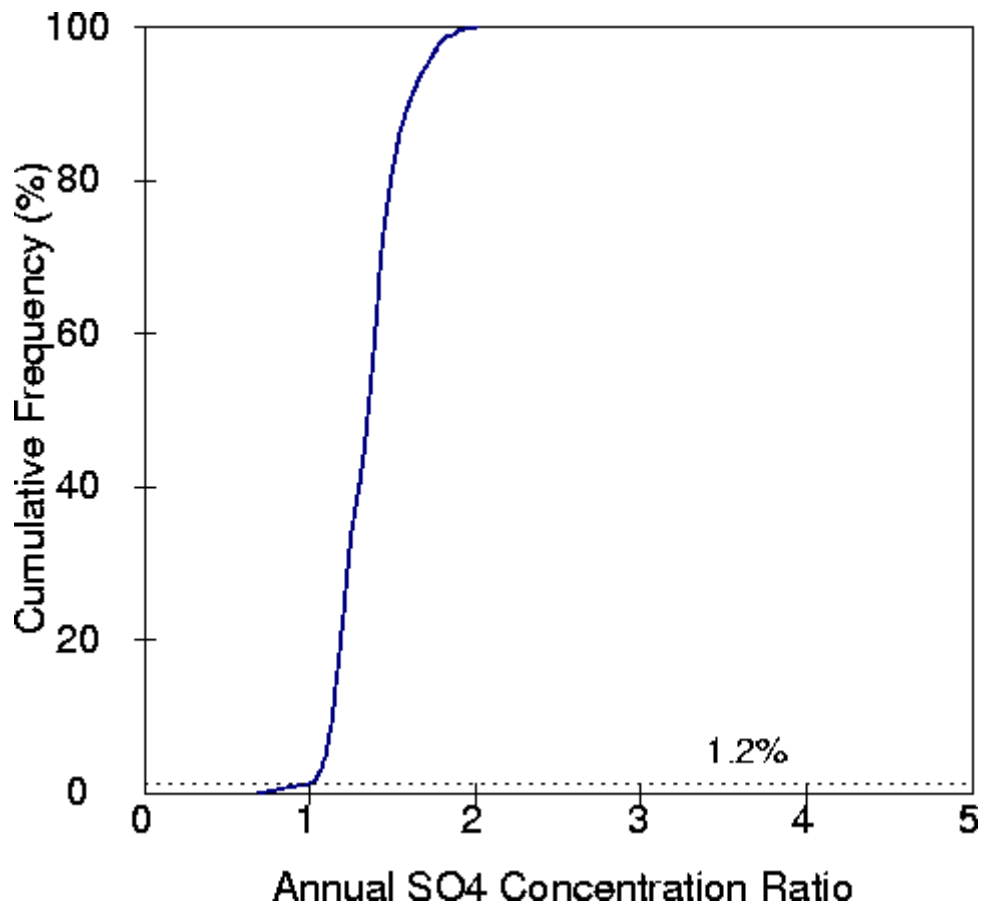


Figure 4-42. Cumulative frequency distribution of design ratios of sulfate concentrations from ships at 125 km from the Atlantic Ocean coastline.

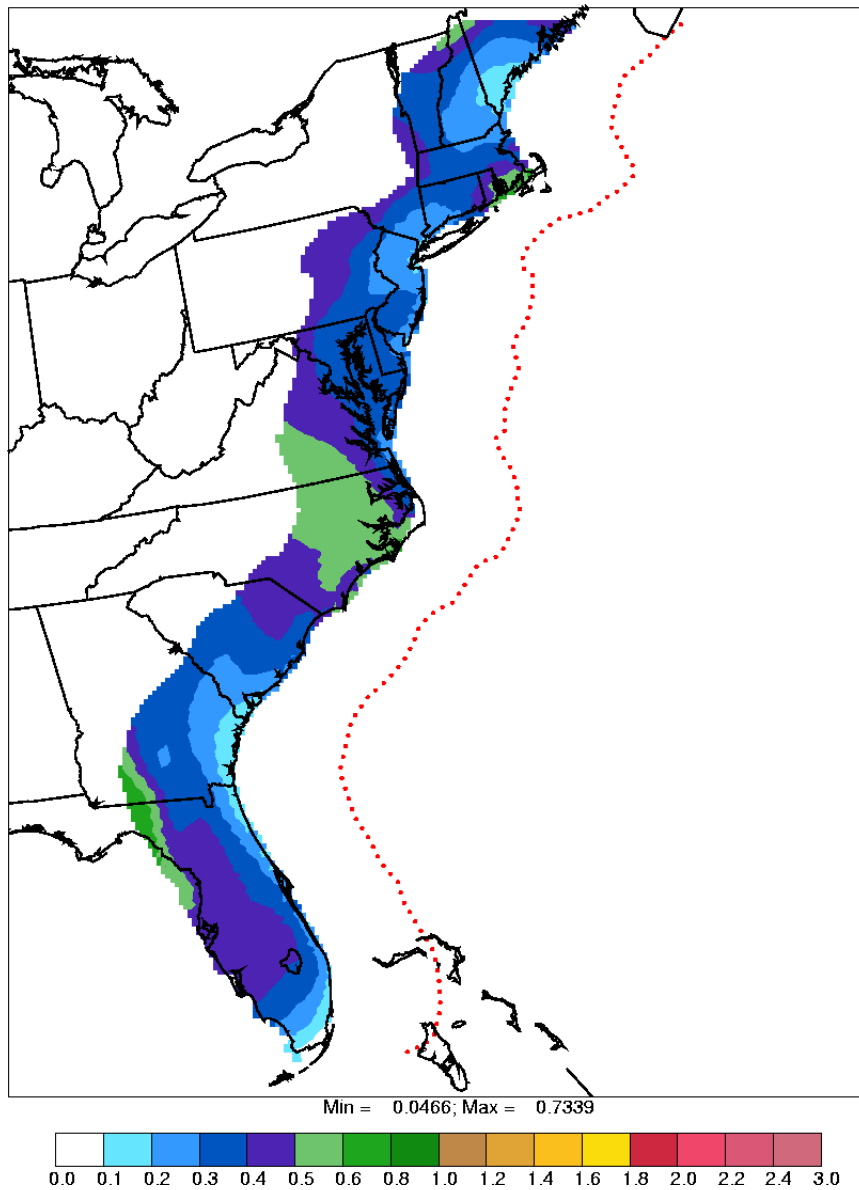


Figure 4-43. Ratios of annual-average SO_2 concentrations due to sea-going ships burning high-sulfur fuel at 250 km from the Atlantic Ocean coastline to the concentrations (target values) due to dockside ships at the coastline burning low-sulfur fuel. The red dots represent the locations of the sea-going ships.

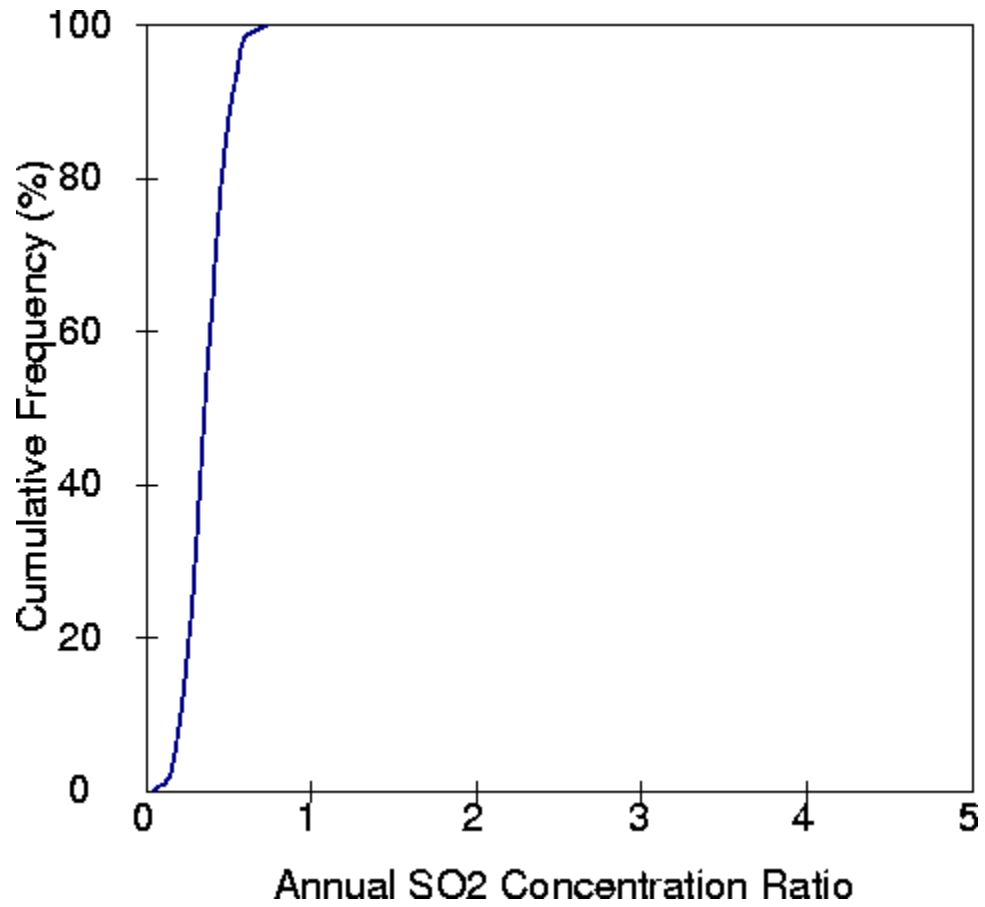


Figure 4-44. Cumulative frequency distribution of design ratios of SO₂ concentrations from ships at 250 km from the Atlantic Ocean coastline.

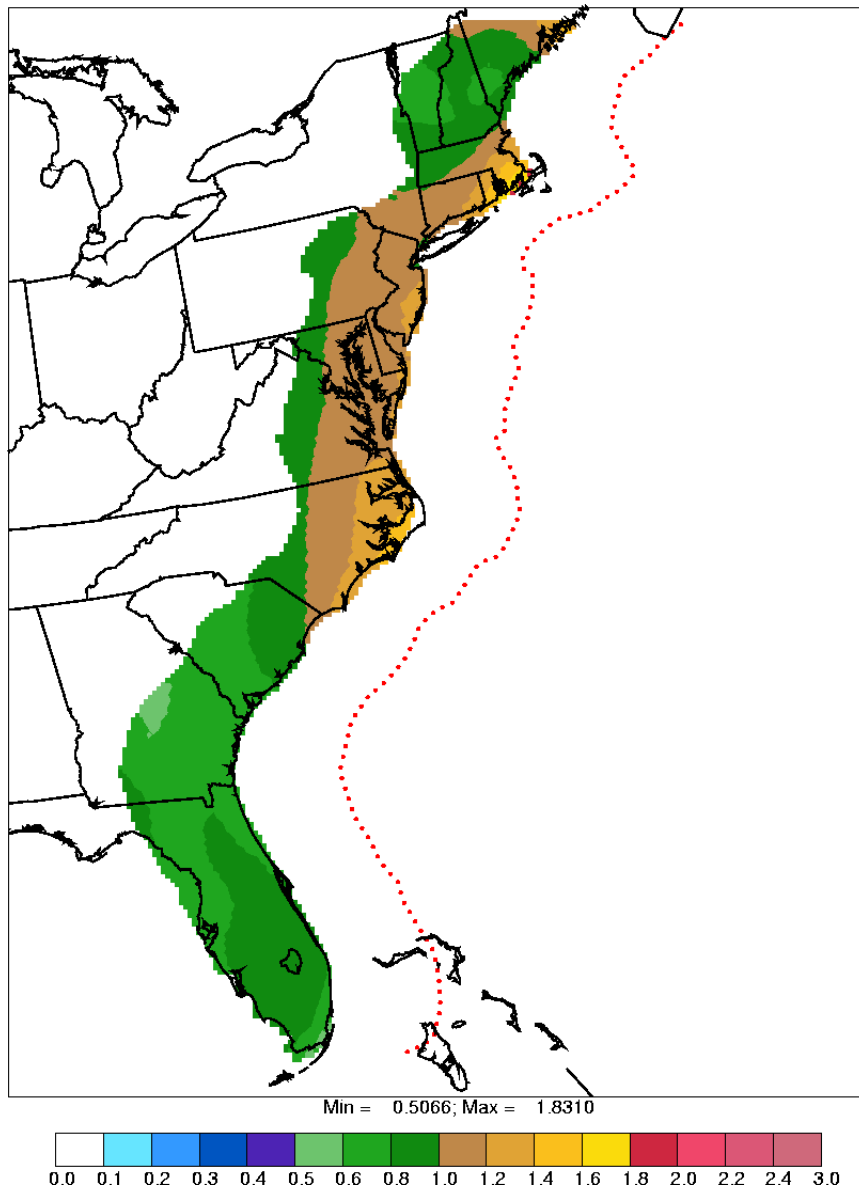


Figure 4-45. Ratios of annual-average sulfate concentrations due to sea-going ships burning high-sulfur fuel at 250 km from the Atlantic Ocean coastline to the concentrations (target values) due to dockside ships at the coastline burning low-sulfur fuel. The red dots represent the locations of the sea-going ships.

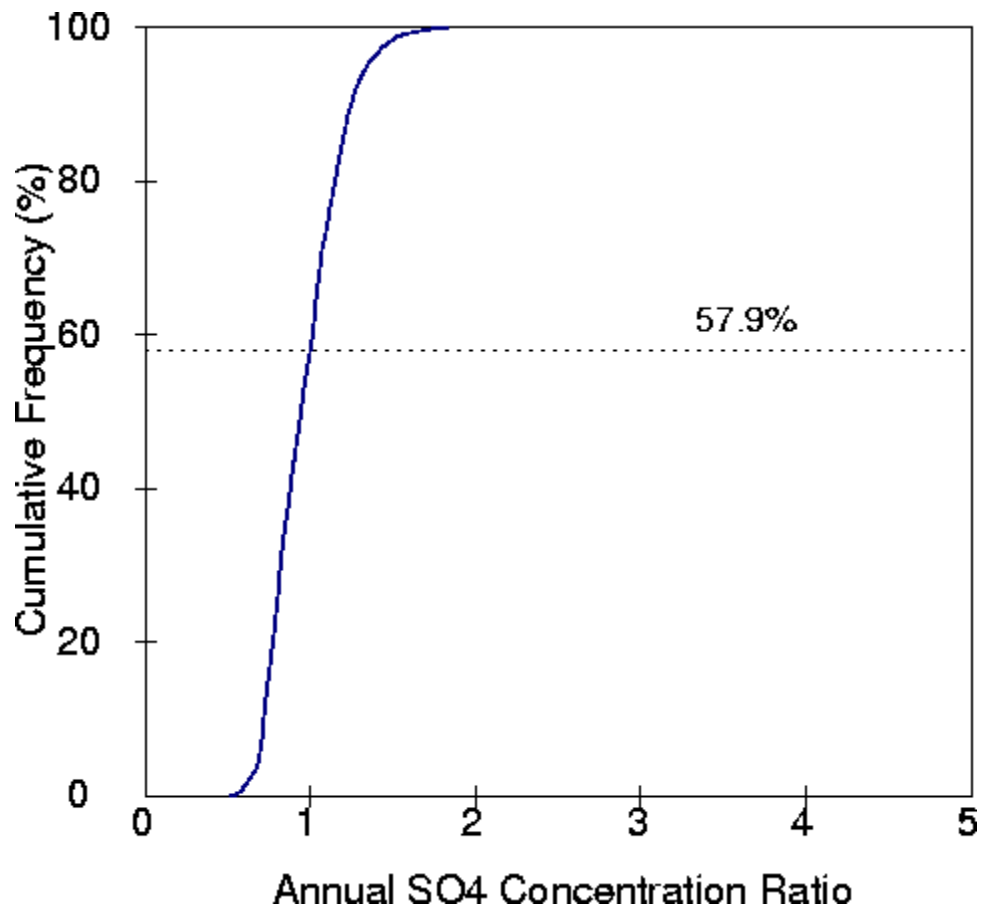


Figure 4-46. Cumulative frequency distribution of design ratios of sulfate concentrations from ships at 250 km from the Atlantic Ocean coastline.

Figure 4-47 shows the spatial distribution of sulfate ratios for ships at 375 km from the Atlantic Ocean coastline. We see that the sulfate ratios are less than one almost everywhere, except in portions of eastern North Carolina and southern Massachusetts. As shown in Figure 4-48, the sulfate ratios are less than one at over 92% of the receptors.

For ships at 500 km from the Atlantic Ocean coastline, the sulfate ratios are less than one everywhere as shown in Figures 4-49 and 4-50.

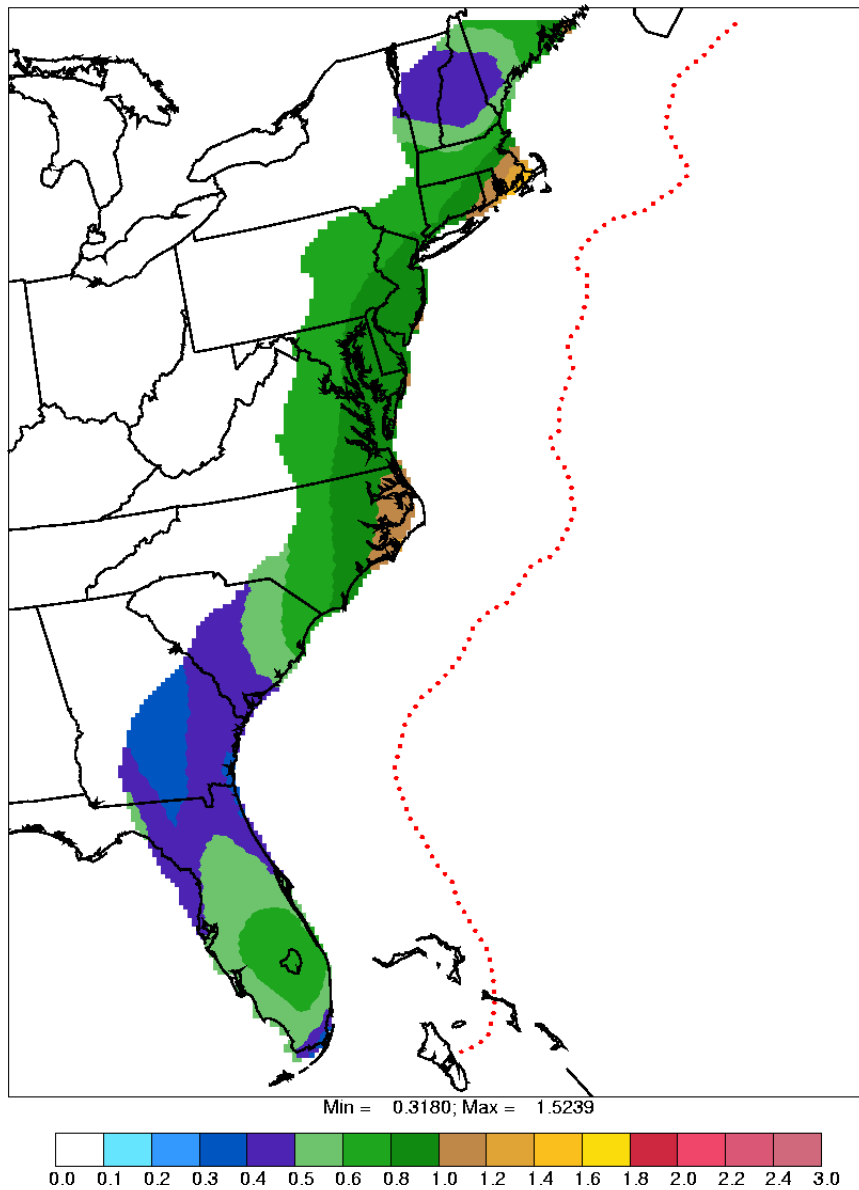


Figure 4-47. Ratios of annual-average sulfate concentrations due to sea-going ships burning high-sulfur fuel at 375 km from the Atlantic Ocean coastline to the concentrations (target values) due to dockside ships at the coastline burning low-sulfur fuel. The red dots represent the locations of the sea-going ships.

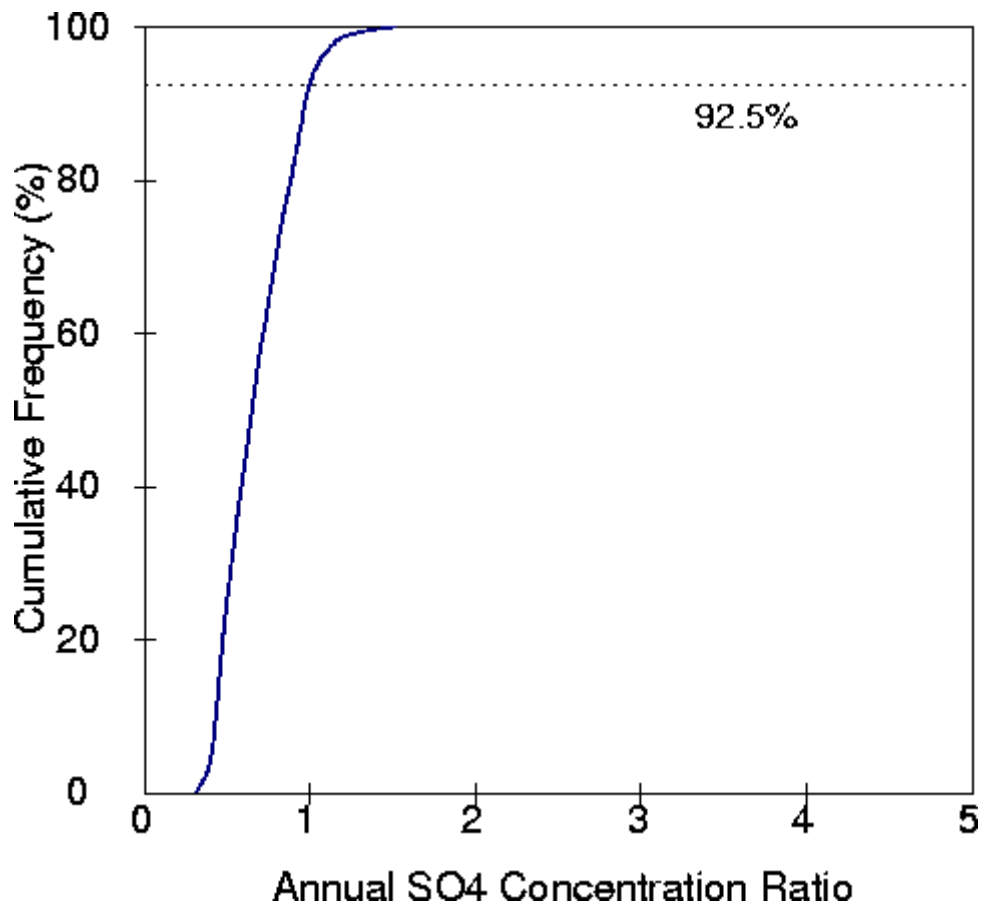


Figure 4-48. Cumulative frequency distribution of design ratios of sulfate concentrations from ships at 375 km from the Atlantic Ocean coastline.

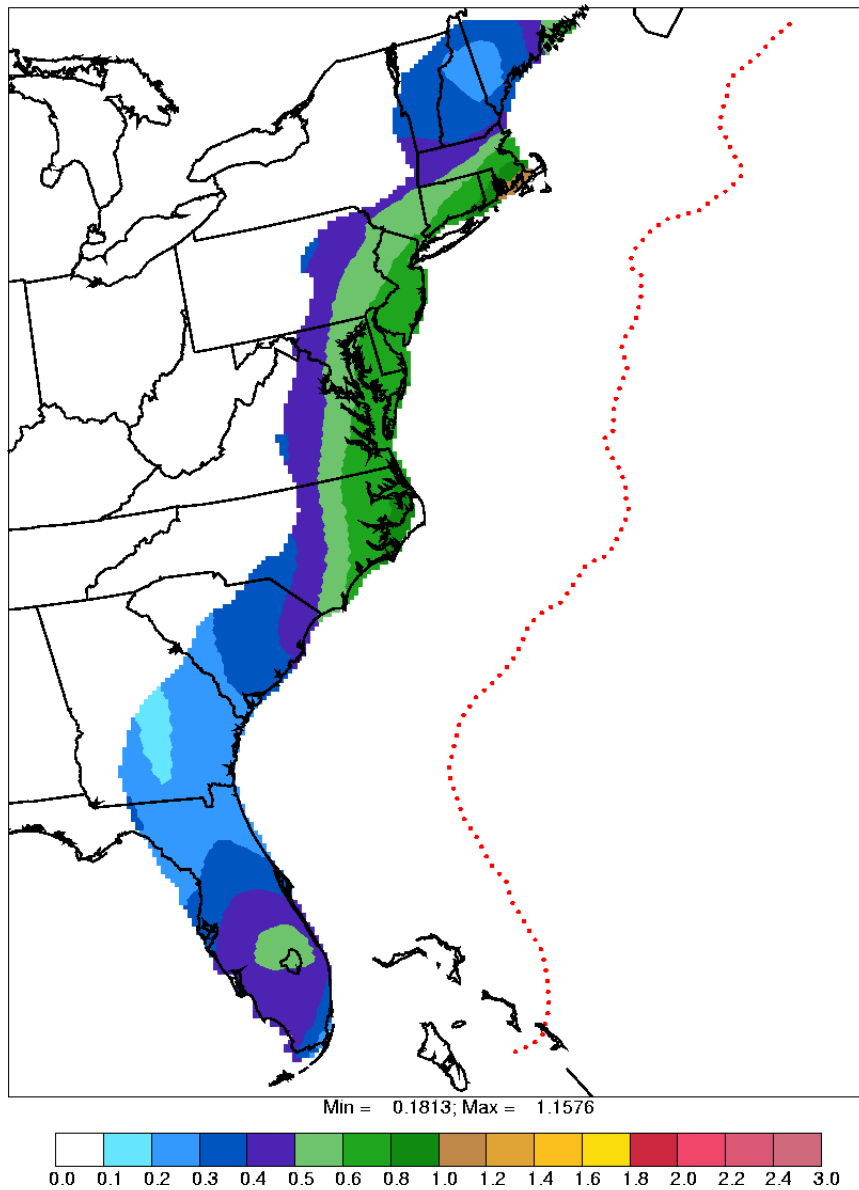


Figure 4-49. Ratios of annual-average sulfate concentrations due to sea-going ships burning high-sulfur fuel at 500 km from the Atlantic Ocean coastline to the concentrations (target values) due to dockside ships at the coastline burning low-sulfur fuel. The red dots represent the locations of the sea-going ships.

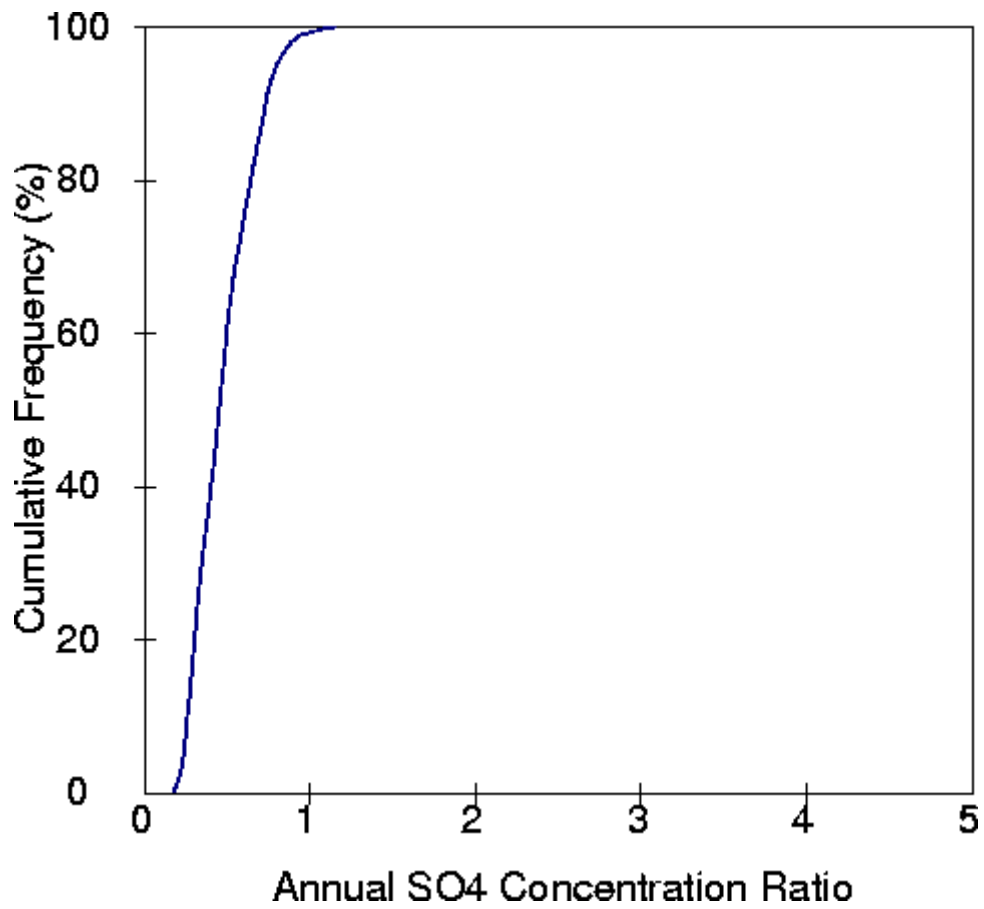


Figure 4-50. Cumulative frequency distribution of design ratios of sulfate concentrations from ships at 500 km from the Atlantic Ocean coastline.

5. SUMMARY AND CONCLUSIONS

A screening study with the CALPUFF dispersion model was conducted to determine the air quality impacts (annual average ground-level concentrations of SO₂ and sulfate) at an array of land-based receptors due to SO_x emissions from ships burning high-sulfur fuel at sea at various distances from the coastline. CALPUFF tends to overestimate the conversion of SO₂ to sulfate in the gas phase (Karamchandani et al., 2006) and the results presented here are likely to provide conservative estimates of the impacts of emissions from ships at sea on inland air quality. (Because of the simplified treatment of aqueous-phase chemistry in CALPUFF, this assessment may be altered if the interactions of the ship plumes with fog dominate sulfate formation.) The results were compared with those calculated for ships burning low-sulfur fuel at the coastline to determine upper bounds for Sulfur Emission Control Areas (SECAs), i.e., off-shore distances at which the switch to high-sulfur fuel would not impair air quality. For each offshore distance investigated, the percentage of receptors for which the air quality impacts of ships at sea were lower than the impacts of ships at the coastline was calculated.

The U.S. coastlines considered in this study include the Pacific Ocean coastline, the Gulf of Mexico coastline, and the Atlantic Ocean coastline. The northern and southern parts of the Pacific Ocean coastline were studied separately. The results are summarized in Tables 5-1 and 5-2 for concentration ratios of SO₂ and sulfate, i.e., the ratio of the concentration calculated for ships at sea to the concentration calculated for ships at the coastline.

The results for SO₂ were different from those for sulfate, primarily due to differences in the behavior of these two species downwind of a source. For all the coastlines studied, the majority of the SO₂ concentration ratios were less than one at shorter off-shore distances than for sulfate. Thus, sulfate concentration ratios were the limiting factor for defining the upper bounds of the SECA for each coastline.

Table 5-1. Percentage of SO₂ concentrations below the design value as a function of the distance from the coastline.

Distance from coastline	125 km	250 km	375 km	500 km
Southern Pacific	40.7%	90.7%	100%	100%
Northern Pacific	46.6%	97.9%	100%	100%
Gulf of Mexico ^a	84.4%	98.1%	100%	100%
Atlantic	86.6%	100%	100%	100%

^aNote that Florida values correspond to a shorter ship-coastline distance and the values presented in the table should be seen as lower limits.

Table 5-2. Percentage of sulfate concentrations below the design value as a function of the distance from the coastline.

Distance from coastline	125 km	250 km	375 km	500 km
Southern Pacific	4.4%	24.9%	41.9%	48.7%
Northern Pacific	0.01%	3.6%	20.3%	55.7%
Gulf of Mexico ^a	40.4%	72.0%	80.5%	84.0%
Atlantic	1.2%	57.9%	92.5%	100%

^aNote that Florida values correspond to a shorter ship-coastline distance and the values presented in the table should be seen as lower limits.

The results showed some differences in results among the various coastlines studied. These differences are due to differences in the wind fields bringing the offshore ship emissions and their secondary products to land as well as differences in precipitation, which removes pollutants from the atmosphere.

The results from the two Pacific Ocean coastline simulations were qualitatively similar. For both Pacific Ocean coastlines, over 90% of the receptors showed SO₂ concentration ratios less than one for ships at 250 km from the coastline. For sulfate, only about 49% and 56% of the receptors had concentrations less than one for ships at 500 km from the southern Pacific Ocean and northern Pacific Ocean coastlines, respectively.

For the other two coastlines (Atlantic Ocean and Gulf of Mexico), the SO₂ results were qualitatively similar to those for the Pacific Ocean coastlines, i.e., over 90% of the receptors showed SO₂ concentration ratios less than one for ships at 250 km from the coastline. However, there were some large differences for sulfate. For the Gulf of Mexico coastline, over 70% of the receptors showed sulfate concentration ratios less than one for ships at 250 km from the coastline. For the Atlantic Ocean coastline, nearly 60% of the receptors showed sulfate concentration ratios less than one for ships at 250 km from the coastline.

These results suggest that an off-shore distance of 500 km should be sufficient when conducting refined modeling of the potential impacts of ship emissions on air quality inland, if a criterion of about 50% of inland receptors having sulfate concentrations below the design value is acceptable to define the SECA.

6. REFERENCES

- ARB, 2000. *Air Quality Impacts from NO_x Emissions of Two Potential Marine Vessel Control Strategies in the South Coast Air Basin*, California Air Resources Board, Sacramento, CA.
- Corbett, J.J. and H.W. Koehler, 2003. Updated emissions from ocean shipping, *J. Geophys. Res.*, **108**, doi:10.1029/2003JD003751.
- Corbett, J.J., 2005. Private communication to Christian Seigneur, AER, July 2005.
- EPA, 2002. *Commercial Marine Emission Inventory*, Final Report from PECHAN, prepared by ENVIRON International Corporation, U.S. Environmental Protection Agency, Office of Transportation and Air Quality, Ann Arbor, MI.
- Fleischer, F., E.J. Ulrich, R. Krapp and W. Grundmann, 1998. Comments on particulate emissions from diesel engines when burning heavy fuels, *Proc. Of the 22nd CIMAC Internat. Congress on Combustion Engines*, Vol. 6, Copenhagen, Denmark, May 18-21.
- ICOADS, 2002. *International Comprehensive Ocean Atmospheric Data Set*, as transmitted from ERG by Office of Transportation and Air Quality, U.S. Environmental Protection Agency, Washington, D.C.
- Karamchandani, P., A. Koo, and C. Seigneur, 1998. A reduced gas-phase kinetic mechanism for atmospheric plume chemistry, *Environ. Sci. Technol.*, **32**, 1709–1720.
- Karamchandani, P., and C. Seigneur, 1999. Simulation of sulfate and nitrate chemistry in power plant plumes, *J. Air Waste Manage. Assoc.*, **49**, PM-175–181.
- Karamchandani, P., S.-Y. Chen, N. Kumar and M. Gupta, 2006. A comparative evaluation of two reactive puff models using power plant plumes measurements, *AWMA Guideline on Air Quality Models Conference*, Denver CO, 26-28 April.
- Morris, R.E., R.C. Kessler, S.G. Douglas, K.R. Styles and G.E. Moore, 1988. *Rocky Mountain Acid Deposition Model Assessment: Acid Rain Mountain Mesoscale Model (ARM3)*, report prepared for the U.S. EPA, Research Triangle Park, NC.
- Scire, J.S., D.G. Strimaitis and R.J. Yamartino, 2000a. *A User's Guide for the CALPUFF Dispersion Model (Version 5)*, Earth Tech, Inc. Report, Concord, MA, January 2000.

- Scire, J.S., F.R. Robe, M.E. Fernau and R.J. Yamartino, 2000b. *A User's Guide for the CALMET Dispersion Model (Version 5)*, Earth Tech, Inc. Report, Concord, MA, January 2000.
- Scire, J.S., 2005. Communication via e-mail of Christian Seigneur, AER, with Joe Scire, EarthTech, 18-19 March 2005.
- Scire, J.S., D.G. Strimaitis and F.R. Robe, 2005. Evaluation of enhancements to the CALPUFF model for offshore and coastal applications, *Proceedings of the 10th International Conference on Harmonisation with Atmospheric Dispersion Modelling for Regulatory Purposes*, Crete, Greece, 17-20 October 2005.
- Scire, J.S., 2006. Private communication to Prakash Karamchandani, AER, February 2006.
- Seigneur, C., K. Lohman and P. Karamchandani, 2005a. *Review of Technical Information relevant to Sulfur Oxides (SO_x) Emissions Transport for Ships at Sea*, Final Report to Office of Transportation and Air Quality, U.S. Environmental Protection Agency, Washington, D.C.
- Seigneur, C., P. Karamchandani and K. Lohman, 2005b. *Analysis Plan - Modeling Sulfur Oxides (SO_x) Emissions Transport for Ships at Sea*, Final Report to Office of Transportation and Air Quality, U.S. Environmental Protection Agency, Washington, D.C.

APPENDIX A

**REVIEW OF TECHNICAL INFORMATION RELEVANT TO
SULFUR OXIDES (SO_x) EMISSIONS TRANSPORT
FOR SHIPS AT SEA**

Prepared by

Christian Seigneur

Kristen Lohman

Prakash Karamchandani

Atmospheric & Environmental Research, Inc.

2682 Bishop Drive, Suite 120

San Ramon, CA 94583

Prepared for

U.S. Environmental Protection Agency

Office of Transportation and Air Quality

1200 Pennsylvania Avenue, NW

Washington, DC 20460

Document CP212-05-01b

June 2005

INTRODUCTION

Marine shipping represents a major and growing source of uncontrolled air pollution in coastal regions and inland areas downwind of coastal regions in many parts of the world, particularly North America and Europe. This can be attributed to both growth in global trade and port activity, as well as controls on land-based emissions. In 1973, an international conference of the International Maritime Organization (IMO) adopted the *International Convention for the Prevention of Marine Pollution from Ships* (MARPOL) designed to prevent pollution from ships. In 1997, the IMO agreed to MARPOL Annex VI, a global treaty to reduce air emissions from ships. This treaty went into effect on May 19, 2005. The treaty sets limits on emissions of sulfur oxides (SO_x) and nitrogen oxides (NO_x) and prohibits the international emissions of ozone-depleting substances, such as chlorofluorocarbons. One key element of Annex VI is the establishment of “SO_x Emission Control Areas” (SECAs) near coastal regions where controls on SO_x emissions from ships are more stringent (1.5% fuel content or 15,000 ppm) than in the open seas (4.5% or 45,000 ppm).

Countries wanting to obtain SECA designation for their coastal areas must submit a formal application to the IMO. The U.S. Environmental Protection Agency (EPA) is currently in the process of exploring the feasibility of a SECA for U.S. coastal areas and plans to work with affected states to obtain the necessary data. As part of the application process, emissions inventories will be developed and air quality modeling analyses will be conducted.

EPA will conduct the air quality modeling analyses for the SECA application in-house using three-dimensional (3-D) grid-based models such as CMAQ and/or CAMx. One of the issues of interest for this modeling exercise is the determination of the “scales of interest”, i.e., a delineation of the extent and scope of the SECA for each coastal region that will be considered in the analysis. This determination will be performed using a “screening-level” modeling analysis, in which a methodology will be developed and applied to estimate SO_x emissions transport from ships at sea to areas off the U.S. coasts (Pacific, Atlantic, and the Gulf of Mexico) using realistic ship emissions and meteorology. SO_x emissions transport from ships on the Great Lakes will be addressed separately under the U.S.-Canada binational program.

This document describes the first component of the SO_x emissions transport methodology, which is a literature review of available tools and data to quantify the transport and residence times of SO_x over water. The fate and transport of pollutants over water has long been of interest because of the potential impacts of off-shore platforms on air quality over land and the potential impacts of ship emissions on global climate change and air quality over land. Consequently, there is a significant body of information available on the atmospheric transport, dispersion and chemistry of pollutants emitted over water.

The Minerals Management Service (MMS) has conducted several studies to investigate the meteorology and the fate and transport of oil platform emissions in the Gulf of Mexico (e.g., Yocke et al., 1998). Those studies are not directly applicable to the present study because the emission source is different; nevertheless, some valuable data and useful experience were obtained in the MMS studies that are relevant to the present study. The relevant aspects are discussed in this report. The U.S. Navy investigated the potential of ship emissions reaching shore and that report provides useful information regarding the different meteorological regimes along the U.S. coastline (Eddington and Rosenthal, 2003). The California Air Resources Board (2000) also conducted a modeling study of the transport and dispersion of NO_x emissions from ships in the southern California region. There have also been several academic investigations on the fate and transport of pollutants emitted from ships. The most recent and relevant one (Song et al., 2003) pertains to the simulation of sulfur chemistry in a ship plume released in the marine boundary layer. The authors used a simple box model to simulate the plume. They concluded that, in the presence of non-precipitating clouds, non-sea salt sulfate could attain about 2 µg/m³ after a few hours of plume travel time. The SO₂/sulfate chemistry was found to be linear (i.e., a change in SO₂ emissions would lead to a proportional change in sulfate concentrations) except near the ship where SO₂ concentrations exceeded the hydrogen peroxide (H₂O₂) concentrations.

In this report, we first examine the fate and transport models available for simulating the transport of pollutants over water. Then, available data sources are discussed for some of the most important input data beginning with meteorology, then emission factors, and finally ship activity data.

AIR QUALITY MODELS

Air quality models can be grouped in two major categories: grid-based Eulerian models and Lagrangian plume (or puff) models. Eulerian models are well suited to address air quality for urban and regional pollutants that are emitted from a large variety of sources. However, their spatial resolution is limited by the grid size and they are not well suited for addressing air quality impacts associated with individual sources or groups of sources. Plume or puff models are better suited for such air quality impacts since their formulation takes into account the dispersion of the emitted material from the source to the downwind distances of interest.

For this screening study of the potential impacts of SO_x emissions from ships at sea, we are considering Lagrangian plume and puff models since they are the most suitable. We are considering three models: OCD, CALPUFF and SCICHEM. We briefly describe these models below and discuss their advantages and shortcomings before making our recommendations for the air quality model to be used for this study.

OCD

OCD was developed under funding from the Minerals Management Service (MMS) to simulate plume dispersion and transport from offshore sources to receptor areas on land or water.

OCD is a steady-state Gaussian model that uses hourly inputs. The steady-state assumption implies that the wind direction and speed are constant for an air parcel after it leaves the source regardless of the time needed for an air parcel to travel between the source and the receptor point. Its formulation includes enhancements that take into account differences between overwater and overland dispersion characteristics, the sea-land interface and off-shore platform aerodynamic effects.

OCD requires both overwater and overland meteorological data (i.e., including wind speed and direction, water surface temperature, overwater air temperature, mixing height and relative humidity). Missing overwater meteorological data such as turbulence intensities are parameterized using bulk aerodynamic wind and temperature profile relationships.

The effect of the source on plume dispersion (stack-tip downwash and building downwash) can be taken into account. Corrections are made for the presence of complex terrain. The evolution of the thermal boundary layer near the coast is simulated. Transitional plume rise and the partial penetration of elevated temperature inversions are simulated.

OCD can simulate the chemical decay of pollutants using first-order transformation rates that are user-specified. However, the formation of secondary pollutants from an emitted primary pollutant (e.g., formation of sulfate from emitted SO₂)

cannot be simulated; this is a major deficiency for this study since it addresses the possible impacts of sulfate concentrations on air quality. Removal processes (e.g., dry deposition) are simulated using a first-order decay.

OCD is listed by EPA as a guideline model but only for primary pollutants (Federal Register, 2003). Therefore, it is not recommended by EPA for secondary air pollutants such as sulfate formed from SO₂ oxidation in the atmosphere.

CALPUFF

CALPUFF was originally developed under funding from the California Air Resources Board (ARB) along with its associated meteorological model, CALMET (Scire et al., 2000a, 2000b).

CALPUFF is a non-steady-state puff dispersion model that can simulate the effects of time- and space-varying meteorological conditions on pollutant transport, transformation, and removal. It can accommodate arbitrarily varying point, area, volume, and line source emissions.

The recommended meteorological inputs for applying CALPUFF are the time-dependent outputs of CALMET, a meteorological model that contains a diagnostic wind field module and overwater and overland boundary layer modules. Optionally, CALMET can use the outputs of prognostic meteorological models, such as MM5 and CSUMM, to create the meteorological fields required by CALPUFF.

CALPUFF includes algorithms for near-source effects such as building downwash, transitional plume rise, partial plume penetration, sub-grid scale terrain interactions as well as longer range effects such as pollutant removal due to wet and dry deposition, simplified chemical transformations, vertical wind shear, overwater transport and coastal interaction effects.

CALPUFF offers several options to simulate the formation of secondary sulfate and nitrate particles from the oxidation of the emitted primary gaseous pollutants, SO₂ and NO_x respectively. The oxidation of SO₂ to sulfate is of interest for this study. The more advanced chemistry module available in CALPUFF uses the RIVAD/ARM3 chemical mechanism (Morris et al., 1988). This simple mechanism treats the conversion of NO to NO₂ accompanied by its further transformation to total nitrate and conversion of SO₂ to sulfate. It is assumed that background concentrations of reactive hydrocarbons (VOC) are low and, therefore, this mechanism is not considered suitable for urban regions. It may be suitable for overseas situations where VOC concentrations are not too high. However, in areas such as southern California, where urban coastal pollution may be transported over the ocean via the land-sea breeze, the assumption of low background VOC concentrations may sometimes be invalid.

In the RIVAD/ARM3 chemical mechanism, the NO-NO₂-O₃ chemical system is first solved to generate pseudo-steady-state concentrations of NO, NO₂, and O₃. During

the day, this system consists of the NO_2 photodissociation to yield NO and O_3 and the NO-O_3 titration reaction to yield NO_2 . During the night, only the NO-O_3 titration reaction is considered. The steady-state daytime concentration of the hydroxyl radical (OH) is calculated from the O_3 concentration after the solution of the $\text{NO-NO}_2\text{-O}_3$ system. Gupta et al. (2001) have noted that the O_3 concentrations are incorrectly treated in CALPUFF, resulting in the overestimation of OH concentrations, and thus overestimations in the gas-phase oxidation rates of SO_2 to sulfate and NO_x to nitrate. The RIVAD/ARM3 mechanism does not explicitly calculate the aqueous-phase oxidation of SO_2 to sulfate. Instead, a constant heterogeneous SO_2 oxidation rate (0.2% per hour) is added to the gas phase conversion rate. The partitioning of semi-volatile chemical species (ammonium nitrate) between the gas phase and the particulate phase is simulated with a simple thermodynamic model.

CALMET is the companion meteorological model that is used with CALPUFF. A weakness of CALMET has recently been identified (Wheeler, 2005). CALMET does not correctly handle cases of unstable convective atmospheric conditions over water (when water temperature is warm and air temperature is cold, for example) because it assumes near-neutral conditions over water. Consequently, the mixing height is calculated based on a neutral mixing relationship and, under conditions of light wind speeds when the mechanical mixing heights are small, CALMET underpredicts the actual mixing height. This weakness can be an issue in areas such as the Gulf of Mexico where warm water temperatures are possible. EarthTech, the developer of CALMET is addressing this problem by adding a convective mixing height calculation in CALMET. This new version of the model is currently being tested but it is not yet publicly available. Based on our discussion with EarthTech (Scire, 2005), we will circumvent this potential problem by inputting measured or modeled mixing heights directly into CALMET (meteorological data are discussed in Section 3).

CALPUFF is listed by EPA as a preferred air quality model for assessing the long-range transport of air pollutants and on a case-by-case basis for certain near-field applications involving complex meteorological conditions (Federal Register, 2003). CALPUFF is also recommended by the Federal Land Managers' Air Quality Values Workgroup (FLAG) for assessing the effects of distant plumes on atmospheric visibility.

SCICHEM

SCICHEM is an extension of the Second-order Closure Integrated PUFF model (SCIPUFF) that includes atmospheric chemical transformations. It has been developed under funding from EPRI and the Defense Threat Reduction Agency (DTRA) ((Sykes et al., 1988, 1993; Sykes and Henn, 1995; Karamchandani et al., 2000; EPRI, 2000).

SCICHEM is a non-steady-state multi-species model that incorporates a comprehensive treatment for gas- and aqueous-phase chemistry, and PM formation.

SCIPUFF represents a plume with a multitude of three-dimensional puffs that are advected and dispersed by the local micrometeorological conditions. Each puff has a Gaussian representation of the concentrations of individual species. SCIPUFF simulates the plume transport and dispersion using a second-order closure approach to solve the turbulent diffusion equations, which provide a direct connection between measurable velocity statistics and predicted dispersion rates.

SCIPUFF can assimilate observational data ranging from a single wind measurement to multiple profiles. Alternatively, three-dimensional gridded wind and temperature fields generated by a prognostic model or other analyses can be used as input to the model. SCIPUFF can simulate the effect of wind shear since individual puffs evolve according to their respective locations in an inhomogeneous velocity field. As puffs grow larger, they may encompass a volume that cannot be considered homogenous in terms of the meteorological variables. A puff splitting algorithm accounts for such conditions by splitting puffs that have become too large into a number of smaller puffs. Conversely, individual puffs that are affected by the same (or very similar) micrometeorology may also merge to produce a larger single puff. Also, the effects of buoyancy on plume rise and initial dispersion are simulated by solving the conservation equations for mass, heat, and momentum.

For PM related regulatory applications, it is important that the underlying model should account for processes responsible for phase-dependent chemical transformations and PM characterization. We provide a brief description of chemical and PM components of SCICHEM.

In SCICHEM, the gas-phase chemical reactions within the puffs are simulated using a general framework that allows any chemical kinetic mechanism (e.g., CBM-IV, SAPRC) to be treated. Therefore, SCICHEM can simulate atmospheric conditions ranging from the clean atmosphere to polluted areas. To minimize the need for computational resources needed to treat the typical chemical mechanisms, the gas-phase puff chemistry can optionally be simulated using a three-staged chemical kinetic mechanism where the number of reactions treated increases as the puff mixes with background air (Karamchandani et al., 1998). This multistage approach offers reasonable accuracy (within $\pm 10\%$) with increased computational speed.

Chemical species concentrations in the puffs are treated as perturbations from the background concentrations. This approach allows the treatment of overlapping puffs and, therefore, provides great flexibility for simulating processes such as calm conditions, wind shear and overlapping plumes for different sources. Optionally, SCICHEM can explicitly simulate the effect of turbulence on chemical kinetics.

SCICHEM includes aqueous-phase chemistry. It is simulated using the RADM chemical mechanism. When the aqueous-phase chemistry option is selected, the wet deposition of pollutants is computed from the cloud water concentrations of pollutants

and the precipitation rate. Otherwise, scavenging coefficients are used to calculate wet deposition. The partitioning of semi-volatile chemical species between the gas phase and the particulate phase is simulated with the thermodynamic model ISORROPIA.

EPA has added SCIPUFF to the list of alternate models (Appendix B of the EPA Guideline on Air Quality Models, Federal Register, 2003) for the simulation of the long-range transport and dispersion of air pollutants.

Recommendations

Table 2-1 presents a summary of the advantages and shortcomings of the three models reviewed here. The major shortcomings of OCD are its use of the steady-state assumption and its lack of treatment of chemical transformations. The steady-state assumption implies that the wind direction and wind speed are assumed to be constant for a puff released from the source, whereas the other two models allow for changes in wind direction and wind speed. Chemical transformations in OCD are limited to a simple decay of the emitted pollutants and do not allow the treatment of secondary pollutant formation (such as the formation of sulfate from SO_2). The major shortcoming of CALPUFF is its simplified chemistry that tends to overestimate sulfate formation in the gas phase and uses a simple parameterization for the cloud/fog aqueous phase. CALPUFF offers the major advantage of being widely used and being an EPA preferred guideline model for the long-range transport of SO_x . SCICHEM offers a more comprehensive formulation than CALPUFF. However, SCICHEM is not yet an EPA preferred guideline model. It is still considered a research-grade model and its computational requirements are significantly greater than those of the other two models.

On the basis of this review, we recommend that CALPUFF be used to simulate the transport, transformation and deposition of SO_x emissions from ships, with the caveat that one must bear its limitations in mind.

Table 2-1. Comparison of the advantages and shortcomings of three plume/puff models for emissions from off-shore sources.

Characteristics	OCD	CALPUFF	SCICHEM
Steady-state vs. transient	Steady-state	Transient	Transient
Spatial resolution	Gaussian plume	Puffs	Puffs
Wind-shear	No	Yes	Yes
Plume overlaps	Yes	Yes	Yes
Near-source effects	Yes	Yes	Yes
Chemical transformations	First-order decay	Simplified chemistry	Comprehensive chemistry
Dry deposition	First-order decay	Yes	Yes
Wet deposition	No	Yes	Yes
Source types	Point, line and area	Point, line, area and volume	Point
Regulatory status	EPA preferred guideline model for primary pollutants released over water	EPA preferred guideline model for long-range transport and visibility impacts of air pollutants	EPA alternate guideline model
Computational requirements	Low	Moderate	High

METEOROLOGICAL DATA

Meteorological data are necessary to run an air dispersion model. For the CALPUFF model, the meteorological input data must first be formatted by the CALMET pre-processor. CALPUFF requires standard surface and upper air meteorological data. CALMET also has an overwater option that allows the use of special overwater measurements for grid cells that are over the ocean. The data required for the overwater option are: air-sea temperature difference, air temperature, relative humidity, wind speed and wind direction. Two optional measurements, overwater mixing height and overwater temperature gradients, may be supplied if available. If the optional parameters are not supplied, CALMET uses default values.

Land-based Measurements

Land-based meteorological measurements are required for both surface and upper air observations above land portions of the domain. The data required are standard format data from the National Climatic Data Center (NCDC) (Scire et al., 2000). The upper air data required are standard NCDC format TD6201 radiosonde data including pressure, elevation, temperature, wind direction, and wind speed for each sounding level. The surface observations that are needed are provided in the NCDC Integrated Surface Hourly Observations. These include wind speed, wind direction, temperature, and dew point temperature.

Fixed Overwater Measurements

The required parameters are all available for the Pacific and Atlantic oceans near the U.S. coastline and for the Gulf of Mexico and Great Lakes from the National Data Buoy Center (NDBC) (NDBC, 2005). The measurements are taken from buoys. The buoys are at varying distances from the coast. Those near the coast are frequently near harbors or bays. Though the coverage is not uniform, the full length of the continental U.S. coastline is covered by those data. Most of the buoys are owned and operated by NDBC but there are also several other agencies that submit their data to the NDBC database. Figures 3-1 through 3-6 show the locations of the NDBC buoys as well as those that are run by other agencies and are included in the NDBC database.

The Minerals Management Service (MMS) has performed modeling for the Breton National Wilderness Area which is on the Coast of the Gulf of Mexico. The MMS has provided us additional overwater data for the Gulf of Mexico including both surface and upper air data. The availability of upper air data will allow a more thorough modeling of the unique conditions above the Gulf of Mexico. These data are available for the years 1999-2001.

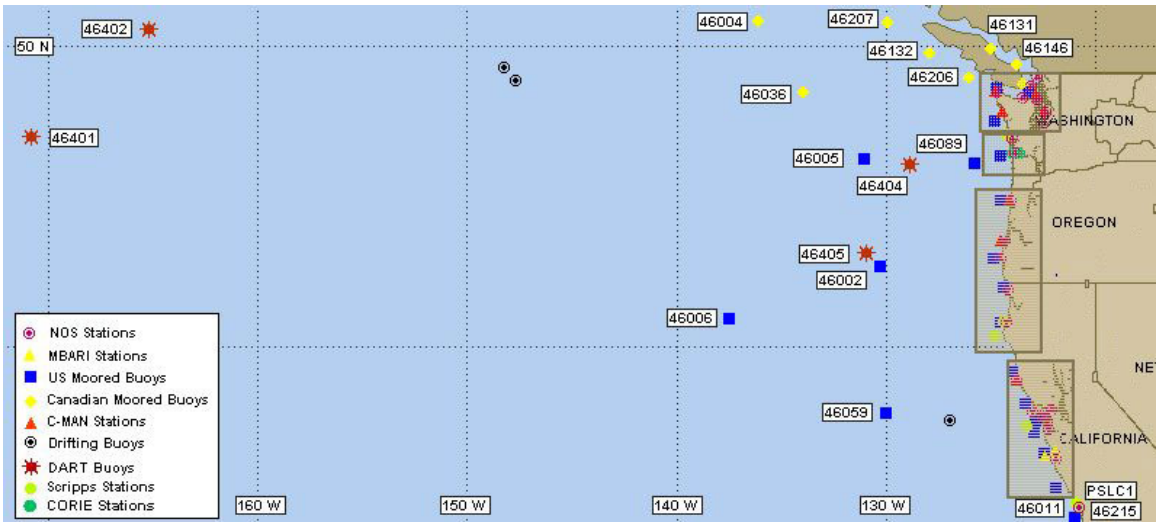


Figure 3-1. NDBC buoys along the Washington, Oregon, and northern California coastline.

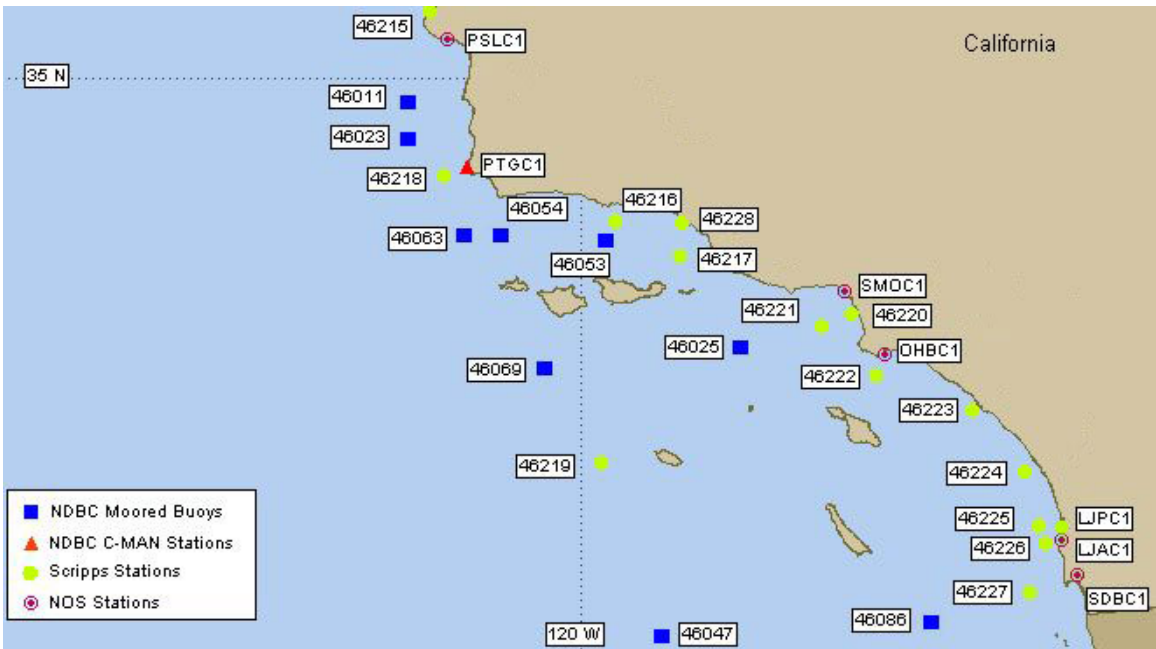


Figure 3-2. NDBC buoys along the southern California coastline

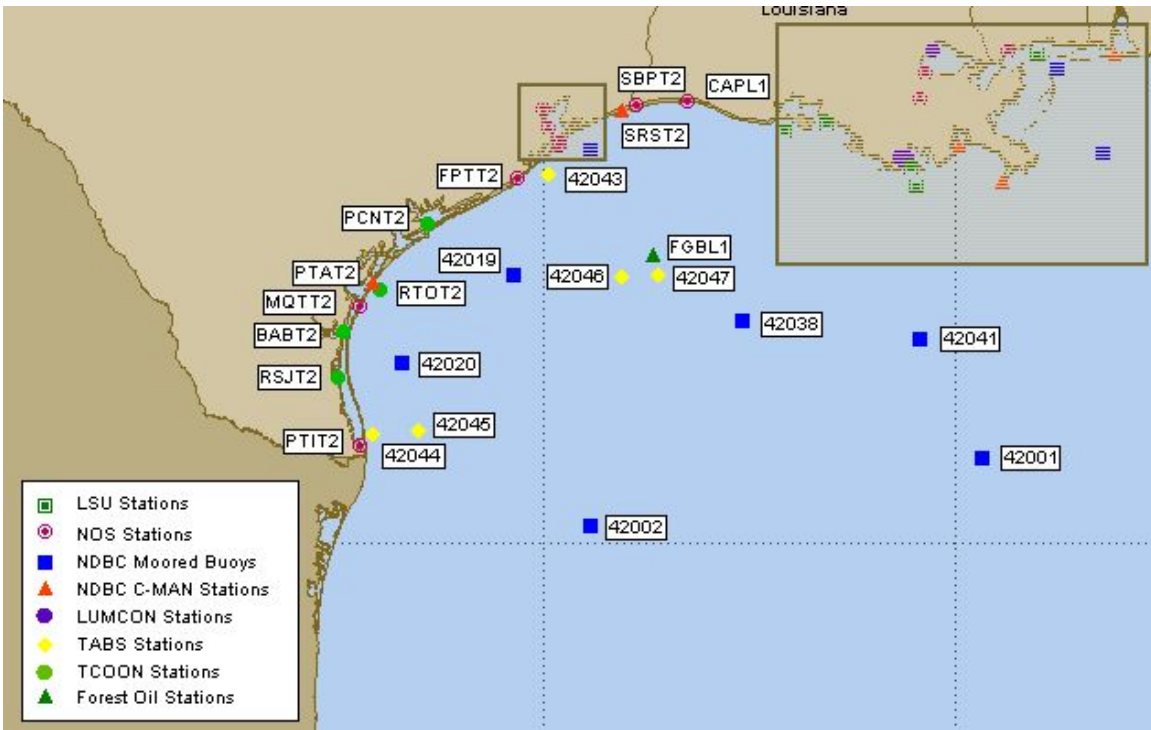


Figure 3-3. NDBC buoys along the western Gulf of Mexico

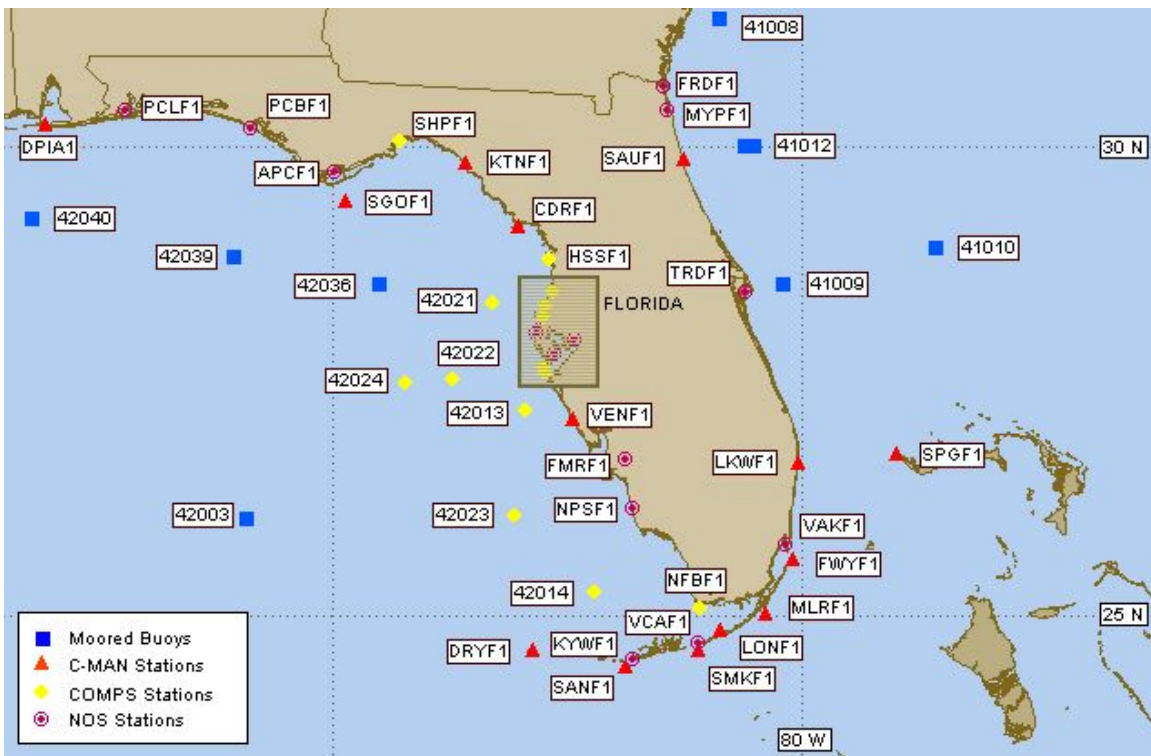


Figure 3-4. NDBC buoys along the eastern Gulf of Mexico

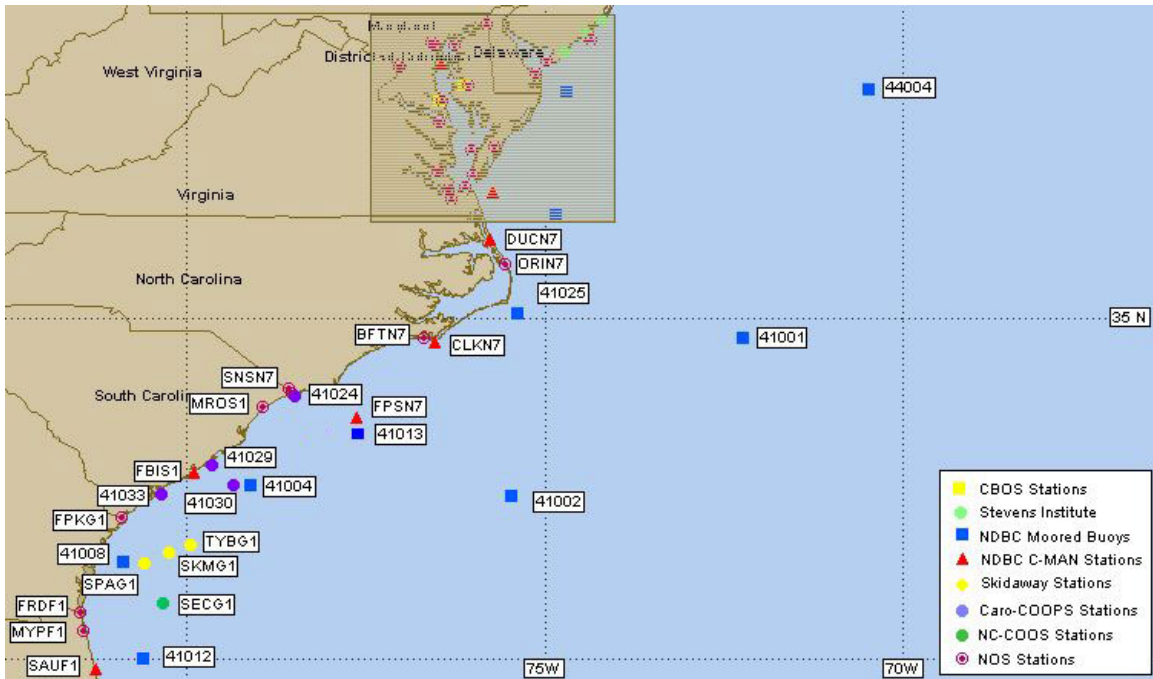


Figure 3-5. NDBC buoys along the southeastern U.S. coastline

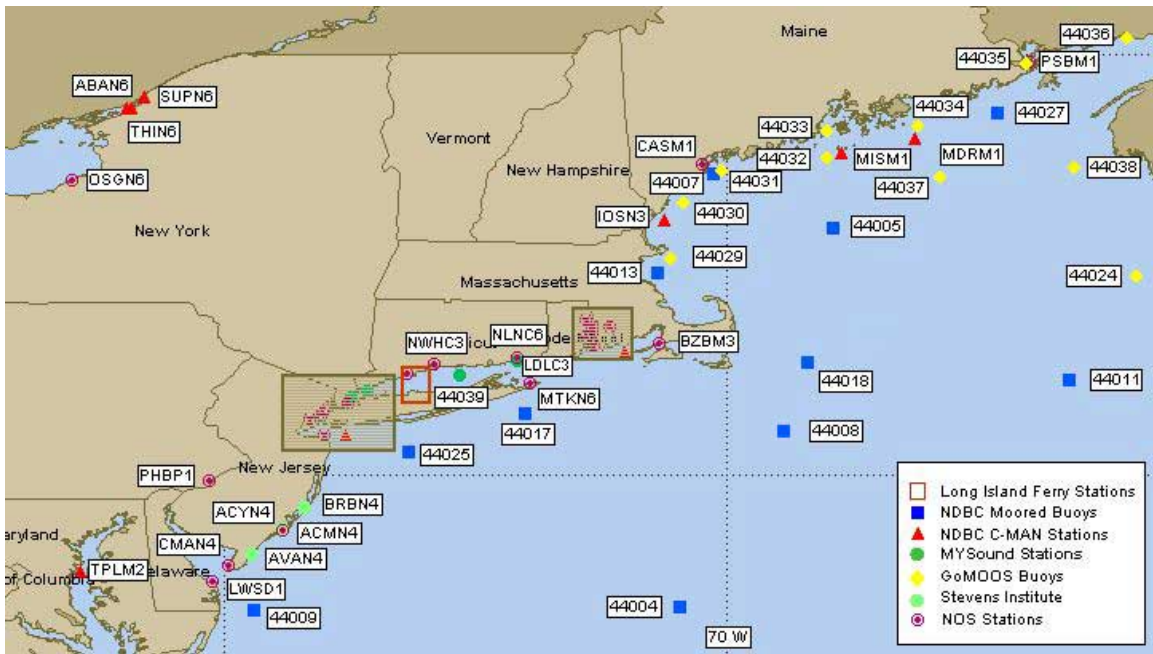


Figure 3-6. NDBC buoys along the northeastern U.S. coastline.

Data from Ships

The CALMET preprocessor also allows for the location of meteorological observations to vary so that measurements made from ships can be used for modeling as well. NCDC as well as other agencies have shipboard measurements.

One available database is the International Comprehensive Ocean-Atmosphere Data Set (ICOADS) from NOAA (NOAA, 2005). It provides data on the location of the ship, as well as air temperature, sea temperature, wind speed and direction, pressure, and dew point. These data are available from 1950 through 2002.

Model Outputs

The outputs of meteorological models can be used, particularly in cases where there are insufficient meteorological observations. This may be the case for upper air data in the Atlantic and Pacific Oceans. Examples of model outputs that could be used as surrogates for upper air data include those from the 2001 or 2002 MM5 simulations sponsored by EPA, those from the NCEP/NCAR reanalysis project and those from the Advanced Climate Modeling and Environmental Simulations (ACMES) database.

Recommendations

There appears to be sufficient meteorological data to model the transport of SO_x emissions from ships. The availability of upper air data for the Gulf of Mexico will be particularly valuable. In the absence of upper air data over water for the other areas, either some default assumptions will need to be made regarding atmospheric stability or the outputs of archived meteorological simulations will be used. We will discuss our proposed technical approach in the Analysis Plan that will be prepared in Task 2.

4. EMISSION FACTORS

Emission factors are needed to estimate the emissions of SO_x associated with various ship activities. We reviewed available emission factors and provide our recommendations below.

EPA (2000) Emission Factors

Emission factors for air pollutant emissions from ships are provided in the report titled “Analysis of Commercial Marine Vessels Emissions and Fuel Consumption Data” (EPA, 2000). Emission factors are provided for several air pollutants including SO_2 and PM. Those emission factors are provided for different oceangoing ship categories that include bulk carriers and tankers, general cargo ships, container/RoRo/auto carriers/refrigerated ships, and passenger ships. The emission factors are a function of the operating mode of the engine; four modes were considered: normal cruise, slow cruise, maneuvering and docking (hoteling).

For SO_2 , the emission factor is a function of the fuel consumption rate and sulfur content of the fuel. The fuel consumption rate is provided per unit of work (i.e., g/kW-h) as a function of the fractional load. The engine work (kW-h) is a function of the ship type (see above) and ship deadweight. The fractional load is the ratio of the actual engine output and rated engine output; it is a function of the engine mode and ship type.

If one assumes a fuel sulfur content of 3%, the SO_2 emission factor per unit of work is 16 g/kW-h for a cruising ship and 20 to 25 g/kW-h for a maneuvering ship. The SO_2 emission factor per unit of fuel is 71 kg/metric ton.

EC Emission Factors

A recent report from the European Commission (EC) provides emission factors for air pollutants from ships (EC, 2002). Emission factors are reported for pollutants including SO_2 and PM. The emission factors are provided either by engine type and fuel type (15 combinations) or by ship type (16 oceangoing ship types); different factors are provided for at sea and in port activities (emission factors for PM are only provided for in port activities).

The emission factors are reported in g/kW-h. Thus, the engine horsepower must be estimated as a function of the ship type and activity.

The SO_2 emission factor per unit of work is in the range of 10 to 13 g/kW-h for a ship at sea and 11 to 13 g/kW-h for a ship at port. The SO_2 emission factor per unit of fuel is in the range of 46 to 54 kg/metric ton. These emission factors are slightly lower (by 20 to 35%) than those reported in the EPA report cited above.

EPA (2002) Emission Factors

A recent EPA report (2002) presents a review of emission factors available from several sources. The emission factors reviewed were for ships with engines with displacement exceeding 30 liters (so-called Category 3 engines).

Emission factors are reported for three different engine types (slow speed, medium speed and steam boiler) for transit modes and hoteling modes.

For slow and medium speed engines, the SO₂ emission factor per unit of work is about 13 g/kW-h for a ship in transit mode, and 1.4 g/kW-h for a ship in hoteling mode. For steam boilers, the SO₂ emission factor per unit of work is 20 g/kW-h for a ship in both transit and hoteling modes. The SO₂ emission factor per unit of fuel is assumed to be 60 kg/metric ton in transit and 7 kg/metric ton when hoteling (steam boilers were assumed to use the same fuel while hoteling as in transit, i.e., 30 kg/metric ton). These emission factors appear to be consistent with those from the EC and lower than those from the EPA 2000 report.

Recommendations

This brief review of available emission factors for SO₂ emissions from ships show that there is some general consistency among the different sources of information. The differences among the various references are well within the uncertainty ranges that one would expect for emission factors of air pollutants. We propose to use the most recent EPA emission factors (EPA, 2002) for this study because they represent the most recent source of information. These emission factors combined with ship type and ship activity data will provide emission rates of SO₂.

It should be noted that there are no emission factors for sulfate. SO₂ emission factors are estimated as a function of the sulfur content of the fuel and the implicit assumption is that all sulfur is emitted as gaseous SO₂. There is evidence that particulate sulfate emissions are associated with diesel engines. For example, sulfate may account for up to 12% of PM emissions from cars and trucks (Shi et al., 2000). PM emission factors are available for ship emissions. By using the EPA (2002) PM emission factor for diesel engines of a ship in transit and assuming that PM is 12% sulfate, we obtain an emission factor of 0.2 g/kW-h. This value corresponds to 1.6% of the SO₂ emission factor. Data from the Navy Pilot Emission Control Program (NPECP) on PM emissions from marine diesel engines confirm these results, although the sulfate fraction of PM depends on the fuel type and the engine regime, ranging from 2 to 19% of PM. Furthermore, EPA assumes that 2% of sulfur is emitted as primary sulfate PM from Category 3 marine diesel engines (i.e., those engines with displacement > 30 liters per cylinder). Because the rate of oxidation of SO₂ to sulfate is slow in the absence of fog or clouds (on the order of 1% per hour), emissions of sulfate from ships may contribute significantly under such conditions to the sulfate concentrations over land that are due to ship emissions. Therefore, we will treat 2% of total sulfur emissions as sulfate emissions

and the SO₂ emission factor will be adjusted down accordingly to maintain the sulfur mass balance.

5. SHIP ACTIVITY DATA

Ship activity data must be determined so that the emission factors can be applied to provide air pollutant emissions from ships. The activity data are typically calculated based on four types of information: port locations, vessel descriptions, trip records, and shipping lane definitions. Port locations are available from the United States Army Corps of Engineers (USACE) (USACE, 2005). For efficiency, these data should be aggregated so that all nearby ports are treated as one.

Once port data have been aggregated, trip data need to be added. Trip data are necessary to track how many of each type of ship move between each port. The emission factors will be applied according to ship type, therefore, it is important to characterize the ship types per shipping lane per year. The USACE provides data on entrances and clearances (USACE, 2005) for vessels traveling under foreign flags. This database lists each entry and departure of a vessel bearing a foreign flag. Through these databases, a ship can be traced through its travels through U.S. ports. Information on domestic ship traffic is also compiled by the USACE.

The entrances and clearances databases list a ship code that can then be matched up to another USACE database. This database provides data on each foreign ship that has registered at a U.S. port providing information on type, size, and power.

Once all of these data have been gathered and processed, they can be combined to provide a list of potential trips (e.g., Portland to San Francisco) by type of ship. The final step is to provide a geographic location for the ship emissions. Since CALPUFF allows the modeling of line sources, we need to determine the geographic definitions of the shipping lanes that will be input into the model. These data are available from the USACE in the form of the Waterways Network (USACE, 2005). It provides information on the latitude and longitude of each node in the U.S. waterways.

Alternatively, the ICOADS database that provides meteorological measurements from ships can be used to determine shipping lanes (NOAA, 2005). ICOADS provides time- and space-resolved meteorological data. Because each record provides both the ship code and a latitude and longitude, ships can be traced along their actual route. In some places this approach may vary significantly from the theoretical ship lanes available from the USACE Waterways Network.

Recommendations

Information on ship activity data is not currently available in a format ready to use for an air quality modeling study. For the Pacific coast, a moderate amount of work would be required to complete the processing of the available data into a format suitable for air quality modeling. For the other areas, a large amount of work would be required based on the data that we identified. One may consider using hypothetical ship emissions

for this air quality modeling study; however, those hypothetical emissions should be representative of actual ship emissions in order to lead to realistic air quality predictions.

6. REFERENCES

- California Air Resources Board. 2000. Air Quality Impacts from NO_x Emissions of Two Potential Marine Vessel Control Strategies in the South Coast Air Basin. Final Report, prepared by the California Air Resources Board and the South Coast Air Quality Management District in Consultation with the Deep Sea Vessel/Shipping Channel Technical Working Group, Sacramento, CA.
- EC, 2002. Quantification of emissions from ships associated with ship movements between ports in the European Community, Final Report prepared by Entec UK Limited.
- Eddington, L. and J. Rosenthal, 2003. The Frequency of Offshore Emissions Reaching the Continental United States Coast Based on Hourly Surface Winds from a 10 Year Mesoscale Model Simulation, Naval Air Systems Weapons Division, Point Mugu, CA.
- EPA, 2000. Analysis of Commercial Marine Vessels Emissions and Fuel Consumption Data, EPA-420-R-00-002, U.S. Environmental Protection Agency, Office of Transportation and Air Quality, Washington, DC
- EPA, 2002. Commercial Marine Emission Inventory, Final Report from PECHAN, prepared by ENVIRON International Corporation, U.S. Environmental Protection Agency, Office of Transportation and Air Quality, Ann Arbor, MI.
- EPRI, 2000. *SCICHEM Version 1.2: Technical Documentation*, EPRI Report 1000713, EPRI, Palo Alto, CA.
- Federal Register, 2000. Environmental Protection Agency, 40 CFR Part 51, *Requirements for Preparation, Adoption, and Submittal of State Implementation Plans (Guideline on Air Quality Models); Proposed Rule*, Vol. 65, No. 78, Friday, April 21, 2000, pp. 21506–21542.
- Federal Register, 2003. 40 CFR Part 51, Revision to the Guideline on air quality Models: Adoption of a Preferred Long Range Transport Model and Other Revisions; Final Rule, 18440-18482, April 15, 2003.
- Gupta, M., N. Kumar, P. Karamchandani, and S.-Y. Wu, 2001. Intercomparison of SCICHEM and CLAPUFF models using Cumberland plume data, *Air & Waste Management Association Conference on Guidelines on Air Quality Models: A New Beginning*, April 4-6, Newport, RI.
- Hanna, S., L. Schulmann, R. Paine, and J. Pleim, 1984. The Offshore and Coastal Dispersion (OCD) Model User's Guide Revised, MMS 84-0069, Minerals Management Service.

- Hanna, S., L. Schulman, R. Paine, J. Pleim and M. Baer, 1985. Development and evaluation of the offshore and coastal dispersion (OCD) model, *J. Air Pollut. Control Assoc.*, **35**, 1039-1047.
- Karamchandani, P.; A. Koo; C. Seigneur, 1998. *Environ. Sci. Technol.*, **32**, 1709–1720.
- Karamchandani, P.; L. Santos; I. Sykes; Y. Zhang; C. Tonne; C. Seigneur, 2000. *Environ. Sci. Technol.*, **34**, 870–880.
- Morris, R.E., R.C. Kessler, S.G. Douglas, K.R. Styles and G.E. Moore, 1988. Rocky Mountain Acid Deposition Model Assessment: Acid Rain Mountain Mesoscale Model (ARM3), Report prepared for the U.S. EPA, Research Triangle Park, NC.
- National Ocean and Atmospheric Administration (NOAA), 2005. <http://www.cdc.noaa.gov/coads/> “ICOADS” Last accessed April 20, 2005.
- National Data Buoy Center (NDBC), 2005. <http://www.ndbc.noaa.gov/index.shtml> “National Data Buoy Center” Last accessed April 20, 2005.
- Scire, J.S., D.G. Strimaitis and R.J. Yamartino, 2000. A User’s Guide for the CALPUFF Dispersion Model (Version 5), Earth Tech, Inc. Report, Concord, MA, January 2000.
- Scire, J.S., F.R. Robe, M.E. Fernau and R.J. Yamartino, 2000. *A User’s Guide for the CALMET Dispersion Model (Version 5)*, Earth Tech, Inc. Report, Concord, MA, January 2000.
- Scire, J.S., 2005. Communication via e-mail of Christian Seigneur, AER, with Joe Scire, EarthTech, 18-19 March 2005.
- Shi, J.P., D. Mark and R.M. Harrison, 2000. Characterization of particles from a current technology heavy-duty diesel engine, *Environ. Sci. Technol.*, **34**, 748-755.
- Song, C.H., G. Chen and D. Davis, 2003. Chemical evolution and dispersion of ship plumes in the remote marine boundary layer: investigation of sulfur chemistry, *Atmos. Environ.*, **37**, 2663-2679.
- Sykes, R. I., W. S. Lewellen, S. F. Parker and D. S. Henn, 1988. *A Hierarchy of Dynamic Plume Models Incorporating Uncertainty, Volume 4: Second-order Closure Integrated Puff*, EPRI, EPRI EA-6095 Volume 4, Project 1616-28.
- Sykes, R. I.; S. F. Parker; D. S. Henn; W. S. Lewellen, 1993 *J. Appl. Met.*, **32**, 929–947.
- Sykes, R. I.; D. S. Henn, 1995. *J. Appl. Met.*, **34**, 2715–2723.

United States Army Corps of Engineers, 2005.
<http://www.iwr.usace.army.mil/ndc/data/data1.htm> “Navigation Data Center –
U.S. Waterway Data” Last accessed April 20, 2005.

Wheeler, N., 2005. Private communication from Neil Wheeler, Sonoma Technology,
Inc. to Christian Seigneur, AER, 14 March.

Yocke, M.A. et al., 1998. Meteorology of the northeastern Gulf of Mexico. ENVIRON
International Corp. U.S. DOI. OCS Study: final report, data from 1995 to 1997.
2000. 154 p. Available from GOM (with 3 CD's). MMS 2000-075.

APPENDIX B

**ANALYSIS PLAN
MODELING SULFUR OXIDES (SO_x) EMISSIONS TRANSPORT
FOR SHIPS AT SEA**

Prepared by

Christian Seigneur

Prakash Karamchandani

Kristen Lohman

Atmospheric & Environmental Research, Inc.

2682 Bishop Drive, Suite 120

San Ramon, CA 94583

Prepared for

U.S. Environmental Protection Agency

Office of Transportation and Air Quality

1200 Pennsylvania Avenue, NW

Washington, DC 20460

Document CP212-05-02a

July 2005

INTRODUCTION

This document describes the analysis plan for modeling the SO₂ and sulfate concentrations due to emissions of SO_x from ships at sea. The results of this screening modeling study will provide quantitative information on the shortest distance at which ships burning higher sulfur fuel (here, 27,000 ppm) will have air quality impacts at land receptors that are less than those anticipated from emissions from ships burning low sulfur fuel (here, 15,000 ppm) within coastal waters. This resulting distance can subsequently be used as the basis for defining the modeling domain for sources to be included in a subsequent modeling study using an Eulerian model (CMAQ). The results of the CMAQ modeling will yield information to define the outer boundary of a Sulfur Emission Control Area (SECA). We focus here on the southern Pacific coast. The methodology presented here is consistent with an approach developed by the Office of Transportation and Air Quality (OTAQ) of the U.S. Environmental Protection Agency (EPA) which included input from EPA regional modelers, and staff from the U.S. Navy.

We first describe the overall modeling approach including the fate and transport model, CALPUFF, that will be used to simulate the transport, transformation and removal of pollutants over water and land. Then, we describe the selection of the model input data including meteorological data, SO_x emissions and ship activity data.

2. AIR QUALITY MODELING APPROACH

Air Quality Model

For this screening study of the potential impacts of SO_x emissions from ships at sea, we will use the CALPUFF model (Scire et al., 2000a, 2000b). CALPUFF is a non-steady-state puff dispersion model that can simulate the effects of time- and space-varying meteorological conditions on pollutant transport, transformation, and removal. The rationale for selecting CALPUFF was described in the Task 1 report (Seigneur et al., 2005).

The recommended meteorological inputs for applying CALPUFF are the time-dependent outputs of CALMET, a meteorological model that contains a diagnostic wind field module and overwater and overland boundary layer modules. Optionally, CALMET can use the outputs of prognostic meteorological models, such as MM5 and CSUMM, to create the meteorological fields required by CALPUFF. The preparation of the meteorological data inputs for CALPUFF for this study is described in Section 3.

CALPUFF includes algorithms for near-source effects such as building downwash, transitional plume rise, partial plume penetration, sub-grid scale terrain interactions as well as longer range effects such as pollutant removal due to wet and dry deposition, simplified chemical transformations, vertical wind shear, overwater transport and coastal interaction effects. Because the latter features are relevant to simulating the transport and chemistry of SO_x emissions from ships, they will all be activated for our study.

CALPUFF offers several options to simulate the formation of secondary sulfate and nitrate particles from the oxidation of the emitted primary gaseous pollutants, SO₂ and NO_x respectively. Since the oxidation of SO₂ to sulfate is of interest for this study, we will select the more advanced chemistry module available in CALPUFF which is based on the RIVAD/ARM3 chemical mechanism (Morris et al., 1988). The limitations of this chemistry module were discussed in the Task 1 report (Seigneur et al., 2005).

Modeling Domain

The modeling domain for the southern Pacific coast will extend from about 32 degrees North to 36 degrees North and will, therefore, cover southern California. (Northern California will be grouped with Oregon and Washington, i.e., from 36 degrees North to 50 degrees North, to constitute the modeling domain for the northern Pacific coast.) The modeling domain will extend 240 km (150 miles) inland to allow enough distance to assess the potential air quality impacts of emissions from ships at sea. It will extend over water at a distance from the coast that corresponds to air quality impacts below the target concentration at all receptors.

Physiographic data (coastline and terrain elevation) will be obtained from the U.S. Geological Survey.

Receptors

Receptors will be located on land as follows. A line of receptors will be located at the coastline, 10 km apart. Such a distance provides a finer spatial resolution than that of the ship emissions along the coast (see Section 5). Inland receptors will then be located eastward at 10, 10, 20, 20, 30, 30, 40, 40 and 40 km apart from each other, i.e., up to 240 km (150 miles) from the coastline; there will, therefore, be 10 lines of receptors from the coast (included) up to 240 km inland. All receptors will be located at ground level. The total number of receptors is, therefore, estimated to be on the order of 500.

Sources

Ship emissions will be represented by a set of stationary point sources. Each point source will represent a ship. They will be located at a selected distance from shore (see below) and apart at a distance to be defined based on ship traffic (see Section 5). The use of stationary sources to represent moving ships is an appropriate approximation for this screening modeling study, because using stationary sources will overestimate the downwind air quality impacts (emissions will be concentrated in specific locations rather than continuously distributed along the shipping lane, thereby leading to greater ambient air concentrations).

We considered but rejected an alternative approach. The approach would treat each ship as an individual source and simulate its impact on air quality inland. Target concentrations would be calculated from individual ships at the coast (dockside mode) with the highest concentration obtained at each receptor being selected as the target concentration for that receptor. Then, the impacts of individual ships would be evaluated against those target concentrations. This alternative approach offers the advantage of providing more detailed information regarding the impacts from ships since it addresses individual ships rather than a shipping lane; thus, different SECA distances could be identified in different parts of the domain. Such an approach requires many more model simulations than the approach proposed here, however, and, therefore, could not be considered for this screening study. Also, comparing with the highest concentration obtained for that receptor does not account for variability of concentrations at receptors, and may result in an overestimation of the boundary distance. Nevertheless, we point out below how the variability of the SECA distance within the study domain will be addressed.

Modeling Approach

Our modeling approach will consist of two phases. In the first phase, we will calculate, at each inland receptor, the target values for the SO₂ and sulfate concentrations that correspond to emission from ships at dockside; i.e., those ships that are within the SECA and therefore must burn low sulfur fuel; i.e., 15,000 ppm). These will be annual average concentrations. (It is not necessary to calculate the light extinction coefficient because it will be proportional here to the sulfate concentration.) In the second phase, we will calculate the annual average values of the SO₂ and sulfate concentrations corresponding to emissions from ships burning high sulfur fuel (i.e., 27,000 ppm) at various distances from the coast and will compare those values to the target values obtained in the first modeling phase.

All simulations will be conducted for one year and we will calculate and use annual average values in our analysis. We propose to use 2002 as our reference year because it corresponds to the year that will be used for grid-based air quality modeling by the EPA Office of Air Quality Planning and Standards (OAQPS).

For the first phase, we will locate the ships at the coastline (dockside mode). They will be distributed spatially according to their estimated density in a shipping lane (see Section 5). The SECA SO_x emission rates will be used (see Section 4). We will calculate the annual SO₂ and, sulfate concentrations at each receptor. These values will be defined as the target values that will be used as benchmarks for the Phase 2 modeling.

For the second phase, we will locate the ships at various distances from the coastline. For a given modeling scenario, all ships will be at the same distance from the coastline; they will be distributed spatially according to their estimated density in a shipping lane (see Section 5), and for all modeling scenarios the number of dockside ships will equal the number of off-shore ships. The SO_x emission rates outside of the SECA will be used (see Section 4). The objective is to determine a set of distances at which those ship emissions will lead to air quality impacts that are less than or equal to the target values calculated in Phase 1 for the following percents of onshore receptors: 50, 60, 70, 80, and 90. To that end, we will conduct CALPUFF annual simulations for various distances from the coastline. We will start with a 100 km distance, and receptor percentage of 50. If the modeling results show air quality impacts lower than the target values, at 50 percent or more of the onshore receptors we will then use a shorter distance (50 km). Conversely, if the modeling results show air quality impacts greater than the target values at 50 percent or more of the onshore receptors, we will use a greater distance (200 km). This process will be repeated until we identify the distance of interest (i.e., the distance where air quality impacts are commensurate with the target values). For example, if the modeling results conducted for a distance of 50 km show air quality impacts lower than the target values, for at least 50 percent of the onshore receptors, we will next use a shorter distance (20 or 30 km). If those modeling results show air quality impacts greater than the target values for at least 50 percent of the onshore receptors, we

will then use a greater distance (70 or 80 km). We will stop when we have identified a distance that leads to air quality impacts commensurate with the target values. This process will be repeated for the other percentages of onshore receptors (60, 70, 80 and 90). For all percentages, a tolerance of plus/minus 2 percent will be used. We propose to use a resolution of 10 km (i.e., we will not refine those distances within less than 10 km increments).

The criterion of percentages of onshore receptors is used as an initial investigation. As we approach the distance of interest, some receptors will show values greater than the target values whereas other receptors may show values lower than the target values. The distribution of these receptors is significant. For example, by definition, fewer receptors have concentrations in excess of target concentrations at the 60% level than 50%. But if the receptors in excess of the target concentrations at both the 50 and 60% levels are located say, within 10 km of the coastline, then even at the greater distances comparable levels of population may still be exposed to concentrations greater than target levels. In this example, the distribution may indicate that a greater distance should be considered. Therefore, evaluation of these various distances will be conducted by the modeling review team as part of the Task 3 analysis.

Another reason for using the criterion of percentages of onshore receptors is that SO₂ and sulfate concentrations will display different behaviors downwind of the ships. SO₂ concentrations will decrease continuously with distance from the source (due to dilution, removal, and conversion to sulfate), whereas sulfate concentrations will first decrease (dilution and removal of primary, i.e., directly emitted sulfate), then increase (formation of secondary sulfate from the oxidation of SO₂) before finally decreasing (dilution and removal exceeding formation).

This behavior of sulfate introduces an additional complication: the sulfate target values at receptors near the coastline will be determined by the directly emitted sulfate, while the target values at larger distances inland will be determined by some combination of primary and secondary sulfate, with the secondary sulfate component increasing and the primary sulfate component decreasing. Even further inland, both components will decrease as the rate of dilution and removal exceeds the formation of sulfate.

To understand how this complex behavior of sulfate may impact the analysis, let us consider the extreme case of no primary sulfate, i.e., all the SO_x is emitted as SO₂. In this case, the target sulfate values next to the coastline will be negligible because there will be minimal time for conversion of SO₂ to sulfate. However, there will be some plume travel time for emissions from ships at sea that will allow some conversion of SO₂ to sulfate. Consequently, it may be impossible in this extreme case to meet target values at the coastline receptors unless a very large SECA is defined.

Therefore, it is possible that all sulfate concentrations may not fall below the target values as we approach the distance of interest for the SECA. Accordingly, we will

need to report the results in terms of the fraction (or percentage) of receptors that exceed the target values for each pollutant.

We will report the results for each distance in terms of maximum concentration, average concentration and fraction of receptors above the target value for SO₂ and for sulfate (all values will be for receptors over land). If significant differences appear for different areas of the study domain (e.g., one area shows impacts above target concentrations for at least 50 percent of the onshore receptors for a shorter distance than another area), we will identify those differences and discuss whether they suggest the need for some variability for the SECA distance within the study domain.

3. METEOROLOGICAL DATA

CALMET is the companion meteorological model that is used to prepare the meteorological fields used by CALPUFF.

A weakness of CALMET has recently been identified (Wheeler, 2005). CALMET does not correctly handle cases of unstable convective atmospheric conditions over water (when water temperature is warm and air temperature is cold, for example) because it assumes near-neutral conditions over water. Consequently, the mixing height is calculated based on a neutral mixing relationship and, under conditions of light wind speeds when the mechanical mixing heights are small, CALMET underpredicts the actual mixing height. This weakness can be an issue in areas where warm water temperatures are possible, such as the Gulf of Mexico, the southern Pacific coast and the southern Atlantic coast. Therefore, we address this potential issue here as it is important for this area as well as for subsequent modeling areas. Based on our discussion with the CALMET developer, EarthTech (Scire, 2005), we will circumvent this potential problem by inputting measured or modeled mixing heights directly into CALMET. For the southern Pacific coast, no upper air measurements are available over water and we will, therefore, use modeled mixing heights, as described below.

Meteorological data are necessary to run an air dispersion model. For the CALPUFF model, the meteorological input data must first be formatted by the CALMET pre-processor. CALPUFF requires standard surface and upper air meteorological data. CALMET also has an overwater option that allows the use of special overwater measurements for grid cells that are over the ocean. The data required for the overwater option are: air-sea temperature difference, air temperature, relative humidity, wind speed and wind direction. Two optional measurements, overwater mixing height and overwater temperature gradients, may be supplied if available. If the optional parameters are not supplied, CALMET uses default values. We propose to supply temperature gradients obtained from the outputs of a prognostic meteorological model (see below).

Land-based Measurements

Land-based meteorological measurements are required for both surface and upper air observations above land portions of the domain. The data required are standard format data from the National Climatic Data Center (NCDC) (Scire et al., 2000b).

The upper air data required are standard NCDC format TD6201 radiosonde data including pressure, elevation, temperature, wind direction, and wind speed for each sounding level. There are four upper air stations that are located within the modeling domain:

- San Nicolas Island (33.25 degrees North, -119.45 degrees West)
- Miramar (32.87 degrees North, -117.15 degrees West)

- Point Mugu (34.10 degrees North, -119.12 degrees West)
- Vandenberg (34.67 degrees North, -120.58 degrees West)

The surface observations that are needed are provided in the NCDC Integrated Surface Hourly Observations. These include wind speed, wind direction, temperature, and dew point temperature. There are many surface stations within the modeling domain (255 for the state of California).

Overwater Measurements

The required CALMET parameters are all available for the Pacific Ocean near the U.S. coastline from the National Data Buoy Center (NDBC) (NDBC, 2005). The measurements are taken from buoys. The buoys are at varying distances from the coast. Those near the coast are frequently near harbors or bays. Most of the buoys are owned and operated by NDBC but there are also several other agencies that submit their data to the NDBC database. Though the coverage is not uniform, there is a fairly comprehensive coverage for the southern Pacific coast. Figure 3-1 shows the locations of the NDBC buoys as well as those that are run by other agencies and are included in the NDBC database.

Model Outputs

The outputs of meteorological models can be used, particularly in cases where there are insufficient meteorological observations. This is the case for upper air data over water in the Pacific Ocean. Examples of model outputs that could be used as surrogates for upper air data include those from the 2001 or 2002 MM5 simulations sponsored by EPA, those from the NCEP/NCAR reanalysis project and those from the Advanced Climate Modeling and Environmental Simulations (ACMES) database.

CALMET can take as input the output of MM5. It can also combine MM5 output with observations. An interface program (CALMM5) converts the MM5 data into a form compatible with CALMET. A new version of this processor has been added to the CALPUFF-CALMET Download BETA-Test page recently (May 25, 2005). This beta version (not yet officially approved by the EPA) of CALMM5 processes MM5 Version 3 output data directly. Using the output of another meteorological model (e.g., ACMES) would require the development of a new CALMET pre-processor that would be outside the scope of this project. Therefore, we will use the MM5 output for this application. Another advantage of using the MM5 outputs is that it will provide consistency with the subsequent grid-based modeling that will be conducted by OAQPS using the Community Multiscale Air Quality model (CMAQ), because CMAQ will be driven with the MM5 meteorology.

The MM5 modeling domain covers the entire contiguous United States and extends significantly over the oceans. For the southern Pacific coast domain, it extends at least 400 to 900 km westward from the coast. Therefore, it will cover the CALPUFF modeling domain needed to address the SECA.

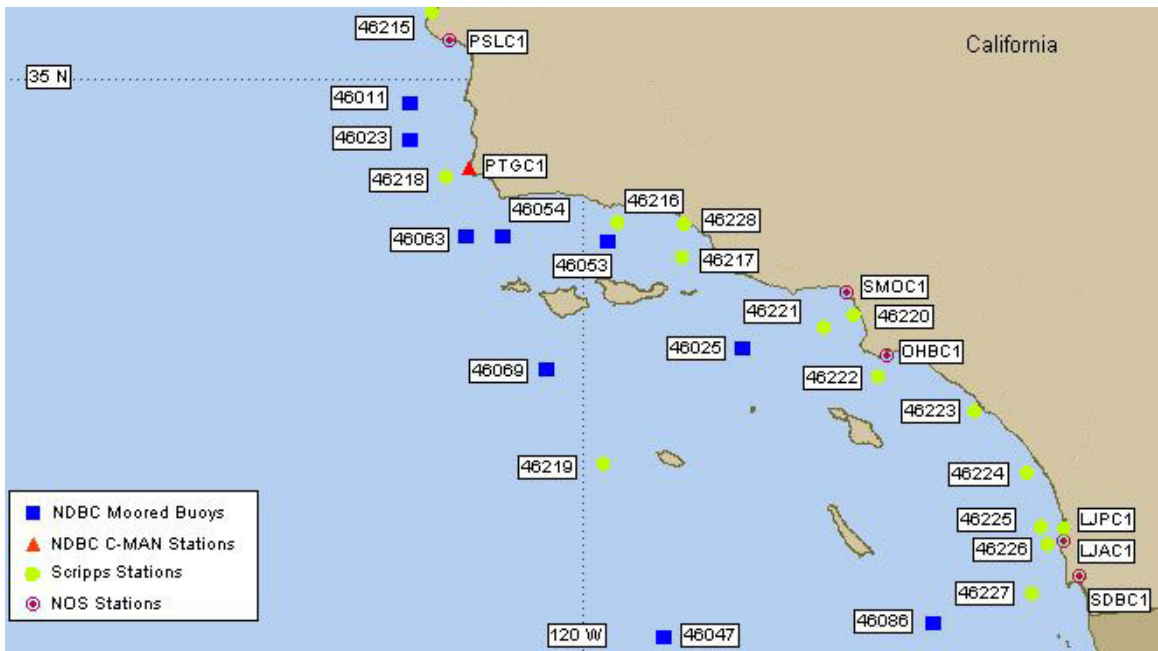


Figure 3-1. NDBC buoys along the southern California coastline

Summary

We will use a combination of MM5 model output, surface observations over water from the NDBC database, surface observations over land from the NCDC database and upper air observations over land from four stations from the NCDC database. These data will be processed by CALMET to prepare a three-dimensional meteorological data set for CALPUFF.

4. SO_x EMISSIONS

Emission factors are needed to estimate the emissions of SO_x (gas-phase SO₂ and particulate-phase sulfate) associated with various ship activities. Based on the review of available emission factors of Seigneur et al. (2005), the most recent EPA emission factors were selected (EPA, 2002). Those emission factors pertain to ships with engines with displacement exceeding 30 liters (so-called Category 3 engines).

Emission factors are reported for three different engine types (slow speed, medium speed and steam boiler) for transit modes and hoteling modes. For this study of ships at sea, we are interested in medium speeds for transit modes.

The SO₂ emission factor per unit of work is reported to be 9.56 g/hp-h for a 3% sulfur fuel (i.e., 30,000 ppm) for a ship at slow or medium speed in transit mode. This is equivalent to 12.8 g/kW-h.

For a ship within the SECA, a fuel sulfur content of 15,000 ppm will be assumed. Therefore, the emission factor will be 6.4 g/kW-h.

For a ship at sea outside of the SECA, a fuel sulfur content of 27,000 ppm will be assumed. Therefore, the emission factor will be 11.52 g/kW-h.

EPA assumes that 2% of sulfur is emitted as primary sulfate PM from Category 3 marine diesel engines. Therefore, we treat 2% of total sulfur emissions as sulfate emissions and the SO₂ emission factor is adjusted down accordingly to maintain the sulfur mass balance. (Note that for the same amount of S, the sulfate emission factor is 1.5 the SO₂ emission factor to account for the different molecular weights.)

Therefore, within the SECA, the gas-phase SO₂ and particulate-phase sulfate emission factors will be 6.27 g/kW-h and 0.19 g/kW-h, respectively. Outside of the SECA, the gas-phase SO₂ and particulate-phase sulfate emission factors will be 11.29 g/kW-h and 0.35 g/kW-h, respectively.

The sulfate emission rates calculated above are consistent with available data on the sulfate fraction of particulate matter (PM) emitted from ship diesel engines. Fleischer et al. report that 20 to 30% of PM emissions from ship diesel engines are sulfate (for a 3% sulfur fuel content). The EPA (2002) emission factor for PM is 1.3 g/hp-h, i.e., 1.74 g/kW-h. These values lead to an emission factor for sulfate in the range of 0.31 to 0.47 g/kW-h for a sulfur fuel content of 27,000 ppm. The emission factor of 0.35 g/kW-h calculated above falls within this range.

Based on data from Corbett and Koehler (2003), the power of a typical ship was estimated to be 16,000 kW (Corbett, 2005). It should be noted that there is a wide range of power among various ships, with the largest container ships having power exceeding 65,000 kW.

The gas-phase SO₂ and particulate-phase sulfate emissions per ship are then calculated to be 100,320 g/h and 3,040 g/h, respectively, within the SECA and 180,640 g/h and 5,600 g/h, respectively, outside the SECA.

5. SHIP ACTIVITY DATA

Ship activity data must be estimated so that the density of ships within the modeling domain can be calculated. Knowing the average number, N , of ships in transit along the southern Pacific coast per year and assuming an average cruising speed, V (km/h), we can calculate the average distance, D (km), between two ships along a shipping lane.

$$D = V * (24 \text{ h/day} * 365 \text{ days/yr}) / N$$

The annual number of ships transiting along the southern California coast was estimated to be 13,000 (ICOADS, 2002). This number includes all ships transiting to and from ports located on the southern Pacific coast as well as ships transiting southward/northward from/to ports located on the northern Pacific coast. It is likely to be an overestimate of the number of ships transiting along the coast because a fraction of those ships will be transiting along shipping lanes that extend from the ports westward into the Pacific Ocean. The cruising speed varies according to ship type. It is about 24 knots for container ships and about 16 knots for tankers. Here, the average ship cruising speed was estimated to be about 20 knots, i.e., 36 km/h (ICOADS, 2002). Thus, the average distance is estimated for the southern Pacific coast as follows.

$$D = 36 * 24 * 365 / 13,000 = 24.3 \text{ km}$$

Based on this analysis, we propose to use a distance of 25 km between ships to calculate ship emissions.

6. REFERENCES

- Corbett, J.J. and H.W. Koehler, 2003. Updated emissions from ocean shipping, *J. Geophys. Res.*, **108**, doi:10.1029/2003JD003751.
- Corbett, J.J., 2005. Private communication to Christian Seigneur, AER, July 2005.
- EPA, 2002. Commercial Marine Emission Inventory, Final Report from PECHAN, prepared by ENVIRON International Corporation, U.S. Environmental Protection Agency, Office of Transportation and Air Quality, Ann Arbor, MI.
- Fleischer, F., E.J. Ulrich, R. Krapp and W. Grundmann. Comments on particulate emissions from diesel engines when burning heavy fuels.
- ICOADS, 2002. International Comprehensive Ocean Atmospheric Data Set, as transmitted from ERG by Office of Transportation and Air Quality, U.S. Environmental Protection Agency, Washington, D.C.
- Morris, R.E., R.C. Kessler, S.G. Douglas, K.R. Styles and G.E. Moore, 1988. Rocky Mountain Acid Deposition Model Assessment: Acid Rain Mountain Mesoscale Model (ARM3), Report prepared for the U.S. EPA, Research Triangle Park, NC.
- Scire, J.S., D.G. Strimaitis and R.J. Yamartino, 2000a. A User's Guide for the CALPUFF Dispersion Model (Version 5), Earth Tech, Inc. Report, Concord, MA, January 2000.
- Scire, J.S., F.R. Robe, M.E. Fernau and R.J. Yamartino, 2000b. A User's Guide for the CALMET Dispersion Model (Version 5), Earth Tech, Inc. Report, Concord, MA, January 2000.
- Scire, J.S., 2005. Communication via e-mail of Christian Seigneur, AER, with Joe Scire, EarthTech, 18-19 March 2005.
- Seigneur, C. K. Lohman and P. Karamchandani, 2005. Review of Technical Information relevant to Sulfur Oxides (SO_x) Emissions Transport for Ships at Sea, Final Report to Office of Transportation and Air Quality, U.S. Environmental Protection Agency, Washington, D.C.
- Wheeler, N., 2005. Private communication from Neil Wheeler, Sonoma Technology, Inc. to Christian Seigneur, AER, 14 March.